On the intrinsic control properties of muscles and reflexes

Exploring the interaction between neural and musculoskeletal dynamics in the framework of the equilibrium-point hypothesis

Thomas Buhrmann

Submitted for the degree of D. Phil.

University of Sussex

November, 2010

Declaration

I hereby declare that this thesis has not been submitted, either in the same or different form, to this or any other university for a degree.

Signature:

Acknowledgements

I would like to thank my supervisor, Ezequiel Di Paolo, for his unfailing encouragement and his patience, which was undoubtedly required to see me through this thesis. I am also grateful to Inman Harvey and Phil Husbands for the useful feedback they have provided as members of my research committee. Many thanks go to my friends and colleagues in the CCNR, particularly Eduardo Izquierdo and Edgar Bermúdez, for inspiring discussions and for making my time at Sussex more enjoyable. I am grateful to the EPSRC for funding my Master's degree and to the University of Sussex for providing me with a Graduate Teaching Assistantship. Finally, I would not have been able to complete this thesis, was it not for the unwavering support of my mother Ilona and my girlfriend Sonia. For all they had to endure I am deeply indebted.

On the intrinsic control properties of muscles and reflexes

Exploring the interaction between neural and musculoskeletal dynamics in the framework of the equilibrium-point hypothesis

Thomas Buhrmann

Summary

The aim of this thesis is to examine the relationship between the intrinsic dynamics of the body and its neural control. Specifically, it investigates the influence of musculoskeletal properties on the control signals needed for simple goal-directed movements in the framework of the equilibrium-point (EP) hypothesis. To this end, muscle models of varying complexity are studied in isolation and when coupled to feedback laws derived from the EP hypothesis. It is demonstrated that the dynamical landscape formed by non-linear musculoskeletal models features a stable attractor in joint space whose properties, such as position, stiffness and viscosity, can be controlled through differential- and co-activation of antagonistic muscles. The emergence of this attractor creates a new level of control that reduces the system's degrees of freedom and thus constitutes a low-level motor synergy. It is described how the properties of this stable equilibrium, as well as transient movement dynamics, depend on the various modelling assumptions underlying the muscle model.

The EP hypothesis is then tested on a chosen musculoskeletal model by using an optimal feedback control approach: genetic algorithm optimisation is used to identify feedback gains that produce smooth single- and multijoint movements of varying amplitude and duration. The importance of different feedback components is studied for reproducing invariants observed in natural movement kinematics. The resulting controllers are demonstrated to cope with a plausible range of reflex delays, predict the use of velocity-error feedback for the fastest movements, and suggest that experimentally observed triphasic muscle bursts are an emergent feature rather than centrally planned. Also, control schemes which allow for simultaneous control of movement duration and distance are identified.

Lastly, it is shown that the generic formulation of the EP hypothesis fails to account for the interaction torques arising in multijoint movements. Extensions are proposed which address this shortcoming while maintaining its two basic assumptions: control signals in positional rather than force-based frames of reference; and the primacy of control properties intrinsic to the body over internal models. It is concluded that the EP hypothesis cannot be rejected for single- or multijoint reaching movements based on claims that predicted movement kinematics are unrealistic.

Submitted for the degree of D. Phil.

University of Sussex

November, 2010

Contents

List of Figures

List of Tables

Chapter 1

Introduction

The following section provides a brief overview of the aims and methods of investigation used in this thesis. This is followed by a short description of the contents of each chapter and a list of original contributions.

1.1 Overview

The aim of this thesis is to examine the relationship between the intrinsic dynamics of the body and its control. Specifically, it investigates the influence of musculoskeletal properties on the control signals needed for simple goal-directed movements in the framework of the equilibrium-point (EP) hypothesis. The EP hypothesis suggests that coordinated movement can be produced without the need for internal models by relying on the intrinsic dynamics of the body. This notion is challenged by proponents of the force-control hypothesis, who suggest that the central nervous system uses internal simulations of the body and its environment to explicitly calculate the muscle forces required for a desired movement. Much of their criticism regarding the EP hypothesis is based on simplified models of the motor apparatus. However, the importance of the body in shaping the behaviour of an agent is now well established in both the fields of biomechanics (Gribble et al., 1998) and cognitive science, with the introduction of concepts such as embodiment (Beer, 2009), passive dynamics (McGeer, 1990), and the dynamical systems approach (Gelder, 1997). This thesis investigates whether the neuromusculoskeletal system (i.e. the skeleton, the muscles that actuate it, and the networks of neurons innervating them) possesses intrinsic control properties that facilitate coordinated movement. To this end, muscle models of varying complexity are studied in isolation and when coupled to different feedback laws derived from the EP hypothesis. Their steady state and transient dynamics are compared to natural kinematics and several criticisms brought forward by proponents of the force-control hypothesis are addressed. These include, for example, the (in-)ability to deal with reflex delays or interaction torques, and the suggestion that observed biomechanical invariants must be the result of central planning. The results suggest that the EP hypothesis cannot be rejected on the basis of such claims. They also stress that predictions about motor control signals are sensitive to assumptions regarding the musculoskeletal system.

Finally, extensions to the simplest instantiation of the EP hypothesis are proposed, which address its limitations in the context of multijoint movements.

1.2 Thesis organisation

Chapter 2 places the research undertaken in this thesis in the context of the controversy between force- and position-based theories of motor control. First, it details the various problems encountered in any motor control task, such as redundancy, signal noise or feedback delay. It then summarises the arguments for and against the two dominant, and conflicting, approaches to motor control: the force-control hypothesis and the equilibrium-point hypothesis. Parallels are drawn to notions of embodiment, situatedness and the dynamical system perspective in cognitive science, and their influence on the methodology used in this thesis is described.

Chapter 3 provides some background about the physiology of skeletal muscles and details the approach taken in modelling musculoskeletal dynamics. This is followed by an analysis of the steady state and transient dynamics of antagonist muscles with static control signals. Specifically, it is studied whether the dynamical landscape formed by muscle models features a stable attractor in joint space, and if so, whether properties of this equilibrium, such as position, stiffness and viscosity, can easily be controlled through simple adjustments of muscle activations. This is a prerequisite of the equilibrium-point hypothesis. The chapter also investigates how modelling assumptions underlying various components of the muscle model influence its dynamical properties. It ends with a demonstration of the benefits of muscle material properties when open-loop control signals are learnt using a genetic algorithm.

In chapter 4, the EP hypothesis is tested on a chosen musculoskeletal model by using an optimal feedback control approach: genetic algorithm optimisation is used to identify the feedback gains and control signals which produce the smoothest single- and multijoint movements of varying amplitude and duration. The importance of different feedback components in reproducing natural kinematics is studied and it is asked whether the resulting controllers correctly predict the response to reflex delays and the experimentally observed triphasic burst patterns in muscle activity. The chapter also aims to identify the form of control signals required for simultaneous control of both movement duration and distance.

A lumped neuromuscular model is introduced in chapter 5 which combines the convergent dynamics of muscle and reflexes into a single equation of force production at the joint level. Experiments are carried out to test whether this model, which is essentially an extended non-linear proportional derivative controller, can approximate the behaviour observed in the detailed muscle-reflex model. In chapter 6 the lumped model is then used to study extensions of the EP hypothesis which aim to solve the problem of interaction torques arising during multijoint movements. A long-standing critique of equilibrium-point models is that they do not account for such torques, and it is often argued that internal models alone can solve this problem. This is challenged here with a proposal for an extension of the EP hypothesis that couples the feedback control laws of neighbouring joints.

The last chapter summarises the results of this investigation, discusses its implications and proposes work that could be undertaken to address remaining questions.

1.3 Summary of contributions

The contributions of this thesis can be summarised as follows.

It is shown in chapter 3 that the stability of joint equilibria and other steady-state characteristics created by antagonistic muscles depend on assumptions about muscle paths and moment arms, the inclusion of series elasticity and the modelling of chemical dynamics. It is also demonstrated that a setup consisting of two monoarticular muscles can qualitatively, and in some respects quantitatively, approximate the steady-state and transient behaviour of a system that also includes biarticular muscles.

It is shown in the second part of chapter 3 that the material properties of muscles allow for flexible motor control (e.g. freedom concerning the energy requirements of a movement), and that they might facilitate motor learning by smoothing and linearising the space of possible control signals.

Chapter 4 confirms that an extended version of the λ-formulation of the EP hypothesis can reproduce the kinematics and force patterns of natural single-joint movements when driven by simple monotonic control signals. It is shown that the range of static musculoskeletal properties represented in the controller needs to be extended to account for movements of arbitrary speeds. It is further demonstrated that velocity error feedback is crucial for high velocity movements without oscillations, and open-loop co-contraction for dealing with feedback delays. The results suggests that experimentally observed movement invariants are not necessarily centrally planned, but can emerge from the interaction of reflex components and the dynamics of the body.

A lumped model of neuromuscular dynamics is developed in chapter 5 that can approximate the kinematic data of a detailed muscle-reflex model during single-joint movements. While other simple models, such as mass-spring systems, have been shown to necessitate complex control signals, the nonlinear model proposed requires only a simple monotonic shift in desired position. Crucially though, the model is shown to predict different control signals than the detailed muscle model.

Most importantly, it is shown in chapters 3-5, that in an equilibrium-point framework smooth multijoint movements do not result from independent control of each joint. Intersegmental dynamics lead to perturbations that are not rejected at realistic stiffness level. Two mechanisms are therefore proposed in chapter 6, which couple the control of individual joints so that interaction torques are compensated for. The two models make specific predictions about the spinal circuits required for their implementation.

Chapter 2

Background

The following chapter provides an overview of the computational and dynamical approaches to motor control. After summarising the complexities involved in controlling a body that exhibits strong redundancy, complex internal interactions, and non-linear material properties, the force-control and equilibrium-point hypotheses are introduced as conflicting paradigms for addressing them. The methodology employed in this thesis is then placed in the context of these research avenues, as well as in the broader field of embodied cognition.

2.1 The problem of motor control

To study behaviour is to study the patterns of interaction between an agent and its environment. From the perspective of the agent, this interaction forms a continuous and closed sensorimotor loop: motor commands initiated by the agent have physical consequences in its environment; these are perceived via sensory feedback, and together with proprioceptive signals influence future motor commands. The field of motor control is concerned with the question of how an agent can consistently produce stable coordinated movement patterns in a complex and constantly changing environment.

Though humans and other animals perform most of their movements seemingly without effort or particular attention to their actions, complex unconscious processes, involving the interaction of many anatomical and neural structures, are needed to produce appropriately coordinated motion. Coordination, in the context of motor control, is understood with respect to a particular task, or movement objective. For an agent, to realise a motor task means to produce changes in its many biomechanical degrees of freedom (DOFs) that are coordinated in space and time such as to achieve a given objective.

Redundancy

To illustrate the complexity of an apparently simple motor task, consider the act of positioning your hand at a given point in space. Even in this simple case there are an infinite number of different paths along which the hand can move from its initial to the desired position. And for

each path there are an infinite number of possible velocity profiles. Even if a single spatiotemporal trajectory has been chosen, each location of the hand can be realised by an infinite number of joint angle combinations. While the task is described by only three independent variables (the spatial coordinates of the desired hand position), the arm contains many more degrees of freedom. One can, for example, swivel the elbow up and down, or tilt one's torso forward and back, both without changing the position of the hand in space. The problem is therefore underdetermined, and the system said to be redundant with respect to the task. What is more, several different muscles act across each skeletal joint, and infinitely many muscle activation patterns produce the same joint configuration (it is possible, for instance, to stiffen the arm without moving the hand). The system is not only redundant in joint space, but also in muscle space. Even if each muscle is for simplicity assumed to be either contracted or relaxed, then the 700 or so muscles in the human body would allow on the order of 10^{210} different muscle activation patterns. Equally, assuming about 200 joints in the body, and for simplicity only one rotational degree of freedom each (many have three), then each movement would have to be described in a 400 dimensional state space if we wanted to account for position and velocity only (disregarding accelerations, inertia, muscle forces, etc.). The combinatorial explosion does not end there, as each muscle is innervated by between 10 and 1000 alpha motor neurons, with many different firing patterns generating the same muscle force. Not only does any proposed motor control scheme have to address this "curse of dimensionality" (Bellman, 1961) encountered when transforming a single spatial location into activations of about 200 000 alpha motor neurons forming the so-called *final common pathway*. The relationship between a motor command and the resulting motion of the body (and vice versa) is also described by highly complicated and non-linear equations. For example, the effect that the activation of a muscle has on the change in angle of the joint it acts on depends on the orientation of the body segment with respect to gravity, the current pose of the limb, the current length and velocity of contraction of the muscle, its state of fatigue, and the forces that arise from the physical interaction of connected body segments, to name just a few.

Although redundancy might seem a curse from the viewpoint of control theory, it also provides advantages in terms of flexibility and adaptability. The abundance of solutions for a given task implies that different strategies can be chosen depending on secondary constraints in the system. In a reaching task, for example, the elbow position can be varied to avoid obstacles that would be encountered otherwise. Humans can also exploit muscle properties to modulate the effective stiffness at the hand such as to better resist perturbations coming from certain directions (without changing the hand position), thereby tuning the passive dynamics of the arm for a specific context (Gomi and Osu, 1998).

Every sufficiently complex organism, and consequently any approach to motor control, thus faces a trade-off between an internal reduction of degrees of freedom to simplify control, and preservation of redundancy as a means to flexibly respond to different secondary task requirements. Bernstein, arguably the founder of modern biomechanics, was among the first to be concerned with this problem (Turvey, 1990). He asked how a large number of independent variables might be regulated without ascribing excessive responsibility to a single centralised system. According to Bernstein, the solution involves reducing the effective number of independent variables by appropriately organising the control of the motor apparatus. Turvey gives an illustrative example of this approach

(Turvey, 1990). Imagine a marionette in which each individual body segment is controlled via a dedicated wire that is manipulated by a puppeteer. Here, the responsibility of coordinating the various moving parts is attributed utterly and exclusively to the puppeteer who, in a homuncular fashion, has to determine the state of all variables over time. Now consider a second marionette, one in which internal wires connect some of the parts to each other so that they move together in a coordinated manner. Pulling a certain wire, here, might for example produce a stepping movement in the puppet's legs. Clearly, the burden of control for the puppeteer is reduced. The number of wires under his control is smaller, as he now controls a few internal mechanisms rather than each individual part. Bernstein called these internal, dimensionality-reducing mechanisms coordinative structures, or *synergies*. He was fast to realise that these are not to be confused with reflexes, which could be considered hard-wired mechanisms of coordination. In Bernstein's view, synergies constitute context-dependent muscle-linkages whose functions can be configured for the task at hand. Central pattern generators can be considered examples of synergies. Here, a neural network innervates a group of muscles that act across many different joints, and creates coordinated movement patterns that achieve a specific goal such as swimming or stepping.

Delays

In addition to redundancy, the control of the motor system is complicated by the presence of various delays in its neural circuits. It is easy to see that these can potentially have detrimental effects on the performance of feedback-controlled motor circuits. In the extreme case, where a movement is faster than the overall delay, feedback would not be available at all during the actual motion. But accuracy can also be negatively affected for movements on a time scale larger than the delay. The faster the system moves (and the longer the delay), the greater the distances covered before the feedback signal arrives. Many control systems with inherent feedback delay therefore have to deal with a trade-off between speed and accuracy. Another potential problem is that of co-registering actions with their consequences when these signals are separated in time by several hundred milliseconds. Hidler and Rymer (2001) have demonstrated the destabilising effect of high transport delays on ankle stability using a model of the stretch reflex.

One source for feedback delay in neural circuits is the time it takes for a presynaptic action potential to arrive at the input site of the postsynaptic cell. This so-called synaptic delay has been estimated at 1–2 ms (Sabatini and Regehr, 1996). Another source is the conduction delay along the axon of a neuron, which ranges between 1 and 20 ms, depending on the length of the axon and whether or not it is myelinated (Carr and Konishi, 1988; Burke et al., 1994; Macefield and Gandevia, 1992). Resistance and capacitance properties of dendrites can also cause a wide range of delays, with durations depending on the topology of the dendritic tree (Agmon-Snir and Segev, 1993).

It is difficult to measure the overall delay in the motor circuit of an animal. Estimates range from 14 ms for a short spinal reflex to 200–300 ms for a response involving the visual system. St-Onge et al. (1997), for example, have estimated a spinal reflex delay of 14–18 ms by measuring the time between the unloading of an initially loaded elbow, and the first sign of reflex activity as indicated by a change in the electromyographic (EMG) activity generated by the muscles.

Noise

Noise, present on all levels of the sensorimotor hierarchy, can be another source of complication for motor control. In proprioceptors and muscles, for example, noise is generated by the transduction of a continuous mechanical signal into a discrete spike train (Read and Siegel, 1996). Synaptic variability (Allen and Stevens, 1994) and complex network dynamics (van Vreeswijk and Sompolinsky, 1996) can further increase the variance in neural firing rates. In the cortex, it is possible that information is nevertheless transmitted reliably, not in temporal spike patterns of individual neurons, but via rate coding in ensembles of neurons. This was shown to allow for reliable rate estimates within a single interspike interval (10–50 ms), assuming that post-synaptic neurons receive a balanced amount of excitatory and inhibitory inputs (Shadlen and Newsome, 1994, 1998). Ensemble coding is not available in the motor periphery, however, where a single motorneuron innervates many muscle fibres. Many approaches to motor control therefore operate on the premise that the standard deviation of a motor signal is proportional to its magnitude, which means that noise levels are signal-dependent. This is supported empirically by the finding that the standard deviation of isometric force production is proportional to the mean force (Schmidt et al., 1979; Meyer et al., 1988), which is itself the result of the distribution of individual motor unit recruitment thresholds and muscle fibre twitch amplitudes (Jones et al., 2002). Noise in the sensorimotor system implies that state estimation (for example of one's current hand position) is unreliable and that actual movements might differ from intended ones. According to the framework of "task optimisation in the presence of signal-dependent noise" (van Beers et al., 2002), the central nervous system (CNS) aims to minimise the detrimental consequences of noise in the motor system by planning movements so that the redundancy of the motor system can help minimise endpoint variability. Movements predicted within this framework are found to closely resemble those observed in human experiments.

Biomechanical invariants

Despite the vast number of redundancies in the human motor apparatus, most types of movements show high regularity, both across repetitions by the same individual as well as across different individuals. These invariants are often seen as indicators of the organisational structure underlying motor control by the CNS.

Morasso (1981), for example, first discovered that the hand follows an approximately straight line path in point-to-point reaching movements, while the tangential velocity along the path is characterised by a symmetric bell-shape. Individual joint trajectories, in contrast, follow more complex profiles. This observation led to the hypothesis that such movements are planned in external Cartesian coordinates rather than in terms of joint angles or muscle lengths. The later discovery that reaching movements show in fact systematic deviation from the straight line (Atkeson and Hollerbach, 1985; Soechting and Lacquaniti, 1981; Uno et al., 1989) and that the symmetry of the velocity profile varies with movement speed (Bullock and Grossberg, 1988) led to further elaboration of this hypothesis based on the principles of optimal control (see below).

Lacquaniti et al. (1983) discovered in rhythmic drawing movements, and others later confirmed in different experiments (e.g. Flash and Sejnowski, 2001), that the relationship between the angular velocity of the hand and the curvature of its path follows a power law with an exponent of 2/3.

Physically, there is no reason that movement kinematics and geometry should be related according to this so-called 2/3 power law. Its existence may reflect a principle of movement organisation in itself, or might be a by-product of other processes involved. A study by Sternad and Schaal (1999) suggests that it might indeed be an epiphenomenon. In unconstrained rhythmic movements, systematic violations of the law were observed which were best explained by a system favouring smooth trajectories produced by a pattern generator in joint space.

Rapid aiming and reaching movements are characterised by a trade-off between speed and accuracy. Quantitatively, the movement time of reaching for a target depends logarithmically on the ratio of movement distance and required accuracy (target size), and is described by Fitt's Law (Fitts, 1954). Plausible explanations link the phenomenon to optimisation principles regulating a noisy (Meyer et al., 1990), or delayed (Beamish et al., 2008) motor apparatus. Though it is often used to validate models of motor control, many different approaches readily produce the speed-accuracy trade-off, which has thus limited scope for resolving conflicting proposals.

An important and open question is whether any of the observed invariants reflect a strategy used by the CNS to deal with redundancy, noise or delays, or whether they are epiphenomena reflecting properties of the neuromusculoskeletal system and physical laws.

Optimal control

Optimal control approaches aim to explain the existence of movement invariants in the presence of high redundancy by stipulating that the motor system is constrained by optimisation principles. More specifically, it proposes that the motor system operates at the minimum of a cost function that measures global quantities such as smoothness, efficiency or accuracy. In this framework it would be plausible, for example, to propose that the hand follows trajectories that minimise energy expenditure. One would then employ an optimisation algorithm (such as dynamic programming, Bryson and Ho, 1975) to produce trajectories conforming to the chosen constraint. Any observed invariants are then merely a reflection of the underlying optimisation principle, but can be compared against those found in natural movements to validate the model. It is worth noting that most theories concerned with optimal control do not necessarily suggest that actual movements are the results of a computational optimisation process in the nervous system. The actual mechanisms producing the optimal motor output and their origin are typically outside the scope of these theories.

Most optimal control models proposed for reaching movements fall into one of two classes: kinematic or dynamic optimisation. Kinematics-based models are concerned only with effector positions or joint angles and their derivatives, and employ cost functions that depend on geometrical or time-based properties of the desired motion. An example is the minimum jerk model (Hogan, 1984; Flash and Hogan, 1985). Based on the observation that hand paths are normally smooth in Cartesian space, it suggests that natural movements minimise the square of the first derivative of acceleration, also called jerk. It predicts straight-line hand trajectories and symmetric velocity profiles in accordance with data on rapid movements executed without accuracy requirements. Observed deviations from these invariants, as described above, were attributed to imperfect execution of the movement plan (rather than to a lack of accounting for arm dynamics, posture, or external forces). The model, when applied to movements along constrained paths such as figure

eights, was also found to approximate the solution described by the 2/3 power law. However, in Gribble and Ostry (1996) it was shown that the same law could emerge simply as a consequence of the viscoelasticity of the muscles. Apart from the shortcomings of this particular model, it is not clear a priori why smoothness of trajectories should be an important property in itself.

Kinematic optimisation models directly specify the positions and velocities of the moving system and assume the existence of a separate process responsible for achieving them. A dynamic model, in contrast, is concerned directly with variables such as joint torques, hand forces or muscle tension, and its solution consists of the actual motor commands necessary to achieve the desired movement. The separation of movement planning and execution is thus avoided.

The dynamic equivalent of smoothness optimisation is the minimum (commanded) torque change model (Uno et al., 1989; Nakano et al., 1999), which has been found to account for several of the shortcomings in the minimum jerk model, such as curvilinear paths in large range motion and in the presence of external forces. However, it shares with the minimum jerk model the question of why it is useful to optimise smoothness. Also, movement duration cannot be selected in either model, but is instead a free parameter.

A model based on a cost function that is biologically more relevant than the above is the minimum variance theory (Harris and Wolpert, 1998). It is based on the assumption that noise in motor commands causes trajectories to deviate from the desired path. Accumulated over the duration of a movement, these errors lead to variability in the final position. As noise is assumed to increase with signal strength, rapid movements, which require large control signals, would therefore result in large end point variability. Accuracy would be improved by using small amplitude control signals, but the resulting movements would then be slow. According to the minimum variance model, motor commands are selected so as to minimise variance in the final position, while maximising the speed of motion as much as is compatible with the accuracy requirements of a particular task. Smooth trajectories are the result of this approach, rather than its assumption. This is because abrupt changes in velocity, which require large changes in the control signal, would generate more noise and are therefore avoided. The model also predicts the speed-accuracy trade-off described by Fitt's law, reproduces the 2/3 power law, and its predictions about eye and arm movements are robust to changes in the dynamics of the body.

The above models make no claim as to the actual neural and biomechanical mechanisms producing the predicted motor commands, but employ a purely open-loop optimisation directly on motor commands or limb trajectories. In contrast, stochastic optimal feedback control (Todorov and Jordan, 2002) explicitly takes into account the feedback nature of the sensorimotor loop. In this approach, an estimate of the current state of the system, based on afferent feedback and internal forward modelling (see below), forms the basis for modifications of a task-specific feedback control law that aims to maximise a performance index such as end point variability. An important aspect of optimal feedback control is the minimum intervention principle, according to which deviations from the average trajectory (the system behaves stochastically) are corrected only when they interfere with task performance. Thus, variability due to noise is not eliminated, but allowed to accumulate in redundant, that is task-irrelevant, dimensions (also called the uncontrolled manifolds, Scholz and Schöner, 1999). Importantly, the theory shows that this is in fact the optimal behaviour for a stochastic system. This prediction is observable in human motor coordination. In

goal-directed pointing movements, for example, such as shooting with a laser gun, fluctuations of joint configurations that affect pointing accuracy are much reduced when compared to fluctuations that do not affect this variable (Scholz et al., 2000). Unfortunately, the mathematics required for constructing optimal feedback controllers are so involved that the motor systems studied have to be significantly simplified in most cases. Linearisation of the complex dynamics of the musculoskeletal system, however, has been shown to invalidate predictions regarding its control (Gribble et al., 1998).

Controlled variables and neural correlates

As the variety of different motor control models above illustrate, there is no consensus as to which variables of a movement the nervous system controls. As easily as one can find a model to support the idea of planning in hand coordinates, joint angles or muscle forces, one can find areas in the nervous system whose neural activity correlates with the variable of one's choice. For example, activity in the primary motor cortex (M1) was shown to predict hand direction (Georgopoulos et al., 1982), velocity (Schwartz, 1993), or movement distance (Fu et al., 1995). However, hand motion could equally be predicted from neurons than encode different quantities of the motor performance, such as muscle activity or joint motion (Mussa-Ivaldi, 1988; Todorov, 2000). Also, some neurons in M1 and other motor areas correlate not with hand-related coordinates, but with patterns of muscle activity (Holdefer and Miller, 2002; Bennett and Lemon, 1996) or arm geometry in redundant degrees of freedom (Scott et al., 1997). Recent evidence indicates that these different neural correlates are not mutually exclusive, but rather reflect a more complicated organisation of the motor cortex than previously assumed (Graziano, 2006). Through stimulation of motor cortex sites in the monkey on the time scale of behavioural responses [1], Graziano and colleagues revealed that the known large-scale somatotopic cortical map is locally distorted by clusters of neurons that are tuned to complex motor patterns including many muscles and joints, and which reflect the behavioural repertoire of the animal (e.g. hand to mouth movements, or reaching out and grasping). Furthermore, this tuning is not fixed but can change instantaneously on the basis of feedback from the motor periphery. For example, pulse stimulation of a point on the primary cortex led to biceps activity if the elbow was extended, but to triceps activity when flexed. When the same site was stimulated with an extended train of pulses, the elbow moved to a particular intermediate angle and stabilised there. This implies that the use of feedback allows for tuning of individual cortical neurons to higher-order parameters such as a desired elbow angle.

In summary, it seems unlikely that a single control variable exists that explains all types of observable movements. Rather, cortical networks can be dynamically configured to regulate almost any (combination of) high- or low-level movements parameters in such a way as is appropriate for the task at hand. It is hence important to critically approach any physiological evidence supporting a model of motor control based on simple neural correlates (such as preferred direction) and artificial experimental setups.

[1] stimulation trains of about 500 ms, as opposed to short pulses of about 0.2 ms, which elicit only muscle twitches

2.2 Two motor control paradigms

The following sections aims to summarise the controversy between the computational and the dynamical systems perspective on motor control. The former has its roots in engineering and is represented by theories which are based on internal models of the body and its environment. The latter originates in biomechanical studies that have identified inherent control properties (stable equilibria) in the coupled dynamics of the skeleton, muscles and reflexes.

2.2.1 The force-control hypothesis

According to computational theories of motor control, the problem of movement generation is essentially one of coordinate transformations. Typically, a desired movement is first defined in spatial coordinates and then transformed into the required forces or torques to be applied at the joints by the muscles. In order to compute these variables, the system uses internal representations of the geometry as well as the dynamical equations of motion of the body. The former can be used to calculate inverse kinematics, that is the joint angles required to position the end-effector at a particular point in external Cartesian space. The latter is used in an inverse dynamics process to calculate the joint torques or muscle forces necessary to drive to the desired joint angles. These processes are inverse in the sense that they revert the natural causality of motion, from muscle forces to changes in position. In addition to these inverse internal models, computational approaches often employ forward internal models to predict the consequences of a motor command. A forward model mimics the actions of the motor apparatus, that is the causal relationship between its inputs (e.g. muscle activations) and outputs (e.g. joint torques). When driven by a copy of the motor command (efference copy), it can therefore predict the sensory consequences this command would elicit. It has been argued that forward models are necessary, for example, to adjust control signals on the basis of anticipated sensory consequences rather than actual sensory feedback, in order to mitigate the detrimental effect of delays in the latter.

For a typical example of using forward and inverse models, consider the task of a goal-directed arm movement while the hand is grasping an object between index finger and thumb (Kawato, 1999). The problem involves the control of a grip force that is just sufficient to prevent the object from slipping. Here, an inverse model of the combined dynamics of arm and grasped object would be used to calculate the motor commands necessary for achieving a desired hand trajectory. These commands would then be sent to the arm muscles, and as an efferent copy to a forward dynamics model. Based on the predicted trajectory of the arm, an expected load force could be calculated that would act on the grasped object. Taking into account load, friction and safety margins, a grip force could then be determined that would prevent the object from slipping, and appropriate motor commands sent to the hand muscles.

Theories of motor control such as the one described, summarised from here on under the notion of the force control hypothesis (Ostry and Feldman, 2003), are based on three assumptions: the brain centrally specifies forces to be applied to the body; these forces are derived using an internal inverse dynamics model; the motor system makes use of predictive mechanisms based on internal forward models.

Force control

The idea that the brain directly calculates and controls the forces required to produce desired movements is supported by many studies showing systematic relationships between joint torques, muscle activity, kinematics and task variables (Gottlieb et al., 1990; Corcos et al., 1989; Gottlieb et al., 1996). It has also been demonstrated that torques at the shoulder and elbow joints follow a linear relationship under many conditions (Gribble and Ostry, 1999), and that subjects are capable of judging force output over a wide range of magnitudes (Jones, 1989). Further support is lent by electrophysiological data. Activity of neurons in cortical area 4, for example, has been shown to correlate with the direction of required force output (Georgopoulos et al., 1992). Also, certain cerebellar lesions lead to problems that seem to indicate a failure to control the interaction torques arising in one joint as a result of motion in another (Bastian et al., 1996).

A theoretical limitation of the force control hypothesis, however, is its inability to resolve the "von Holst paradox" (Ostry and Feldman, 2003). In their classic paper, Holst and Mittelstaedt (1950) drew attention to the fact that the body is in any posture stabilised by neuromuscular mechanisms that generate forces in order to resist external perturbations. Yet clearly the organism is also able to intentionally move from one pose to another. The posture-movement problem is the question of how this is possible without triggering resistance by postural reflexes. In force control models it is typically assumed that desired forces are encoded in the group activity of motoneurons as reflected in measured EMG signals. EMG signals, however, cannot predict posture. Recordings from point to point movements show that EMG activity is zero at the initial and final position, and by extension, whenever the system is at rest[2] (Suzuki et al., 2001). Different postures can therefore not be encoded by motoneuron activity or forces directly, but must be controlled by other variables. If it were assumed that forces are specified directly only to transition between different postures, then the stabilising mechanisms would have to be completely or partially suppressed. However, experimental observations do not support this idea. Instead, even intermediate postures, that is to say, any point on the trajectory from initial to final pose, seem to be stabilised by resisting actions (Won and Hogan, 1995). More elaborate versions of the force control hypothesis, which include muscle properties and reflexes, for example, must equally counteract their posture-stabilising effect, instead of utilising it (see Ostry and Feldman 2003 for a more detailed analysis). This failure to establish different poses without inducing resistance, and the resulting mismatch between predicted and empirically observed EMG signals, indicate conceptual gaps in the force control hypothesis.

Inverse models

Most force control models are formulated such that trajectories planned in kinematic coordinates are transformed into necessary torques by an inverse dynamics computation. Typically, the inverse model neither explicitly accounts for the dynamics of the neurons innervating the muscles, nor for the non-linear dynamics of force generation by the muscles themselves. It directly provides trajectories of joint torques over time that will produce the desired movements when applied to the mechanical system. This coordinate transformation allows inverse models to implement open-loop motor control schemes that do not rely on error-correcting feedback. The fact that deafferented

[2] It is also easily observed that one can relax ones arm muscles in any possible joint configuration

monkeys, meaning those whose sensory feedback is eliminated surgically, can still reach a target with their hands (though more crudely) seems to indicate that under such laboratory conditions movements can indeed be executed in a preplanned and purely feedforward manner (Bizzi et al., 1984).

The existence of inverse models is further supported by experiments in which subjects execute reaching movements while exposed to an external force field (Shadmehr and Mussa-Ivaldi, 1994). Such fields, usually generated by a robotic manipulandum, alter the effective dynamic characteristics of the arm by applying forces that depend on its position and velocity. When arm movements are carried out in a force field, observed hand trajectories are initially distorted when compared to natural straight-line paths. Over repeated trials, however, subjects adapt to the load and eventually restore their normal hand paths. If the force field is then suddenly removed, trajectories become distorted once again, but in the opposite direction of the previously applied perturbations. The explanation, according to the force control hypothesis, is that kinematically planned reaching movements are realised by an inverse dynamics model of the arm. This model initially fails to account for the externally applied forces, but over time adapts to their stable characteristics. The resulting model of combined arm and force field dynamics then misrepresents the actual situation when the field is later removed. The idea of an internal model combining arm and load dynamics is supported by experiments with monkeys in which it was shown that neurons in area 4 change their tuning properties with changes in load (Gribble and Scott, 2002). However, neither the behavioural nor the physiological evidence rule out alternative explanations. They merely show that humans (and monkeys) can take loads into account when performing arm movements. Gribble and Ostry (2000) have demonstrated in a framework of position control that load adaptation is possible without representation of forces, inverse dynamics or forward predictive simulation.

Further neurophysiological evidence for internal inverse models is based on firing patterns recorded in cerebellar Purkinje cells (Gomi et al., 1998; Shidara et al., 1993). During reflexive eye movements, their neural activity can be reconstructed from a linear combination of eye position, velocity and acceleration in a way that reflects the relationship between these variables in an inverse dynamics representation of the eye. As Ostry and Feldman (2003) have pointed out, however, correlation does not equal causation. It is not entirely surprising that neural activity correlating with mechanical variables can be identified in a system that couples mechanical, sensorial and neural components. Also, the less than 10 ms lead of Purkinje cell activation over movement initiation failed to account for the observation that antagonist deactivation starts 30–40 ms before reflexive eye movements. In the same experiments, climbing fibres feeding in to the cerebellum were found to carry sensory error signals in coordinates of the motor command. This observation was used to support the so-called cerebellar feedback-error-learning model, in which the error produced by a feedback loop is used to train an inverse model that functions a feed-forward controller (Kawato et al., 1987). Identifying similar relationships between neural activity and movement variables for arm movements however has so far been less successful.

On theoretical grounds, current inverse models are also incapable of resolving the redundancy problem. Even if EMG signals are determined by inverse dynamics computations, for a full account of motor control it would be necessary to determine the motoneuron inputs that produce the desired EMG output. However, non-linearities such as threshold and plateau-potentials cannot be

reversed without significant simplification of the relevant dynamics. As is true for the equations describing force production by the muscles, such simplified models produce questionable results (Gribble et al., 1998; Zajac et al., 2002).

Forward models

Forward dynamics models can be used to predict both the actual movement of the system and its sensory consequences (Karniel, 2002). For example, an efference copy of the motor command could be used in conjunction with a forward dynamics model to predict and cancel out the sensory effect (re-afference) of self-induced motion. This control scheme has been suggested, for example, as a mechanism for stabilising visual space against movements of the head and the eyes (Jeannerod, 1997). Forward models can also be used to implement open-loop control when placed in an internal feedback look (Jordan, 1993).

Another suggested role is the use of forward models to provide internal feedback about the predicted consequences of a motor command when the delay of actual sensory feedback would otherwise lead to instability. An extension of this idea, known to engineers as a Smith predictor, delays the output of the forward model to cancel out the predictable components from the actual feedback. This allows for a feedback system that only corrects the remaining unpredictable, and likely small, errors that cannot be anticipated by the internal model. The cerebellum has been proposed to act as a Smith predictor, for example (Miall et al., 1993).

Forward models have also been implied in a theory of sensorimotor integration based on the Kalman filter (Kalman, 1960), which is a formal solution to the problem of optimal state estimation. In a Kalman filter, the future state of a system is estimated by a forward model that receives as input both a copy of the motor command and the current state estimate. At the same time, a prediction of sensory feedback based on the system's current state is compared with actual feedback. The resulting sensory error is then used to correct the state as predicted by the forward model. In essence, the Kalman filter uses motor commands, sensory feedback and a model of the motor system to reduce uncertainty in its state estimate. It has been proposed, for example, as an explanation for experiments in which subjects estimate the position of their arm after having performed a movement in the dark (Wolpert et al., 1995).

Further evidence for the idea that the nervous system takes body dynamics into account comes from anticipatory postural adjustment and grip force modulation. Rapid arm movements, for example, are usually preceded by adjustments in the rest of the body that mitigate the effect of upcoming interaction torques (Belenkii et al., 1967). Also, when moving their arms while grasping an object in precision grip, subjects make anticipatory adjustments to grip force that cancel the effect of load forces arising due to self-generated movement (Flanagan and Wing, 1997). This grip-force/load-force coupling can be explained in a framework incorporating both inverse and forward models as described above (see paragraph 2 in section 2.2.1). Here, the prediction of load force by the forward model compensates for the delay in sensory detection of the load, which would be too long to prevent slip. Differential neural activity in the cerebellum during anticipatory grip force modulation has been suggested as evidence for the existence of forward models in the brain (Wolpert et al., 2003).

Neurophysiological support for forward models was presented in experiments investigating the

fact that self-produced tactile stimuli are perceived as less ticklish than the same stimuli generated externally (Blakemore et al., 1998). Here it was found that a part of the cerebellar cortex was selectively inhibited by self-produced movements that resulted in tactile stimulation, but significantly activated by externally produced stimuli. The authors reasoned that the predicted sensory consequence of the motor command (predicted tactile stimulation) is used to cancel the percept of the actual tactile stimulus.

Because they affect motor output only indirectly, evidence for forward models is more difficult to establish than for inverse models. This is crucial, because for output prediction every model-based controller can in theory be replaced with a direct control scheme that has exactly the same input-output function (Mehta and Schaal, 2002). Direct controllers map sensory signals to motor commands without the intermediate step of internal models and have been suggested as a model for motor learning in the cerebellum (Barto et al., 1999). Because of their equivalence, none of the studies suggesting the involvement of internal models mentioned above can rule out the use of a non-model based controller for output prediction. Forward models can however be used to fill in missing sensory input, and among a set of different control schemes were shown to best explain the performance of subjects in a pole-balancing task with visual blank-outs (Mehta and Schaal, 2002). The same experiments allowed for further distinction between different use-cases for forward models. The Smith predictor, for example, was rejected formally for control of mechanically unstable systems, of which human balancing is just one example, as it would provably become unstable itself. The most successful model was similar to the Kalman filter proposed for explaining the performance of subjects estimating their arm position after movements in the dark (Wolpert et al., 1995). However, Ostry and Feldman (2003) note that the same data can be explained by an alternative hypothesis that does not involve an internal model.

There is no doubt that human motor control features predictive or anticipatory mechanisms that can detect and compensate for the effects of self-induced motion or novel sensorimotor environments. It is a valid question, though, whether these are implemented in the nervous system as internal models, that is to say detailed and accurate predictive simulations of the body and/or the external world. For example, even a simple feedback mechanism can be described as a predictor if the target state is interpreted as both motor command and expected future state. Also, even comparatively simple animals such as crickets and other insects exhibit anticipatory behaviours and can distinguish between self- and externally produced stimuli (Webb, 2004). Evidence suggests that this can often be achieved through simple sensory gating by an appropriately delayed motor signal. In other words, sometimes a simple scaling (and delaying) of the motor signal provides an accurate enough estimate of its sensory consequence.

2.2.2 The equilibrium-point hypothesis

An alternative to force and internal model based theories of motor control is the equilibrium-point hypothesis. Its origins are found less in formal engineering than in the history of neurophysiological research on muscle and reflex dynamics.

Posture-movement paradox

As early as 1926, Wachholder and Altenburger wondered if humans were able to relax their muscles at different joint positions. It was already known that muscles exhibited spring-like properties, and easy to see that two muscles acting against each other could be in equilibrium at a single position only. By confirming that muscles are indeed relaxed at different positions, it could be concluded that the nervous system modified the spring-like properties of the muscles during voluntary movement. This was in line with Sherrington's finding of reciprocal innervation, that is the inverse proportional activation of antagonist muscle groups, which explained why activation of a muscle does not trigger a resisting stretch reflex in its antagonists. It also supported his idea of reflexes as tunable mechanisms rather than hardwired responses, and his general view of motor control via modulation of reflex parameters. Holst and Mittelstaedt (1950) addressed a similar problem, namely the posture-movement paradox of how voluntary movement to a new position can occur without triggering resistance from posture-stabilising reflexes. Their solution, the reafference principle, proposed that an efferent copy of the motor command changes the reference point relative to which sensory feedback is measured in the posture-stabilising action. This means that stabilising reflexes are re-addressed to a new position, rather than simply inhibited. The physiological basis of this resetting mechanism was demonstrated in experiments by Matthews (1959), in which he showed that stimulation of the spinal cord in the decerebrate cat was associated not with changes in muscle length, activation or force, but with a constant relation between force and length. Muscles would produce force as a function of length along a characteristic non-linear curve that was shifted by the level of stimulation (invariant characteristic). In other words, muscle and reflexes together acted like a non-linear spring whose setpoint was determined by descending inputs. The equilibrium-point (EP) hypothesis was established when Feldman demonstrated similar torque-angle characteristics in elbow movements by non-decerebrate humans, and suggested that central motor commands can change a component (λ) of the threshold length beyond which a muscle becomes activated (Feldman, 1966). The posture-movement paradox was thus resolved. In the EP framework, a change in muscle activation thresholds means that the current position becomes a deviation from the newly specified one, and the posture-stabilizing reflexes will ensure that the system moves to the new target.

The λ-model

To elaborate, the EP hypothesis suggests that when a motor system is at rest, the α-motoneurons innervating the relevant muscles are in a state that is just below their threshold for activation. This is confirmed by the observation that EMG signals before and after a movement are zero, but that muscles become immediately activated when perturbed externally. The observation of subthreshold states at any desired pose implies that muscle activation thresholds are reset in voluntary movements. The proposed motor control scheme is thus one of threshold control. It distinguishes itself from the force-control hypothesis by the fact that it implies a positional coordinate frame. This is because α-motoneurons receive not only the descending motor commands λ, but are also the target of muscle length dependent feedback from the tonic stretch reflex. Therefore, a muscle activation threshold specifies the length of a muscle below which it is silent. If the muscle is stretched beyond the threshold length, the tonic stretch reflex will activate it in proportion to the difference between actual and threshold length as sensed by proprioceptors. Activation of the

muscle in turn will produce contraction, thus bringing its length closer to the threshold value. The continuous interaction of neural and muscular elements will thus drive the system towards a state of minimal activation. However, since the body is usually exposed to external forces (gravity, environment interaction), it will typically reach equilibrium where muscle force equals external load, that is not necessarily at zero activation or exact threshold length. A distinction is therefore made explicitly in the EP hypothesis between the virtual equilibrium as determined by muscle thresholds, and the actual equilibrium at which the system comes to rest.

The EP hypothesis has been extended to account for many features observed in natural limb movements. To explain the coordination of multiple muscles for simultaneous control of position and stiffness, for example, it was suggested that the λ command could be formed by a combination of two components: a reciprocal signal that moves the thresholds of antagonist muscles in the same direction, and therefore activating one, but relaxing the other muscle; and a co-contraction signal that moves the two thresholds in opposite directions, leading not to a change in joint position but a stiffening of it (St-Onge and Feldman, 2004; Feldman, 1993).

To produce smooth voluntary movements it was suggested that central commands specify simple monotonic (e.g. ramp-shaped) shifts of threshold lengths. In other words, instead of specifying a new virtual equilibrium position directly, a virtual trajectory is used to move smoothly from the current to the desired position. The implication is that any point along the trajectory should be a stable equilibrium. This has been confirmed in experiments in which the hand position of subjects was perturbed in the middle of an arm movement (Won and Hogan, 1995). Measurements showed that resisting forces were directed not at the target, but towards the intended trajectory.

The λ-formulation of the EP hypothesis has also been successfully employed as a tool for studying the problem of redundancy (Balasubramaniam and Feldman, 2004), vertical posture stability (Micheau et al., 2003), human walking (Guenther and Ruder, 2003), sense of effort (Feldman and Latash, 1982), and in relating kinematics, dynamics and EMG patterns in point to point reaching movements (Feldman et al., 1990; Latash, 1993; Gribble et al., 1998).

Criticism and clarifications

A crucial proposition of the EP hypothesis is that no inverse dynamics model is required to calculate the EMG signals or forces required for goal directed movements. Instead, these variables emerge from the spring-like dynamics of the combined muscle-reflex system. In other words, by changing the lambda component of the stretch reflex, motor commands set up an equilibrium point (or trajectory) and a force field around it. Movement, in this framework, is simply the relaxation of the system towards the specified attractor. The often-used mass-spring analogy for describing muscle-reflex dynamics, when taken too literally, has led many to wrong conclusions about the validity of the EP hypothesis. It is therefore worth to clarify some of the more subtle points of the hypothesis here.

One important point is that central commands modify the equilibrium position, but they do not do so exclusively. For example, velocity-dependent proprioceptive signals and inter-muscle reflexes also terminate on motoneurons and affect their thresholds. Therefore, the central contribution to threshold values should not be considered an internal representation of the motor goal — it is just the means by which the nervous system can produce movement. Feldman stresses that the target

of a movement is specified in physical variables relevant to the task and environment and does not need to be represented in other internal coordinates (Feldman and Latash, 2005).

The λ-model suggests that smooth movements are created by simple monotonic EP shifts. This was questioned, however, by Gomi and Kawato (1996), who estimated stiffness and damping values of the arm from measured perturbations and used it to calculate the shifts in virtual equilibrium necessary to produce the observed movements. They concluded that this shift is not monotonic but follows a rather complex N-shaped trajectory. This suggested that even in the EP hypothesis, arm dynamics have to be accounted for in planning the correct EP trajectory. However, the experiment assumed that force production by the muscles was a linear function of position, which constitutes a major simplification of the motor system. Gribble et al. (1998) demonstrated that when an adequate muscle model is used instead, simple monotonic EP shifts are in fact sufficient to explain Gomi and Kawato's data.

Other oversimplifications, such as the assumption that the dynamic characteristics of the motor system are the same during movement and at rest, have been used in claims that the EP hypothesis incorrectly predicts values of damping (Gomi and Osu, 1996). Feldman pointed out, though, that when the damping properties of muscles and velocity-dependent feedback components are taken into account the data is in fact consistent with the theory (Feldman et al., 1998; Gribble et al., 1998).

Another controversy regarding predictions of the EP hypothesis concerns the level of joint stiffness during voluntary movements. It has been suggested by several authors that the EP hypothesis requires relatively high levels of joint stiffness (or large mechanical and neural feedback gains) to generate forces large enough to account for fast movements (Kawato, 1999; Wolpert et al., 1995). The observation that stiffness is instead rather low (Gomi and Kawato, 1996), was then argued to conflict with the EP hypothesis (Popescu et al., 2003). However, as Feldman pointed out (Feldman and Latash, 2005), the EP hypothesis has in fact no unique requirement for the levels of stiffness or damping. It is only restricted by physical laws according to which a stable system has to reject perturbations with stiffness and damping coefficients that are larger than those of the external load. The same physical laws equally apply to the force control hypothesis, however. Claims that it requires lower stiffness levels than the EP hypothesis are again the result of misrepresenting major properties of the neuromuscular system (for a more detailed analysis see Feldman and Latash, 2005). Difficulties in reliably measuring the stiffness of a moving system mean that conclusive experiments comparing predicted and actual stiffness have yet to be conducted for both the force hypothesis as well as the EP hypothesis. However, it has been shown recently that an EP model in conjunction with a realistic muscle model can produce fast and smooth single joint movements with EMG signals resembling those measured in human subjects (Kistemaker et al., 2006).

Another argument brought against the EP hypothesis concerns the property of equifinality, that is the assumption that with constant command signals the system should always settle at the same equilibrium point after transient perturbations have ceded. The finding of positional errors in arm movements as the result of coriolis forces[3] seemed to violate this principle (Lackner and Dizio,

[3]The coriolis force, like the centrifugal force, is an example of *pseudo forces*, which result from the effect of inertia in a rotating frame of reference. They can be observed, for example, when movements are carried out on a rotating platform.

1994). As these forces are velocity-dependent they should be transient and not affect the final EP. However, this assumes that control signals remain constant. It can be argued, though, that coriolis forces belong to a class of perturbations that are actively opposed by changes in motor commands such as to ensure stability at the expense of positional error (Feldman et al., 1995, 1998). Even in the simple case where external forces are absent, natural variability in non-central components of muscle activation thresholds mean that equifinality cannot be guaranteed. Only on average will the system settle to the same EP if all other things are equal. Observation of violations of equifinality in healthy humans (Feldman, 1979) or the λ-model are therefore consistent with the EP hypothesis.

The fact that subjects can adapt their movement strategy to external force fields (see above) is often claimed to support the idea of force control and internal models. Although they provide a possible explanation, an alternative approach based on the λ-formulation of the EP hypothesis has been demonstrated to achieve load adaption without the need for inverse dynamics calculations or coordinate transformations between positional error and correcting forces (Gribble and Ostry, 2000). Anticipatory grip force-load force modulation, the most cited evidence for internal models, has also been successfully simulated in a model based on threshold control (Pilon et al., 2007). Again, no calculation of required forces or EMG signals was necessary.

One of the proposed roles for internal forward models is their use in a control scheme that operates on predicted rather than actual sensory feedback. This, it is argued, mitigates the detrimental effects of delays on the stability of the motor system. Such concerns about the destabilising effect of sensory delays might not be justified, however. Firstly, intrinsic viscoelastic muscle properties generate instantaneous stabilizing forces in response to changes in position or velocity, a mechanism termed preflex (Brown and Loeb, 2000). Also, use of both position and velocity feedback, as is the case in sensory input to the motoneurons, can help to minimise instabilities caused by delays (Ali et al., 1998). A model incorporating both preflexes as well as position and velocity feedback was demonstrated to be sufficiently stable for arm movements with reflex delays within the empirically observed range (St-Onge et al., 1997). More recently, (Pilon and Feldman, 2006) have emphasised that the central components of threshold modulation are best viewed as feedforward commands that influence the state of the reflex system prior to activation of the muscles. Consequently, it contributes to muscle activation immediately, not just after an initial lag period. Their model confirmed that threshold control of fast arm movements is indeed stable for proprioceptive delays that cover both spinal as well as transcortical reflex loops.

2.2.3 Summary

The force control hypothesis offers mathematical constructs that provide plausible explanations for many observed aspects of human movements, and its assumption that the nervous system implements internal inverse and forward models is consistent with a number of experimental studies. However, it has failed so far to resolve the posture-movement paradox, and it is in conflict with well-known EMG patterns. The possibility of completing the inverse transformation from desired outcome to required motor commands, including non-linear neural and musculoskeletal dynamics, still has to be demonstrated. Meanwhile, simplified representations of the motor apparatus limit confidence in its predictions. Neurophysiological data is often ambiguous and behavioural

evidence, such as force field learning or anticipatory behaviour, can equally be explained by alternative theories that do not require internal models.

The equilibrium-point hypothesis offers an alternative that is grounded in neuromuscular physiology, solves the posture-movement problem and correctly reflects observed EMG signals. It has so far resisted attempts at falsification (most of which are based on misinterpretations of the theory or overly simplified models) and has provided alternative solutions to many problems in motor control thought to require internal models. While the EP hypothesis cannot currently be rejected, challenges remain. Accurate stiffness predictions and validations, as well as experimental tools for measuring the hypothesised control signals (motoneuron threshold offsets) are still lacking. Also, potential mechanisms are needed to explain how these control signals are produced for a given task and context. It is hoped that this thesis will contribute towards an understanding of how control signals in the EP theory depend on the desired movement and the dynamics of the underlying musculoskeletal system.

2.3 Embodied cognition

The two conflicting motor control hypotheses reflect a broader controversy in the field of cognitive science. This is the question of whether a computational or a dynamical perspective is better suited for studying cognitive agents.

Computationalism

According to traditional views, cognition and behaviour are best understood in a computational framework. The physical symbol system hypothesis (Newell and Simon, 1976), for example, claims that cognitive agents are essentially problem solvers that algorithmically manipulate internal representations of the world via operations on static symbol structures. Such formal systems were claimed to have "the necessary and sufficient means for general intelligent action" (Newell and Simon, 1976). The theory assumes that the world can be divided into discrete objects, actions and states, each of which can be referred to by a symbol. The nature of variables describing such systems is hence discrete and its basic operations are discrete state transitions. Time is represented in this theory only in so far as the system is updated at certain points in time. Events thus have a temporal ordering, but there is no temporal continuity upon which a system's behaviour can depend. What matters is not *when* the system occupies a certain state, but *which* states it passes through and in what order. The computational view focuses more on the internal structure of the system's overall state (e.g. syntax) than on how it is achieved. Proponents of this theory were mainly concerned with abstract thought and rational problem solving. Most work was aimed at explanations of isolated, high-level and disembodied cognitive faculties, such as decision making, knowledge representation or logical reasoning. While the approach led to important advances in computer science (e.g. expert systems and logic programming), its limitations were recognised both on philosophical grounds and whenever attempts were made to apply it to robots acting in the real world. Theoretical issues identified include but are not limited to the frame problem (Dennett and Pylyshyn, 1987), symbol grounding (Harnad, 1990), and the binding problem (Revonsuo and Newman, 1999). With respect to robotics, it was recognised that many adaptive skills, such

as balance, locomotion or object discrimination, do not always require symbolic processes and sometimes are more easily explained and reproduced without them (Brooks, 1990).

Embodiment and dynamicism

A shift in perspective followed, in which the importance of embodiment and dynamicism were emphasised in explaining the adaptive behaviours of agents in continuous coupling with their environment. Behaviour-based robotics (Brooks, 1990), for example, was aimed at understanding all aspects of simple, but complete adaptive behaviours instead of isolating individual components or aiming for general intelligence. It attempts to avoid unrealistic assumptions about the agent or its environment by requiring a robot to interact in real-time with the real world. The approach opposes the computationalist assumption that the brain constructs internal representations of the world, which a homuncular subsystem acts upon. Instead, it claims that for a situated and embodied agent "the world is its own best model" (Brooks 1995), and thus advocates the primacy of perception over internal models. The concept of embodiment refers to the idea that an agent's behaviour depends non-trivially on the unique perceptual and motor capabilities that its particular body affords (Thelen et al., 2001; Beer, 2009). The material properties and morphology of the motor apparatus and its sensory interface both empower and constrain the interactions that an embodied agent is capable of. Notions like morphological computation (Pfeifer and Iida, 2005), cheap design (Iida, 2005), and passive dynamics (McGeer, 1990) further emphasise that the physical properties of an agent's body can be adaptive in the sense that they make behaviours more efficient and robust or simplify its control. Examples of this approach include passive dynamic walkers that exploit gravity for locomotion without actuators and control systems (McGeer, 1990); a fish-like robot that exploits body shape to navigate in three dimensions despite being equipped only with a one degree of freedom actuator (Pfeifer and Iida, 2005); and a robotic hand that grasps arbitrary objects without visual analysis or control by using elastic tendons and deformable fingertips (Pfeifer and Iida, 2005).

The shift towards an understanding of behaviour as the continuous unfolding over time of the interaction between a physical agent and its environment necessitates a corresponding language to describe it. Computationalism deals with discrete ordered events and algorithms only, and cannot account for the real-time dynamics that many behaviours critically depend on. The Dynamical Hypothesis in cognitive science (Gelder, 1997) proposes instead that cognitive agents instantiate dynamical systems (nature hypothesis) and that they are therefore best understood by using the language of dynamical systems theory (knowledge hypothesis). Dynamical systems describe the evolution over time of quantitative variables according to laws that are usually expressed as differential or difference equations. In contrast to the language of computation, it can thus be used to describe any physical process, including the continuous interaction between an agent's brain, body and environment. A dynamical systems approach to behaviour typically involves the modelling of agent and environment as coupled dynamical systems and/or the analysis of such systems in terms of quantitative and qualitative properties of the resulting state space. Particular behavioural features observed experimentally are often explained geometrically by reference to stable and unstable limits sets and basins of attraction, or changes to these dynamical entities as the system's parameters are varied (bifurcations)[4].

[4]For a comprehensive overview of analytical and geometrical methods in nonlinear dynamics see Strogatz (1994)

A cornerstone of the dynamical approach to motor control is the Haken-Kelso-Bunz (HKB) model (Haken et al., 1985). It is based on experiments by Kelso (1984) in which subjects were instructed to produce bimanual tapping movements in synchrony with a pacing metronome. As the desired frequency was slowly increased, several interesting features could be observed in the pattern of coordination between the two hands: if subjects start with an anti-phase pattern they spontaneously switch to in-phase movements at a certain critical frequency; when the frequency is subsequently decreased, subjects maintain the symmetrical pattern and do not switch back to anti-phase (hysteresis); such a transition is not observed when subjects start in the symmetric mode. In the HKB model it was shown that these observations could be derived directly from a simple differential equation that describes the change in relative phase between the hands as a function of frequency (which serves as a control parameter). Analysis confirmed, and the equation was devised so that the two different patterns corresponded to the only fixed point attractors of the system. Bifurcation analysis further showed that both attractors are stable at low frequencies (bistability), while at the critical frequency a phase transition occurs beyond which only the in-phase pattern is stable. The observed hysteresis and absence of transitioning when starting with in-phase movement is explained by the fact that the system is already in a stable equilibrium which is not affected by changes in the frequency parameter. In the HBK model, the equation describing these phase dynamics were then derived from the coupled dynamics that describe individual limb oscillations. It thereby not only provided a complete quantitative description of the observed phenomenon, but also provided an explanation in terms of the relation between the two levels of description.

The work by Thelen and colleagues on Piaget's classic A-not-B task (Thelen et al., 2001) can be regarded as a second milestone of the dynamical systems approach. In this task, 7-12 months-old infants, who have repeatedly managed to uncover a toy at location A, continue to reach for it even when they have watched the toy being hidden in a different but nearby location B. Traditional explanations refer to the infant's incomplete or fragile object representations, or problems with spatial coding, as explanations for this error. Thelen et al., in contrast, were less interested in what infants seem to know than in how they behave. In their dynamic field theory of infant perseverative reaching they demonstrated that the A-not-B error can be understood as the result of the coupled multiple timescale dynamics of actions such as looking, planning, reaching and remembering. The work showed that the same language could be used to describe the time-evolution of both cognitive processes and bodily movement, and that only the history of interactions between the various subsystems could explain the observed behaviour. The idea of cognitive embodiment was further supported by findings that perseveration is tightly linked to developing reaching abilities and that the error disappears when infants adopt different poses between the A and B trials. Smith and Thelen (1993) also used a dynamical systems approach to study the development of motor skills in infants. They demonstrated that the disappearance and subsequent reappearance of kicking behaviour in infants can be explained simply by the fact that their legs become heavier. As the weight increases, the kicking behaviour ceases to be a stable oscillatory pattern. When the infant's muscles grow stronger, however, they compensate for the weight gained. In other words, an infant's leg weight operates as a control parameter whose change can lead to a bifurcation that results in qualitatively different motor behaviours.

---

and Abraham and Shaw (1992).

Evolutionary robotics

Embodiment and dynamicism often play a strong role in evolutionary robotics (ER) experiments (Nolfi and Floreano, 2000). Here, algorithms inspired by natural evolution are used to automatically find robot controllers (Floreano and Mondada, 1994), and sometimes morphologies (Harvey et al., 1994), that maximise a given fitness function. Starting with a random population of candidate robots, individuals are assigned a fitness value based on their performance in the desired task. In a process of selection, this fitness measure determines how variations ("offspring") of the better performing individuals replace the worse ones. Variability is introduced by applying operations such as mutation and recombination to the robot instances. Over many iterations of selection and variation, the population of robots is hoped to converge towards maximum fitness.

The main motivation for an ER methodology is that human intuition often fails to anticipate or comprehend the complex interactions required in a given task between a robot's brain, body and environment. A design approach to robotics thus easily introduces unnecessary or wrong assumptions about the kind of control mechanisms or robot morphologies needed. Such preconceptions can be minimised if aspects of an agent's "brain" and body are allowed to evolve, instead of being specified by the experimenter. By not restricting the kinds of environment interactions that a robot can engage in, one often finds that evolved solutions can exploit unforeseen properties of the body or the environment that allow for simpler control mechanism than those an engineer might have synthesised. This was strikingly demonstrated by Harvey et al. (1994), who evolved continuous-time recurrent neural networks (CTRNNs) (Beer, 1995b) for real-time control of a camera equipped gantry robot. By using an active exploration strategy, the evolved networks were able to distinguish between triangular and rectangular targets using only two pixels (or receptive fields) of the camera's video image.

Beer (1995a) demonstrated the strength of a dynamical and embodied approach by evolving and analysing CTRNN controllers that produce locomotion behaviour when coupled to a six-legged simulated robot. Although successfully evolved networks showed no significant functional organisation, a state space analysis offered insight into the specific dynamics that gave rise to different walking patterns. Specifically, Beer found limit cycles whose projections into motor space caused single legs to rhythmically alternate between stance and swing motion in a fashion appropriate to walking. The limit cycles were produced by periodic bifurcations that in turn were triggered by the current state of the leg. If the leg was in the stance phase, a bifurcation would lead to the appearance of an attractor, the relaxation to which produced a swinging motion. Conversely, in the swing phase a different bifurcation would produce an attractor that pulled the system back into the stance phase. The parameter changes necessary for these bifurcations to occur were produced by sensory signals that indicated whether or not a leg was in contact with the ground. The observed walking behaviour, therefore, could not be attributed to the agent's brain, body or environment individually, but only to the coupled system as a whole. In a series of experiments on minimally cognitive behaviours (Beer, 1996; Slocum et al., 2000), Beer showed how the same approach can be applied to study cognitive performances such as visual orientation, object recognition, selective attention, perception of self-motion, planning of sequential behaviours and learning.

2.4 Approach in this thesis

The methods used in this thesis to model and analyse the interaction between muscles and neural control, as well as the kind of questions asked, are both examples of a dynamical and embodied view of motor control. Firstly, the thesis is concerned with the equilibrium-point hypothesis. This hypothesis is by nature dynamicist, as it suggests that *control* of motor behaviours is done by changing parameters of the coupled neuro-musculoskeletal system, while the *execution* of a motor behaviour is simply the relaxation of its dynamics towards a stable equilibrium. Secondly, the tools used for describing and analysing the models in this thesis are those common to the dynamical systems approach. The behaviour of skeleton, muscles and neural control in this thesis are simulated as coupled dynamical systems described by differential equations. The behaviour of these systems is analysed in terms of the long-term (steady-state) and short-term (transient) features of its phase space. It is shown, for example, that the interaction of antagonistic muscles can produce stable as well as unstable equilibrium points in joint space. Properties of this equilibrium are studied as parameters of the system are varied. Transients, that is individual trajectories that have not yet settled to an equilibrium, are compared to those observed in natural human arm movements.

One aim of this thesis is to identify the kind of control signals that are required to generate natural goal-directed arm movements. An important finding is that this depends crucially on assumptions about the material properties of the muscles. A simplified model, for example, is shown to predict different control signals than a more realistic model. In this way the thesis highlights the importance of embodiment when studying the dynamics of motor control. It also employs evolutionary robotics techniques. Throughout the thesis, genetic algorithms are used to evolve the neural systems controlling individual muscle activations. In most experiments, the neural activity of the stretch reflex is described simply by a lumped model in which muscle activity is calculated directly from a linear combination of various feedback components. This is in essence an optimisation of the standard (λ-) model of the equilibrium-point hypothesis for the task at hand. In other experiments, however, dynamical neural networks are evolved as reflex controllers. These experiments, which extend the standard lambda-model, explore the forms of control possible when assumptions about its structure are relaxed.

Chapter 3

Muscle dynamics

"Behaviour is regular, but there are no regulators" (J. Gibson)

3.1 Introduction

A distinguishing feature of all animals is their ability to move and interact with their environment in complicated and goal-directed ways. The dexterity, robustness and efficiency of movements by even the simplest animal easily surpasses the abilities of current robots. In mammals, skeletal muscles are the sole initiators of movement. They transform energy into motion through contraction and transmit the resulting forces to the skeleton. Hence, to understand the principles of animal movement it is necessary to study the mechanical properties and dynamics of force production by the muscles, their interaction with the skeleton as well as their neural coordination. In this chapter I will use the Hill-type muscle model in conjunction with a physical simulation of a planar two-jointed arm as a tool for studying natural movement dynamics.

Skeletal muscles are different from current robotic actuators in that the force they produce is not simply a linear function of its input. The non-linear relationship between muscle force, length, velocity and activation, a result of intrinsic material properties, play a crucial role, for example, in fast but precisely damped movements or implementation of so-called pre-flexes, a zero lag resistance to perturbations (Brown and Loeb, 2000). The importance of an *ecological balance* between material properties of the body, its morphology and control when interacting with an environment has received much attention recently (Pfeifer, 2007). Through *morphological computation*, agents, whether natural or robotic, can exploit physical dynamics to achieve higher efficiency and simplified control, while maintaining a sufficient level of behavioural diversity (Pfeifer and Iida, 2005). Gribble et al. (1998) e.g. has shown that the non-linearities of biological muscles can simplify the control signals necessary to generate smooth shifts in the position of an arm. He showed that if too simplified a muscle model is used, complex N-shaped inputs signals are needed to drive an arm linearly from one position to another. By including the non-linear relationships on the other hand, the same movement can be achieved with a simple monotonic ramp signal.

In this chapter the material properties of antagonistic muscles are studied for their ability to create an equilibrium-point at the joint level that allows for control of position, stiffness and velocity. This has been demonstrated before (e.g. Kistemaker et al. 2007a). Here, however, a muscle model is studied that is at the same time more complicated than abstract lumped models (Barto et al., 1999), but simpler than those aiming for high levels of biological accuracy (Kistemaker et al., 2007a). This intermediate level was chosen, because the goal of this chapter is not primarily to reproduce human movements quantitatively, but to identify those components of a muscle model that are fundamental for achieving flexible control of a joint's equilibrium position. Care is taken, nevertheless, to ensure a reasonable level of biological relevance. To this end, the steady-state and transient behaviour of various muscle models is analysed and compared to natural human movements. The results determine whether the chosen level of model detail is sufficient for studying the assumptions and implications of the EP hypothesis in the next chapter.

3.2 Methodology: Modelling skeletal muscle

The following sections provide an overview of the anatomy and physiology of skeletal muscles and explain their force-generating mechanism. The well known Hill-type muscle model (see e.g. Zajac, 1989) is then introduced as a tool for studying their dynamics under open-loop control.

3.2.1 Muscle physiology

Muscles create motion by transmitting contraction forces to the skeleton via tendons. Their structure is hierarchical. The body of a muscle, surrounded by connective tissue called epimysium, consists of many bundles (fascicles) of muscle fibres. Hundreds of thousands of these contractile muscle cells are controlled by about a hundred motor neurons. A single motor neuron along with all the muscle fibres it innervates is called a *motor unit*. Muscle fibres themselves are composed of many *myofibrils*. The latter contain the units ultimately producing contraction, the *sarcomeres*. Large numbers of these are connected in series through non-contractile components from which they are separated by so called Z disks. From the disks thin filaments containing actin monomers project inward, while thick filaments, made from myosin molecules, float in the middle of the sarcomere. It is the interaction between the thick and thin filaments that generate contraction of the muscle through a mechanism known as the "sliding filament hypothesis" (see below).

3.2.2 From action potential to force output

Every contraction starts with the transmission of an action potential from the motor neuron to the muscle fibre via a chemical synapse called the end-plate. The action potential then travels along the muscle cell membrane and will eventually trigger the release of calcium from an internal compartment (see figure 3.1). The free calcium ions can now bind to a troponin molecule, which in turn leads to a conformational change in the connected tropomyosin molecule covering the actin filament. A now exposed binding site allows the head part of the myosin molecule to bind to the actin filament and form a so-called *cross-bridge*. With the cross-bridge in place, the myosin head bends and performs the *power-stroke*: it pulls the actin filament in the direction of increased

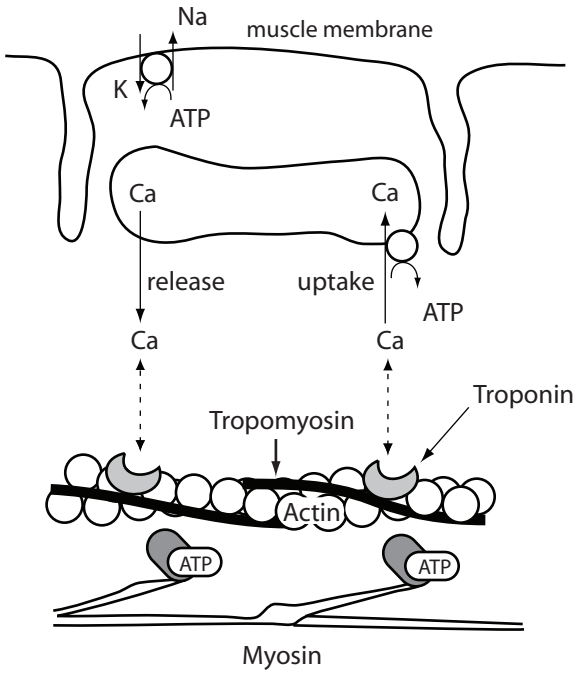

Figure 3.1: Illustration of the sliding filament hypothesis. Calcium released through an action potential triggers ATP powered actin-myosin cross bridge cycling.

overlap, thereby shortening the muscle fibre. During the stroke, the myosin head releases ADP and phosphate. This allows for the binding of ATP instead, which leads to the termination of the stroke. Energy gained from the breakdown of ATP to ADP and phosphate is used to return the myosin head to its initial position. This process is repeated, leading to asynchronous cross bridge cycling at many different binding sites simultaneously. At the end of the action potential, calcium is pumped back into the compartment, actin-myosin binding sites are once more covered by tropomyosin, and the muscle fibre relaxes.

3.2.3 The Hill-type muscle model

One of the most widely used models of biological muscle is the so-called Hill-type model (Zajac, 1989). Here, muscles are treated as input-output systems comprising a contractile element in parallel and in series with a varying number of springs and viscous dampers. A common configuration is shown in figure 3.2.

The model behaviour is described by experimentally observed relationships between the different kinetic and kinematic variables in the form of constitutive relationships. Specifically, these idealised lumped elements describe empirically how a muscle's force output depends on its length, velocity and activation. In this way it differs from models that start from first principles, such as the Huxley-Zahalak equation, which quantitatively models the action-myosin interaction (Zahalak, 1981). The Hill-type model was chosen here because it captures key features of real muscles while computationally being relatively cheap. The following section will explain in detail the different constitutive relationships and their implementation.

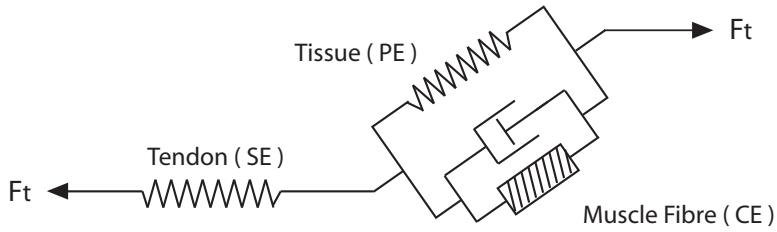

Figure 3.2: Musculotendon unit: a tendon (or series elastic element, SE) is connected in series with a muscle. The latter consists of an active contractile element (CE), a passive elasticity (PE) and a viscous damper.

3.2.4 Activation dynamics

Responsible for the release of sufficient Ca^{2+} to enable the sliding process of thick and thin filaments is an action potential travelling along the surface of a muscle fibre. A single action potential will not allow for all possible cross-bridges to form and hence will produce only relatively little contraction. Consecutive action potentials however can add to the number of active cross bridges if they occur before the re-uptake of Ca^{2+}. Thus, the amount of force produced by a muscle is proportional to the frequency of action potentials. Calcium release and its subsequent uptake are two separate processes and lead to different time courses in the rise and fall of active tension during muscle contraction. In the muscle model, excitation-activation (a) dynamics limit the time course of force production. Effectively, activation a implements a filter on neural excitation (u), interpreted as firing rate, with different activation and deactivation rates:

$$\dot{a} = f_a(a,u) = (u-a)/\tau^\star \tag{3.1}$$

where $\tau^\star = \tau_{ac} = 0.04s$ if $u \geq a$ and $\tau^\star = \tau_{de} = 0.07s$ if $u < a$.

In reality, the rates of calcium release and re-uptake themselves have been shown to depend on stimulation frequency, muscle fibre length and velocity (Brown et al., 1999). Also, different types of muscle fibres (fast and slow twitch) show different rates of activation and deactivation. Here, for simplicity, time constants are assumed to be constant throughout a movement, and represent the lumped effect of a range of different fibre types. Also, where muscle parameters are optimised in this thesis, these constants are excluded. This is a limitation of the work presented here, and could be addressed in future work. The fixed rates specified above fall into the midrange of reported values. Activation rates as low as 10–20 ms and deactivation rates as high as 200 ms have been used in the literature (e.g. Pandy et al. 1990; Pilon and Feldman 2006).

3.2.5 Ca^{2+} dynamics

Another, often neglected, aspect of Ca^{2+} dynamics is that muscle fibres become more sensitive to Ca^{2+} as sarcomere length increases (Konhilas et al., 2002). In other words, force production by the muscle is not only dependent on the amount of calcium released as a result of stimulation, but also on muscle length. In this thesis we modelled this aspect of Ca^{2+} dynamics following the approach detailed in (Kistemaker et al., 2007a), itself based on (Hatze, 1981). In this new scheme,

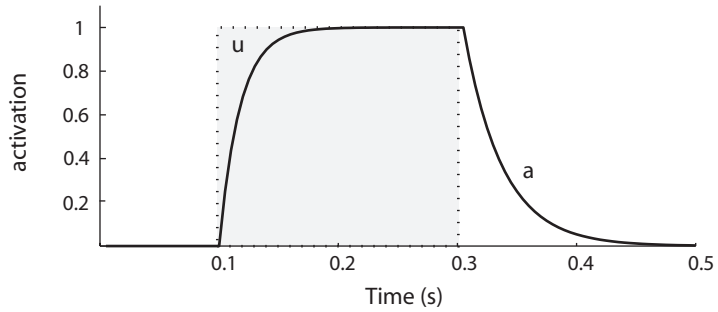

Figure 3.3: Muscle activation dynamics. Muscle activation *a* is a low-pass filtered version of neural input signal *u* with different activation and de-activation rates.

the activation level *a*, described above, is now interpreted as the free Ca^{2+} concentration resulting from muscle stimulation. The final active state q of the muscle, however, that is the amount of Ca^{2+} bound to troponin, now depends on both *a* as well as on muscle length via ρ:

$$\rho = c\eta\frac{k-1}{k-\tilde{L}^M}\tilde{L}^M \tag{3.2}$$

$$q = \frac{q_0+(a\rho)^3}{1+(a\rho)^3} \tag{3.3}$$

where c, η, k and q_0 are constants. The effect of calcium dynamics on the muscle's force-length relationship is shown in figure 3.4. Mechanically, the added Ca^{2+} sensitivity adds to the stiffness of the muscle at lower activations, and captures the experimentally observed shift of its optimum length (Balnave and Allen, 1996; Roszek et al., 1994).

3.2.6 Active force-length relationship

The number of cross bridges formed during a contraction, and hence the force produced, not only depends on the exposing of binding sites through sufficient calcium release, but also on the spatial overlap of thick and thin filaments. As a muscle is stretched, this overlap decreases until no force can be generated when there are no adjacent filaments. Conversely, as a muscle shortens overlap increases and more force can be generated. Beyond the mid-region however, actin filaments start interfering with each other until eventually they are pressed against the Z disks. Increasingly this will oppose the contractile force until at this extreme force can no longer be generated either.

The region where active muscle force can be generated is usually modelled as $0.5L_0^M < L^M < 1.5L_0^M$. Here L_0^M, the optimal muscle fibre length or resting length, is the length at which active muscle force reaches its maximum $F^M = F_0^M$. The following function describes the active generation of force at different muscle lengths:

$$\tilde{F}_a^M(\tilde{L}^M) = 1-(\frac{\tilde{L}^M-1}{0.5})^2 \tag{3.4}$$

For the rest of this thesis variables decorated with a tilde are normalised. Here it means $\tilde{L^M} = L^M/L_0^M$ and $\tilde{F^M} = F^M/F_0^M$. A superscript M will refer to a muscle variable, and a superscript T to the tendon. Plots of the active force-length relationship are shown in figure 3.4. It is usually assumed that activation level *a* scales the active force curve, but not the passive.

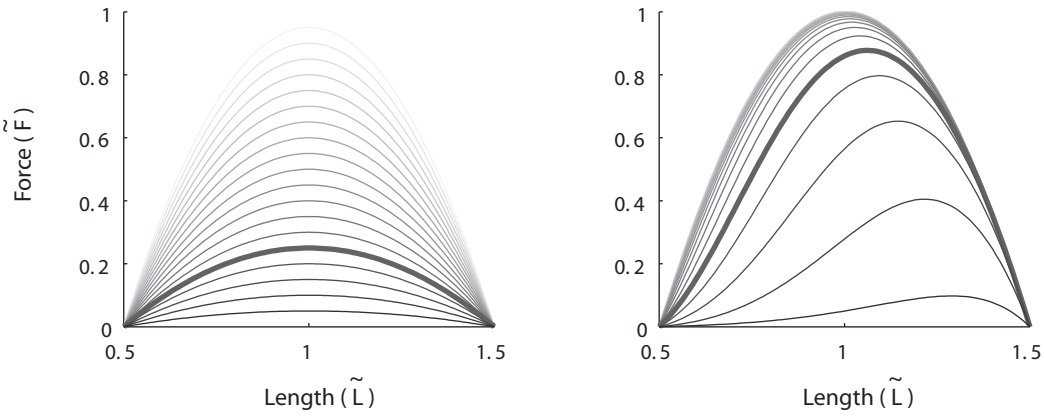

Figure 3.4: Active force-length relationship for muscle activations from 0.05 to 1.0 in steps of 0.05. On the left without, on the right including the effect of calcium dynamics. Notice the change of optimum muscle length when calcium dynamics are modelled as well as its higher stiffness at low activations (for comparison force curves at activation level 0.25 are marked by thick lines).

3.2.7 Passive force-length relationship

In parallel with the active contractile apparatus, several elastic elements passively generate force in a muscle fibre. Connectins, which keep thick and thin filaments aligned, the connective collagen tissue surrounding each muscle fibre as well as the fascicles and the muscle as a whole, all contribute to a springlike restoring force when a muscle is stretched beyond its slack length while being inactive. The combined effect is modelled as a lumped spring with non-linear toe region and linear tail:

$$\tilde{F}_p^M(\tilde{L}^M) = \begin{cases} (\frac{k_{ml}}{k_{me}})(e^{k_{me}(\tilde{L}^M - \tilde{L}_s^M)} - 1) & \tilde{L}_s^M \leq \tilde{L}^M < \tilde{L}_c^M \\ k_{pm}(\tilde{L}^M - \tilde{L}_c^M) + F_c^M & \tilde{L}^M > \tilde{L}_c^M \\ 0 & \text{otherwise} \end{cases} \tag{3.5}$$

where $\tilde{L}_s^M$ denotes normalised muscle slack length (at less than which no force is generated), $\tilde{L}_c^M$ the normalised length of transition from the linear to the non-linear regime (1.5), F_c^M the offset of force produced by muscle at transition length (0.66), and k denote form parameters with values $k_{ml} = 0.4$, $k_{me} = 6.0$ and $k_{pm} = 6.5$. Figure 3.5 shows how passive elasticity and active force-length characteristics combine additively. It should be noted that many different models exist describing force production by the passive elastic element. It can also be modelled, for example, using an exponential increase without linear tail, or even simpler, a quadratic curve. However, since in most experiments carried out in this thesis the muscles will be working mostly in their midrange, rather than at their extreme lengths, the exact shape should not have a significant effect on the overall dynamics. This remains to be confirmed in future work however.

3.2.8 Force-velocity relationship

Not only the number of cross bridges formed determines net force, but also the ability of each individual cross bridge to produce force. The constitutive relationships described above assume an isometric muscle, i.e. a muscle at a fixed length. Naturally however, muscles work against loads and will shorten if the load is less than the contractile force (concentric work) or lengthen if the

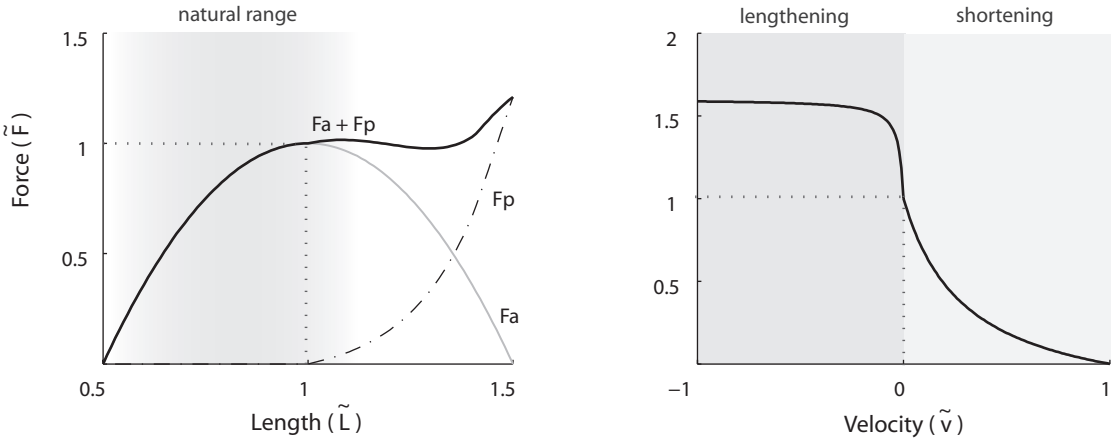

Figure 3.5: The net force-length relationship (thick solid line, left) is formed by addition of an exponential-to-linear elasticity resisting lengthening of the muscle (slash-dotted) and a hyperbolic function with a maximum at resting length describing the active generation of force (thin solid). The curve represents the case of maximum excitation. The force-velocity relationship (right) describes how force production drops with increasing shortening velocity and increases when actively lengthening.

load is larger (eccentric work). Now, the faster a muscle shortens, and the faster the cross bridges are cycling, the less force it can generate. Eventually, contractile force reaches zero at a velocity of v_0^M. Muscles that are actively lengthening, on the other hand, can produce more force than those contracting isometrically. This experimentally observed force-velocity relationship affects overall force output in addition to and independently of the force-length relationship.

For concentric contractions (shortening) the total effect of reduced cross bridge forces and other sources of internal friction can be modelled as a viscous damper in a mechanical system. Mathematically, the following hyperbolic relationship, first formulated by Hill (1938) with regard to muscle thermodynamics, describes the relationship between force and velocity:

$$\tilde{F}_{v_{conc}} = \frac{F_0^M b - a v^M}{v^M + b} \tag{3.6}$$

where F_0^M is the maximum isometric force and a, b are parameters for which $v_0^M = bF_0^M/a$, and which usually are fitted to experimental data. Here we model an average muscle with $v_0^M = 10L_0/s$ (Zajac, 1989). The resulting force-velocity curve is shown in figure 3.6. Damping is the result of force resisting change in velocity. This can be seen in the negative slope of the curve, which leads to decreasing force levels with increasing positive velocities (shortening). Also, due to the non-linearity, the slope itself decreases with faster shortening, indicating that damping decreases for faster movements. The curve can also be interpreted when inverted, meaning that muscles can shorten more rapidly against light loads than they do against heavier ones (in other words, heavier loads will be lifted more slowly than lighter ones).

When eccentrically contracting, i.e. when the load imposed on the muscle exceeds its force and thus leads to stretch rather then flexion, the muscle can generate forces greater than its isometric maximum. The same equation as above can be used with following parameter substitution:

$$a : a', \quad b : b' = \frac{b}{s}\left(\frac{1+a'}{1+a}\right) \tag{3.7}$$

Here s is the slope of the eccentric curve at $v^M = 0$ and is expressed as a multiple of the slope of the concentric curve at the same point. It determines the level of discontinuity at rest, and is usually modelled as a factor of two. Parameter a' determines the asymptote $\lim_{v \to -\infty}$. Reported values, fitted to experimental data, range from 1.4 to 1.8.

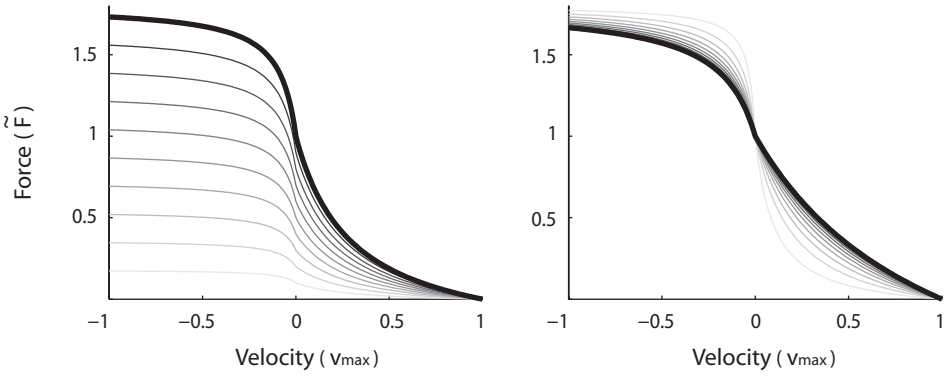

Figure 3.6: Force-velocity relationship. Left: for different levels of muscle activation (0–100% in steps of 10%) with damping parameters $a = b = 0.3$. Right: tetanic activation (100%) and damping parameters $a = b \in [0,1]$. With parameter values increasing, the slopes of the curve around zero velocity increase too. Such models will therefore have stronger internal damping properties.

The force-velocity relationship is crucial for the dynamic behaviour of the muscle model. The steep slope of the curve around the resting state, for example, leads to instantaneous rejection of perturbations and can help stabilise the muscle (the so-called *preflex*). Equally desirable is the model's inherent property of being only lightly damped during fast movements and more strongly damped at slow speeds. The changing slope of the force-velocity curve determines the extent of internal damping and hence the time course of muscle contractions. In section 3.3.4 I will compare muscles having different damping characteristics with respect to the kind of trajectories they produce (also see figure 3.6).

3.2.9 Tendon

Skeletal muscles are not connected to the bone directly. Instead, muscle fibres are arranged at an angle with respect to the muscle's line of pull and held together by connective tissue. This aponeurosis transmits the collective force of all muscle fibres to the tendon, which in turn connects to the bone. Both these in-series elastic elements, especially when long compared to the muscle, can store mechanical energy during muscle contraction. During isometric contractions, tension in the tendon reflects a lengthening of the series element and an internal shortening of the contractile element.

For modelling purposes tendon force is often expressed in terms of strain, i.e. the normalised distance from its slack length. Here, the stress-strain curve is modelled as an exponential to linear function (also see figure 3.7):

$$\tilde{\sigma}^T = \tilde{F}^T(\varepsilon^T) = \begin{cases} \frac{\tilde{F}_t}{e^{k_t}-1}(e^{k_t \varepsilon^T/\varepsilon_t} - 1) & \varepsilon^T \leq \varepsilon_t \\ k_{lin}(\varepsilon^T - \varepsilon_t) + \tilde{F}_t & \varepsilon^T > \varepsilon_t \end{cases} \tag{3.8}$$

where ε^T is tendon strain, $\varepsilon^T = (L^T - L_s^T)/L_s^T$, ε_t the strain at the transition from the nonlinear toe region to the linear regime, $\tilde{F}_t$ the corresponding force, k_{lin} the slope in the linear regime and k_t a form parameter. With $\varepsilon_0 = 0.04$ describing the strain at which the corresponding force equals the normalized maximum isometric muscle force (i.e. $\tilde{F}^T = \tilde{F}_0^M$ at $\varepsilon^T = \varepsilon_0$), following parameter values are used: $\varepsilon_t = 0.609\varepsilon_0$, $\tilde{F}_t = 0.33$ and $k_{lin} = 1.712/\varepsilon_0$. It will also be useful to express the inverted relationship between tendon force and strain:

$$\varepsilon^T(\tilde{F}^T) = \begin{cases} log(\frac{\tilde{F}^T(e^{k_t}-1)}{\tilde{F}_t})\frac{1}{k_t\varepsilon_t} & \tilde{F}^T \leq \tilde{F}_t \\ (\tilde{F}^T - \tilde{F}_t)/k_{lin} + \varepsilon_t & \tilde{F}^T > \tilde{F}_t \end{cases} \tag{3.9}$$

Many experiments in thesis will not actually include the tendon; partly because it constitutes a considerable computational cost (see section 3.2.11), and partly because it does not always affect movement dynamics in a significant way. This is because the length change in tendon is negligible compared to the change in muscle length if the tendon is relatively short, as is the case with elbow muscles for example (Zajac, 1989).

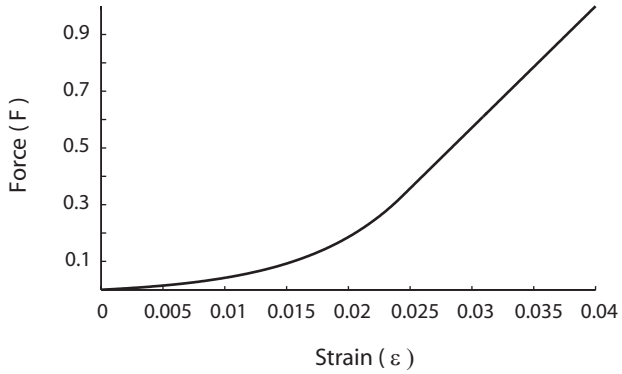

Figure 3.7: Tendon force-stress relationship. Tendon force equals maximum isometric muscle force at 4% strain, and the transition from non-linear to linear occurs at 2.4% strain.

3.2.10 Muscle path

It has been shown in sensitivity studies of similar muscle models that the path of the muscle, from its point of origin to the arc around the joint and eventually its insertion point, is a critical factor for determining its dynamic response. This is because the path determines how the length of the muscle, and its moment arm with respect to the centre of the joint, change as a function of joint angle. This in turn influences where on the force-length and force-velocity curve a muscle resides. There are different ways of calculating muscle length given the current kinematic situation. The simplest is to assume a straight line between origin and insertion. In certain conditions, however, this would lead to a path unrealistically crossing through the bone structure. A more precise method takes into account the arc of the muscle path around the joint. Here though, in order to minimise computational cost, we use dimensionless curves fitted to data from an average type of muscle.

Figure 3.8 shows muscle length and moment arm as functions of joint angle under four different assumptions. For better comparison, all curves have been normalised to the same range. Most

muscles, although many exceptions exist, are connected to the skeleton such that they are mainly using the ascending limb of the force-length curve (Garner and Pandy, 2003). According to the authors, the monoarticular[1] elbow flexors brachialis and brachioradialis, for instance, have a natural range of approximately 60% to 110% of their resting length. This is also the range used for all muscles in this thesis.

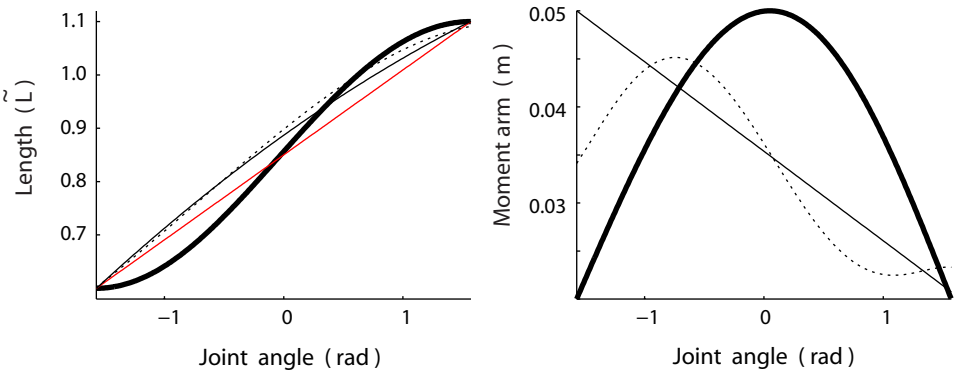

Figure 3.8: Muscle length and moment arm as functions of joint angle. Thick solid lines: Bullock's symmetric model. Thin solid lines: Kistemaker model. Dashed lines: Lemay and Crago model.

For the angle to muscle length mapping a linear curve is compared to two functions that were polynomially fitted to anthropomorphic data (Lemay and Crago, 1996; Kistemaker et al., 2007a), as well as an idealised symmetric setup (Bullock and Grossberg, 1991). For moment arms, a linear curve, a fitted polynomial (Lemay and Crago, 1996) and an idealised bell-shaped function (Bullock and Grossberg, 1991) are considered. Also, a constant moment arm, as is present in the triceps elbow extensor for example, is used for comparison. I will show in section 3.3.1 how these different modelling assumptions qualitatively affect the overall landscape of muscle dynamics.

3.2.11 Simulation

The simultaneous dependence of muscle force on length, velocity and activation can be visualised by the surface:

$$\tilde{F}^M = f(\tilde{L}^M, \tilde{v}^M, a(\tau)) \tag{3.10}$$

$$= a(\tau) F_0^M F_a^M(\tilde{L}^M) F_v^M(\tilde{v}^M) + F_0^M F_p^M(\tilde{L}^M) \tag{3.11}$$

Here velocity and active force exhibit a multiplicative relation scaled by muscle activation, while passive muscle force is unaffected by the activation level. Another way of reading this is to say that active force, scaled by activation, is used to determine the zero intercept of the velocity curve (i.e. the maximum isometric forces are matched). All variables here are dimensionless. As mentioned before, muscle length L^M is normalised by its resting length L_0^M, velocity v^M by maximum shortening velocity v_0^M and force F^M by maximum isometric force F_0^M. This has the advantage that many different types of muscles can be modelled simply by choosing different parameter values for the normalisation, while all constitutive relationships operate over the same dimensionless range. The corresponding surface is shown in figure 3.9 for different levels of activation.

[1] spanning a single joint only

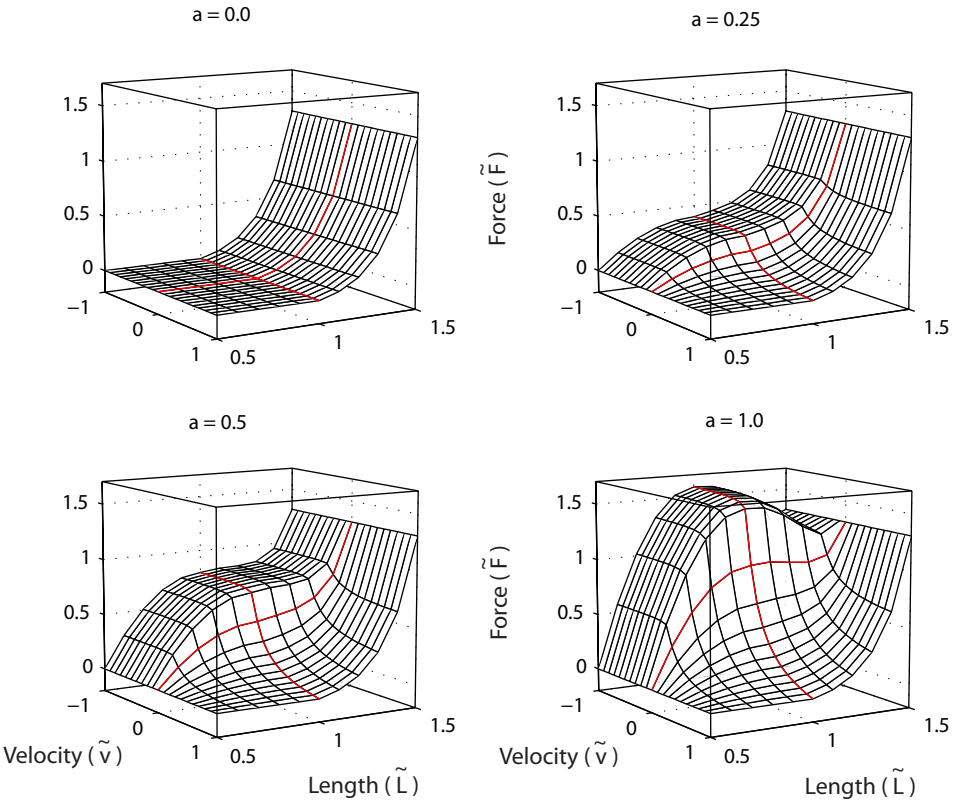

Figure 3.9: Muscle surfaces. Force is represented as a surface over length and velocity for different muscle activations. Red lines indicate the parts of the surface where the muscle is at resting length (1.0) or at zero velocity. It can be seen that higher activation not only leads to larger absolute forces but also to steeper slopes in both length as well as velocity dependent forces. This in turn results in both higher stiffness (slope of f-l) and stronger damping (slope of f-v).

During natural movements, both the length and velocity of a muscle change continuously. As a result, force output will also be altered even if neural activation is constant (although this will rarely be the case, as neural activation is strongly modulated by spinal neuron circuits). Even more, the slopes of the surface, i.e. stiffness and damping, will change as well throughout a single movement. It would thus be reasonable to assume that rather complex dynamics would result from such a system and that it would be difficult to control. I will show in the following sections however, that this is not the case. On the contrary, the non-linear muscle properties seem to have been adapted such that they allow for rather simple forms of control.

Model integration

Without tendon, a simple integration scheme (figure 3.10A) can be used to calculate muscle force according to the model described by equation 3.11. When a tendon is included, the scheme is different, as there is no longer a unique mapping between joint angle and muscle length. Instead, for any length of the combined musculotendon unit (which is unique for every joint angle), the relative length of the muscle and the tendon depends on the force with which the muscle is currently contracting. Hence an algorithm as shown in figure 3.10B is used for integration.

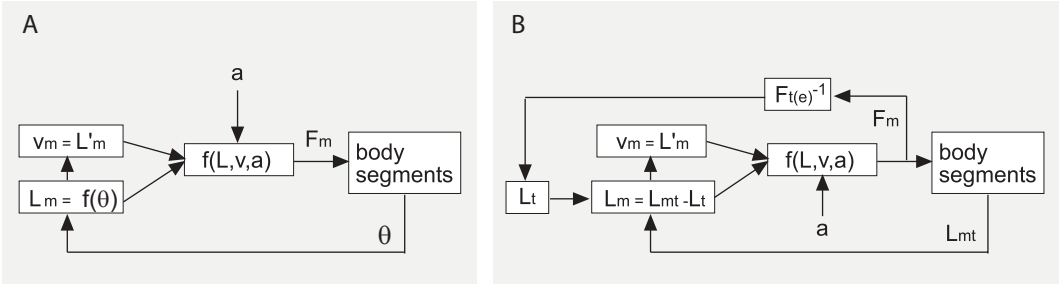

Figure 3.10: Musculotendon unit (MTU) flow chart. A) without tendon: joint angles, readily available in the rigid body physics simulator ODE, are mapped to muscle lengths directly. Velocity, the derivative of muscle lengths, and activation, the input, are used to calculate muscle force. B) including tendon: the length of the tendon can be derived from the inverse of the tendon force-length curve given the current force output. This can be used to calculate muscle length and subsequently its velocity. The same steps are then taken to get force output.

Once the force output has been calculated for a given muscle, it is multiplied by its moment arm and applied as torque to the joint it spans. The resulting motion of the body, i.e. the articulated chain of rigid bodies, is then handled by a physics simulator [2] that takes into account the effects of gravity, inertia, friction and collisions. In the following time step the new positions of the body segments are then used again for the integration of the model equations as described above.

3.3 Results: Muscle dynamics

A muscle never functions in isolation but always interacts with a load. The load can be static, as in holding a weight against gravity, or dynamic. In the latter case the muscle accelerates or decelerates a load that has inertial and possibly viscoelastic properties. This is the case for example when two muscles are arranged antagonistically, each providing a load to the other. As muscles can only pull, they usually come in pairs to actuate a joint (usually in higher numbers though, especially for joints with more than one degree of freedom). In the elbow, for instance, the triceps straightens the joint, while the biceps flexes it (as do brachialis and brachioradialis). In the following experiments this is the setup used, with all muscle properties being symmetrical (including their insertion into the bone).

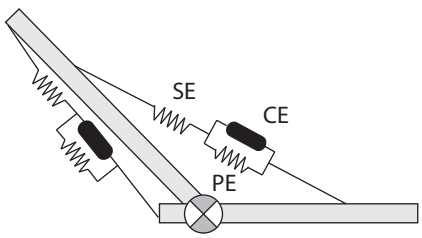

Figure 3.11: Example of an antagonistically arranged pair of muscles. In this thesis, muscles are attached to the skeleton in a symmetrical fashion instead.

[2] ODE - Open Dynamics Engine: http://www.ode.org/

One way of looking at the behaviour of such a system of coupled dynamics is to identify its equilibrium points (EP). These are the states where the force producing characteristics of the two muscles (and external loads) intersect so as to cancel each other out. As a result, no movement occurs at an EP: it defines the points at which the system is at rest. Figure 3.12 shows the force-length curves of an antagonistic muscle pair at different activation levels. Both are plotted as producing positive forces although their effect on the skeleton is of opposite sign. The force-velocity curve need not be considered for now, as the velocity at the EP is zero by definition.

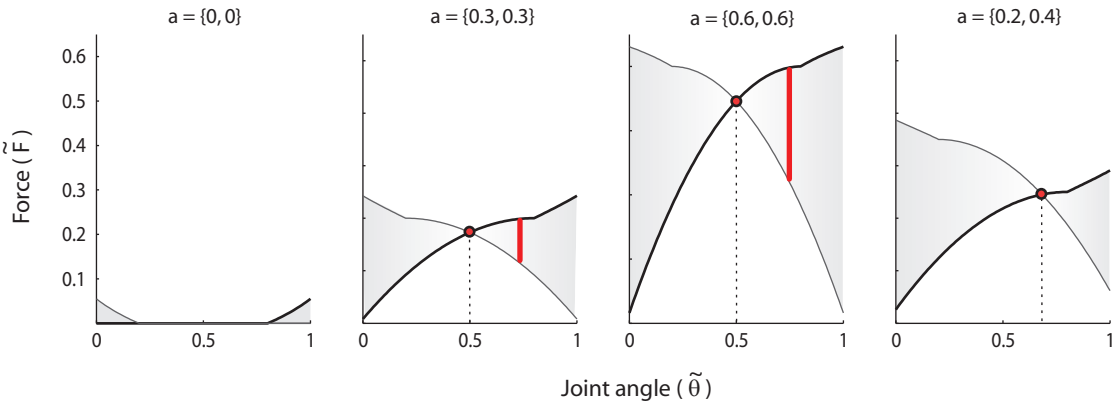

Figure 3.12: Behaviour of an antagonistic muscle setup acting on a hinge joint. Arrangement is symmetric, joint angles in $[-\pi/2, \pi/2]$ and lengths of both muscles vary between $0.6\tilde{L_M}$ and $1.1\tilde{L_M}$. Co-activation of the antagonistic muscles changes the slope of both force-length curves at the EP and increases the overall stiffness (the difference in force as a function of distance from the EP increases). A shift in the difference between activations however, shifts the position of the equilibrium.

When neither muscle is activated, the joint acts completely passive in its mid-region and only lightly resists movement at its extremes (due to passive elasticity). With small and equal activations however, an EP appears to which the joint will converge from any starting point in its range. It will resist perturbations away from this EP with a force that equals the difference between the two curves, which in turn is determined by the slopes at the EP (shaded grey). The equilibrium is therefore stable, i.e. an attractor. It is easily observed that due to the non-linearity of the curves, increasing co-activation of the muscles (simultaneous and of equal amount) leads to higher stiffness of the joint. Differential activation of the muscles on the other hand, does not primarily change the stiffness of the system, but the position of its equilibrium.

Muscles are often assumed to be primarily spring-damper systems. But although they do have viscoelastic properties, their dynamics can be quite different from simple springs. With respect to equilibrium points, compare the above model to the linear spring setup depicted in 3.13. Here the system consists of two antagonistic springs whose resting lengths can be controlled via input signals. Although the intersection of their force-length curves also create an EP whose position can be controlled, its stiffness is always the same. No matter how the individual resting points are modulated, the overall stiffness is always determined by the individual spring constants.

The fact that muscle non-linearities create an equilibrium point whose position and stiffness can be modulated centrally, suggests a particular form of control. With respects to posture, i.e. the

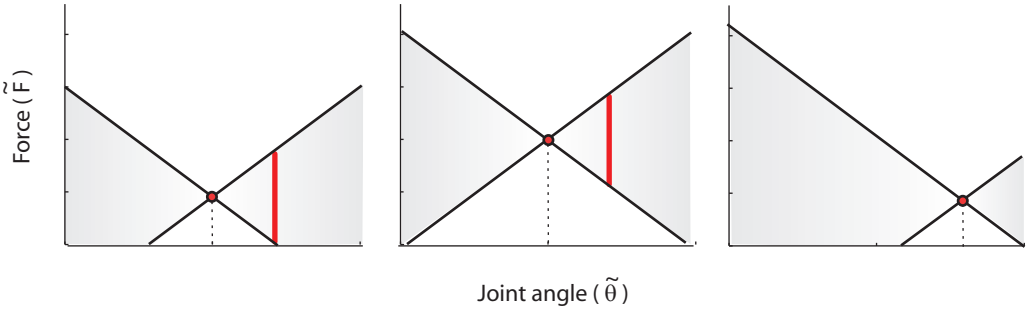

Figure 3.13: Linear spring model of a muscle actuator. Co-activation, i.e. the shift of resting lengths by equal amounts but in opposite directions, increases the force output of individual springs, but doesn't affect their difference. The overall stiffness is thus determined solely by the individuals spring constants.

maintenance of a body configuration, it offers stability for free. If muscle activations are such as to produce a given posture, any perturbation will be rejected automatically. There is no need for the explicit calculation of forces that need to be produced by each muscle to oppose a perturbation. Voluntary movement, in such an EP control scheme, corresponds simply to a shift in posture. Instead of using an internal model of body dynamics to infer the correct forces needed to move the body segments in a desired fashion, a simple shift of the EP is sufficient to induce movement to the target position. This is why the EP-hypothesis offers a solution to the posture-movement paradox: there is no clash between dedicated autonomous systems stabilizing a posture and voluntary movements. Both are aspects of the same system.

For goal-directed movements a mapping between desired joint configuration and muscle lengths is required, but this is considerably simpler than the formation of an internal dynamics model. Also, there exists the possibility that segmental reflex connections develop such as to mirror the anatomical organisation of the muscles (Feldman and Levin, 1995). This would mean that no explicit geometrical representation of the motor apparatus is needed to "map" a desired joint configuration to required muscle length thresholds. Instead, a centrally specified joint reference configuration is distributed to all involved muscles via appropriately organised reflex connections such that their threshold lengths correspond to the desired joint angle.

It is clear, however, that motor control using only static activation levels, as illustrated above, is neither biologically plausible nor energetically efficient. EMG measurements show that at the end of most movements muscle activation goes to zero. A lot of energy would be wasted if for every posture all muscles would be constantly contracting. This is why the λ-formulation of the equilibrium hypothesis proposes that the EP is the result of the combined effect of muscle properties and reflex activity, the latter of which resets the setpoint beyond which muscles start contracting. Another solution would be the creation by the muscles of an EP to induce movement, followed by a gradual decline of activation once the desired position is achieved; or a combination of such an open-loop control-law and reflex activity. But whatever the form of control, the dynamics of an antagonistic muscle pair will always have a significant effect on the movement generated. The following sections will therefore analyse how the dynamical landscape depends on the various components of the muscle model in open-loop mode. The next chapter will then deal with closed-loop control.

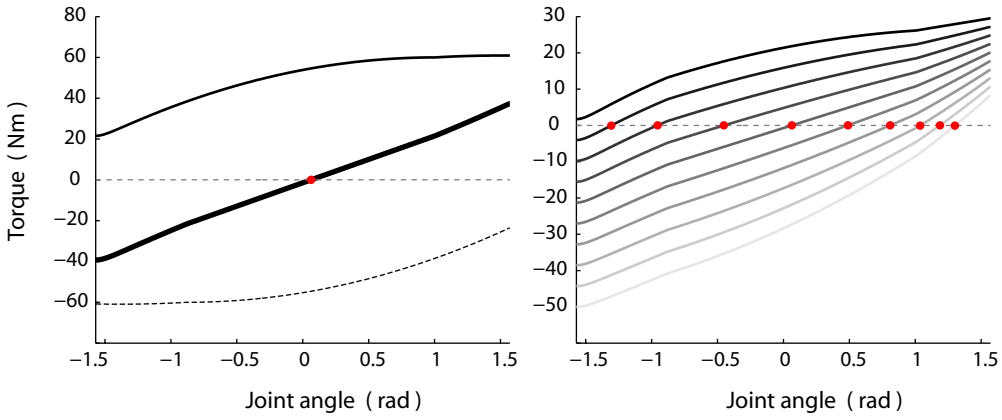

Figure 3.14: Net torque curve of joint at full isometric activation for LC model (left). Right: extensor activation fixed to 0.5 and flexor ranging from 0 to 1.

3.3.1 Steady-state equilibrium points

The equilibrium points of a single hinge-joint actuated by an antagonistic muscle pair can be found where the amounts of torque produced by both muscles are equal. Muscle torque in turn is a function of joint angle: indirectly via the muscle's force-length relationship and directly via changing moment arm. Figure 3.14 plots the torque of each muscle as a function of joint angle for different static activation levels. Since the muscles pull in opposite direction, their torque curves are of opposite sign. Also shown is net joint torque, given by the sum of the two muscle torque curves (thick line). Since the setup is symmetric, the equilibrium point, the point at which net joint torque is zero, can be found in the middle of the joint range. The slope at the same point determines if the point is an attractor or repellor. Here, the flexor (thin solid line) pulls the joint towards negative, the extensor (thin dashed line) towards positive angles. A positive slope thus defines an attracting equilibrium point, as is the case in figure 3.14. While the left part of the picture shows the condition of both muscles being maximally activated, the right shows the movement of the EP with extensor activation fixed at 0.5 and flexor activation ranging from 0.0 to 1.0. It can be observed that the slope at the EP, i.e. the joint stiffness, changes with activation as well.

The same technique of identifying EPs and estimating stiffness from the slope of the net torque curves can be used to fully characterise the steady-state behaviour of the system. In figure 3.15 this was used to display EPs and stiffness over all possible muscle activation pairs. Several salient features of these surfaces are interesting. Firstly, EPs exist for every possible joint angle. Hence any position of the joint can be maintained in a stable fashion and movement between any two positions is possible via a shift in muscle activation. Secondly, each equilibrium position can be achieved with different combinations of muscle activations. In fact, the joint position isocurves (drawn below the surface), that is the curves along which joint position is constant despite changes in activation, form straight lines. The isocurve for joint angle $\theta = 0$ for example is found where $M_{Flex} = M_{Ext}$, while all other isocurves correspond to fixed ratios between flexor and extensor activation. From a control perspective this is a desirable feature because no complex mapping between desired joint position and muscle activation is needed. This is amplified by properties found in the

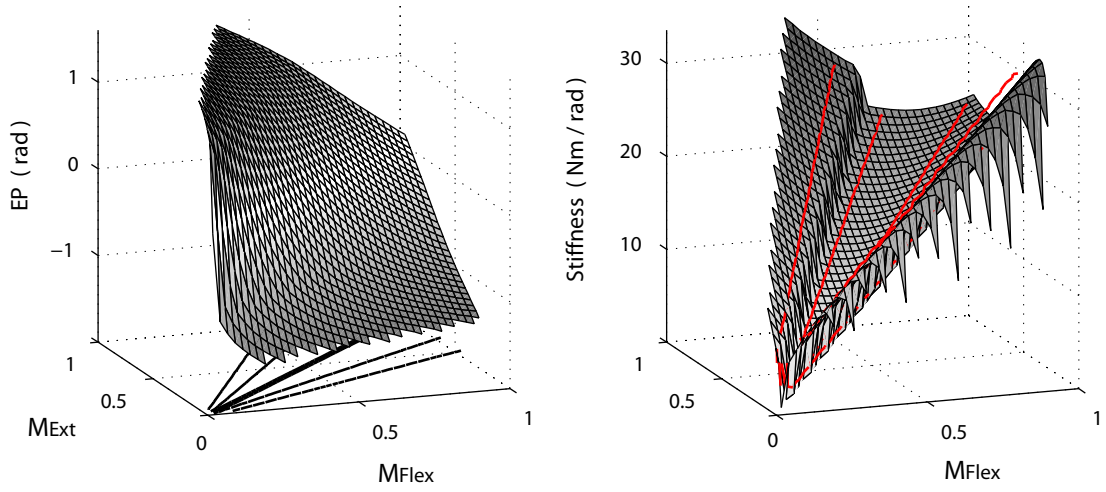

Figure 3.15: EPs and corresponding stiffness in isometric condition as functions of flexor activation (M_{Ext}) and extensor activation (M_{Flex}). Muscles have a linear length function and constant moment arm. EPs exist for each joint angle in the range. Stiffness increases as passive elasticity comes into play.

stiffness map. Here, red lines indicate joint stiffness along the positional isocurves. These too form straight lines. Hence a single number, the flexor-extensor activation ratio, determines joint position while their absolute values determine joint stiffness. A simple strategy for independent control of these variables could therefore be implemented in a straightforward manner.

Above analysis represents a muscle model in which moment arms are constant and muscle lengths change linearly. As mentioned in section 3.2.10 though, each of these can be modelled in various ways. Figure 3.16 summarises the steady-state behaviour of twelve different models. The labels identify each model, with the first letter referring to the muscle length mapping (L = linear, S = sigmoidal), and the second referring to the moment arm function (C = constant, L = linear, A = asymmetric bell-shape). Additionally, the two top rows differ from the two bottom rows in that they do not include calcium dynamics. It was found that the other modelling options mentioned in section 3.2.10 produce results almost identical to the ones shown here. The more realistic muscle length approximation, for example, was not significantly different from linearity, and the bell-shaped moment arm function is equivalent to a constant moment arm if the muscles are arranged symmetrically.

From figure 3.16 it is clear that the model is only slightly sensitive to the shape of the muscle length function. Comparing rows 1 and 2, or 3 and 4, the only difference between a linear and a sigmoidal function is a steeper slope towards the extreme joint angles. More significant is the effect of the moment arm. By using the linear or non-linear functions almost all surfaces are changed such that a wide region in the middle becomes practically uncontrollable. A slight variation in activation will move the joint towards one of the two extremes. Only the LL and SL models with calcium dynamics seem to be well behaved (smooth in the central region). Calcium dynamics itself is another major factor in shaping the surfaces. While not disrupting the emergence of EPs, it leads to non-linear EP isocurves. Consequently these models do not allow for a trivial mapping of equilibrium position to a fixed ratio of agonist-antagonist activation.

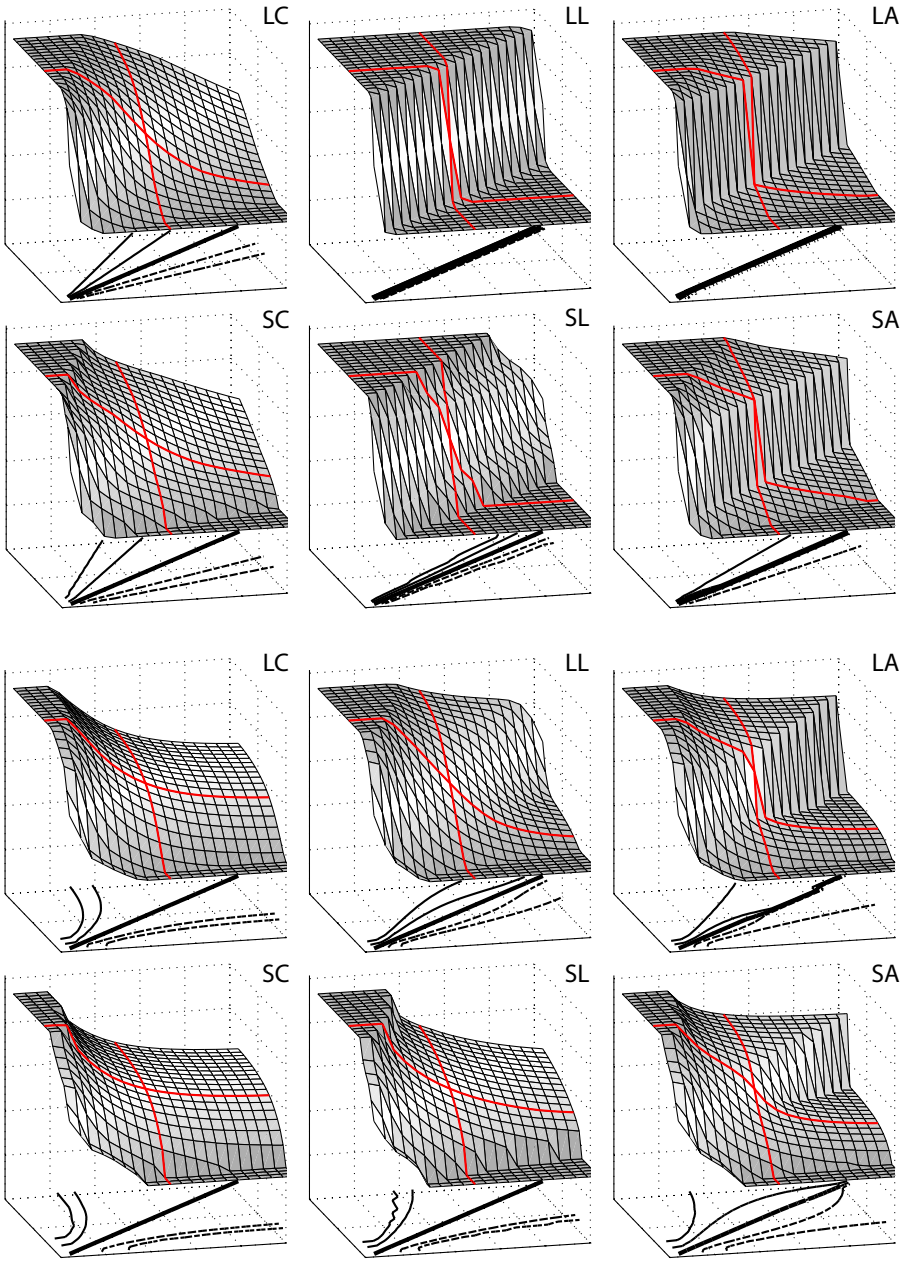

Figure 3.16: Surfaces of equilibrium position over muscle activation pairs comparing different muscle length and moment arm functions as well as the effect of calcium dynamics. The first initial of each label refers to the length mapping: L for linear, S for sigmoidal. The second letter identifies the moment arm mapping: C for constant (0.04 cm), L for linear, and A for the asymmetric bell shape (Lemay and Crago, 1996). The top two rows do not include calcium dynamics, the bottom ones do. For units of axes refer to previous figure.

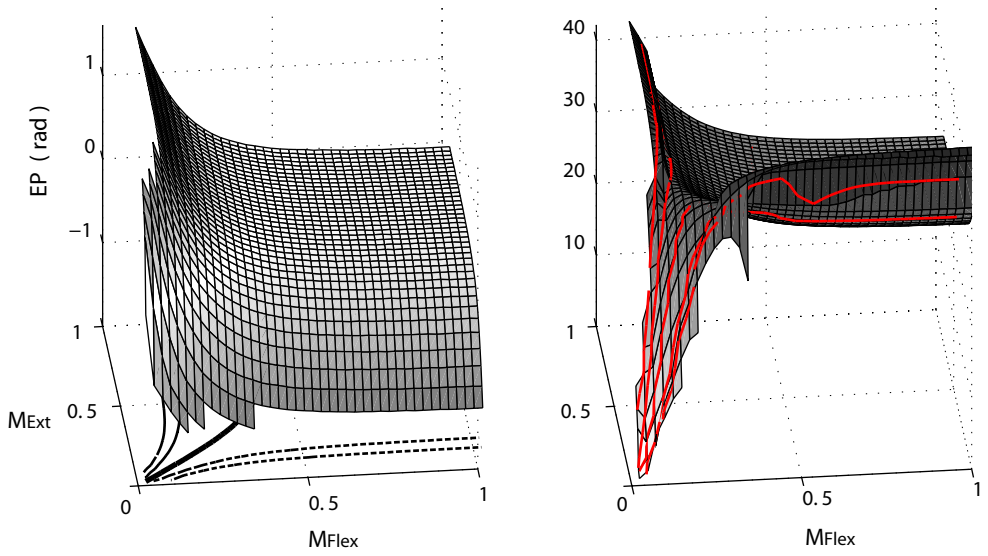

Figure 3.17: EPs and corresponding stiffness determined from isometric condition. Muscles have a linear length function, constant moment arm and calcium dynamics. Note that inclusion of the latter implies that near maximal force production can be achieved in the region below activation levels of 50% (compare figure 3.4), i.e. the flat region in the observed surfaces would fall outside the range of natural human movements.

We can explain the differences observed between the various models by looking more closely at individual EP surfaces and net torque curves. These are shown in figures 3.17 for a model with linear muscle length, constant moment arm and calcium dynamics. Compared to the model without calcium dynamics (figure 3.15), the surface of EPs becomes more nonlinear, resulting in a flat surface beyond activations of approximately 0.5. This is due to the force-length relationship saturating at much lower activations (see figure 3.4). Nevertheless, all positions are attainable with activations below that range. Stiffness also shows a different characteristic and no longer increases linearly along the EP isocurves. It is still a controllable variable, as the same EP can be achieved with different levels of co-contraction, but in a less simplistic fashion.

The position and type of equilibrium points is directly related to the position of peaks in individual muscle torque curves. In both models with linear muscle length and constant moment arm these peaks occurred somewhere between the centre and that extreme at which a muscle is at its longest. As the curves were monotonic and symmetric, the resulting net joint torque was close to being linear. If, however, the muscle torques peak at shorter muscle lengths, and the curves become non-monotonic, the net torque can cross zero several times and hence produce several equilibria. An example of this is the model with sigmoidal muscle length and non-linear moment arm shown in figure 3.18. Here, the system exhibits three equilibria. The two EPs located at the ends of the joint range are attractors, while the EP in the centre is a repellor. This explains why the central region is uncontrollable. Depending on initial conditions, or small random perturbations, the joint will always be pushed into either of the peripheral attractors. From a control point of view this is undesirable. In open-loop mode the system can not be controlled, and if feedback control was used, the gains would have to be so high as to overcome the system's inherent pressure away from the centre. High gains however can easily cause instability themselves.

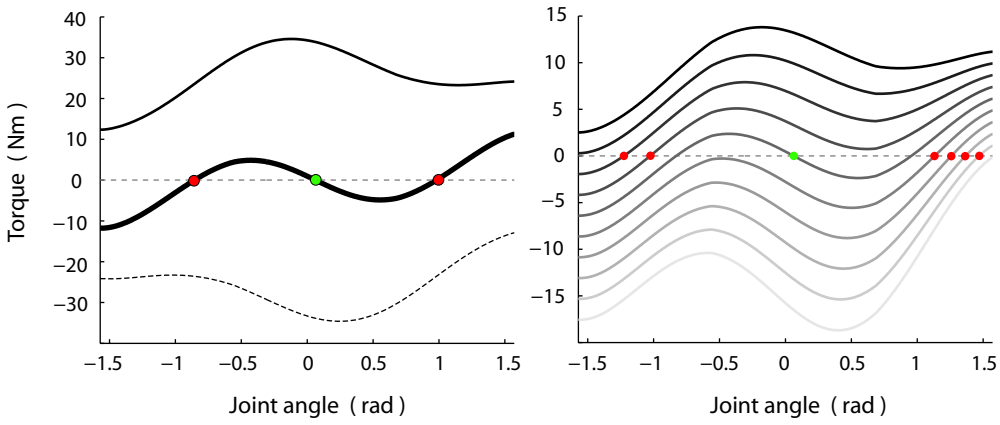

Figure 3.18: Net torque curve of joint at full isometric activation for SA model (left). Right: extensor activation fixed to 0.5 and flexor ranging from 0 to 1.

It should be emphasised at this point, that the muscle setup used in all experiments here is rather abstract when compared to real musculoskeletal morphologies. In humans for example, four muscles are involved in elbow flexion (biceps, brachialis, brachioradialis, pronator teres) and two in extension (triceps, anconeus). All have different torque-angle curves and contribute forces to different degrees depending on the particular movement carried out. The properties of the antagonist muscles modelled in this thesis are not supposed to correspond to any of those real muscles in isolation, but should rather be seen as an abstraction of the whole elbow system. Correspondingly, the dynamics exhibited by the model are assumed to be a subset only of the dynamics of the real system. Models that lead to unstable dynamics, for example, are not studied any further in this thesis, without claiming that natural systems never exhibit such behaviour [3]. Validation of the lumped two-muscle model, i.e. assurance of biological plausibility and relevance, is based on both qualitative and quantitative assessment. A qualitative feature of movement dynamics considered crucial, for example, is the ability to independently control joint position and stiffness across the full range of joint angles. Quantitatively the model is considered plausible if it reproduces features observed in natural kinematics, such as bell-shaped velocity profiles.

3.3.2 Co-contraction and stiffness

So far it has become clear that even with static open-loop control signals, antagonistic muscles can create a dynamic landscape that allows for the control of joint position via equilibrium points. Furthermore, different combinations of muscle activations can lead to the same equilibrium position. How is co-contraction, i.e. the amount of contraction shared by two muscles, related to the stiffness of the joint? Control of stiffness is directly connected with the stability of a system, and it is usually assumed that co-contraction of antagonists increases the stiffness at the joint. Figure 3.19 plots stiffness, measured as before by the slope of the net torque-angle curve, against the level of co-contraction. Irrespective of whether the model includes or excludes calcium dynamics, stiffness increases indeed with co-contraction. In the former case it changes linearly, and in the latter case non-linearly and non-monotonically with a peak at submaximal muscle activation. The maximum

[3] they might do in fact, as demonstrated in (Akazawa and Okuno, 2006)

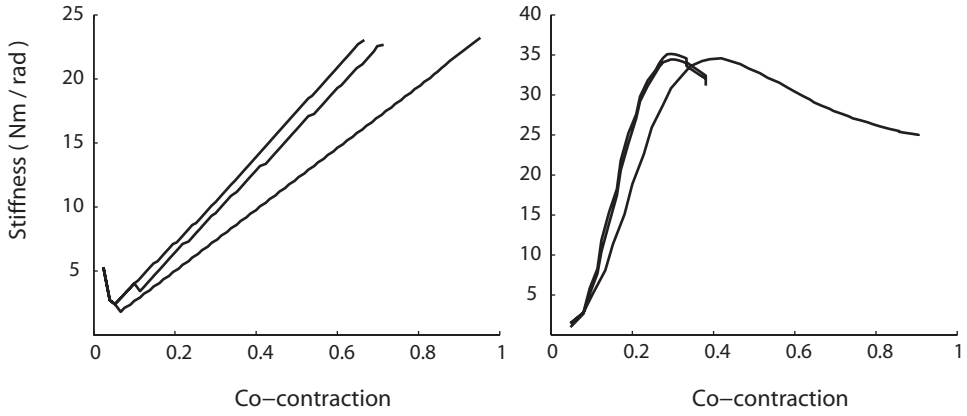

Figure 3.19: Stiffness along EP isocurves as a function of co-contraction. On the left the LC model without, and on the right with calcium dynamics is shown. In both cases some areas are omitted because of numerical inaccuracies in estimating stiffness from torque-angle slopes.

stiffness observed in the model varies between 18 and 45 Nm/rad, depending on the equilibrium-angle. This is within the physiological range, reported as being 14 to 126 Nm/rad (Kistemaker et al., 2007a). The shape of the stiffness curve for the model including calcium-dynamics matches that reported in (Kistemaker et al., 2007a) for a model composed of six individual muscles.

3.3.3 Tendon and EP

In the previous analyses the tendon was omitted from simulations. In the case of the elbow this can be justified by the fact that the ratio of tendon to muscle length is such that the effect of the tendon is minimal (Zajac, 1989). Only when the tendon is comparatively long does it add enough series elasticity to store a significant amount of energy. Nevertheless, in order to test the effect of a short tendon on the dynamic landscape of the antagonist system, the previous analysis was repeated with a tendon present. The musculotendon length was modelled as varying between 7 and 14 cm (Pigeon et al., 1996), with $L_0^M = 9cm$ (Garner and Pandy, 2003), and $L_s^T = 3cm = 0.33L_0^M$. With this setup, the muscle length measured over the same joint range as above varies between 0.5 and $1.2L_0^M$. This is similar to (Lemay and Crago, 1996) where L_s^T was set such that $\tilde{L}^M = 1.2$ when activation $a = 0$ and musculotendon length L^{MT} at maximum physiological length. As figures 3.20 and 3.21 show, inclusion of a tendon does not change the main features of the joint's equilibrium surface. The main difference, similar to the model including calcium dynamics, is that for high activation the EP surface becomes flat. Most change occurs when either activation is low. Also, an effect of change in the range of muscle lengths can be observed. Now between 0.5 and $1.2L_0^M$, force output drops to zero at the joint extreme for the muscle that is at its shortest here. Stiffness increases smoothly with co-contraction as in the models described above, but in a non-linear fashion. As the inclusion of the tendon increases the complexity of the model, but does not affect the properties of interest here, the decision is made to not include it in the rest of this thesis.

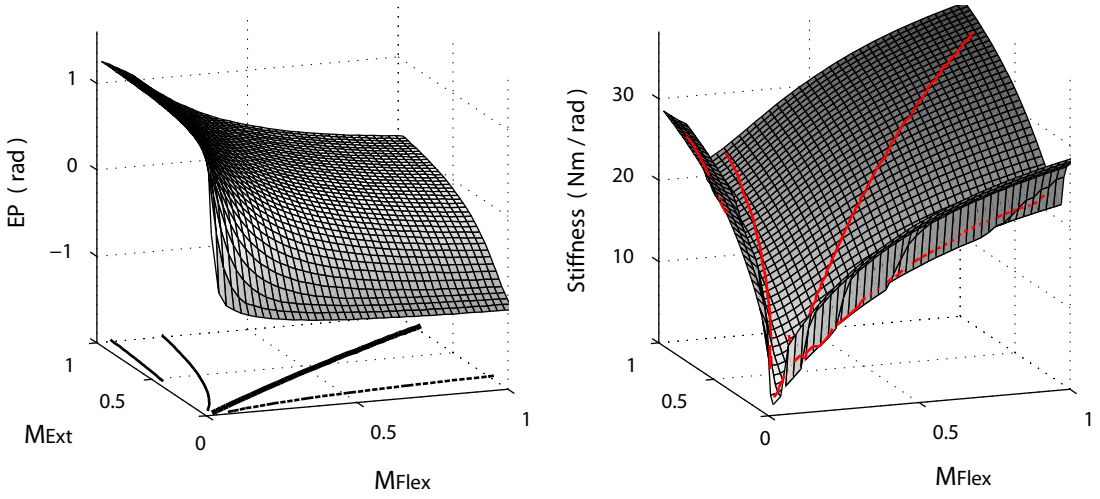

Figure 3.20: EPs and corresponding stiffness determined from isometric condition. Muscle has a linear length function, constant moment arm as well as a tendon element. EPs exist for each joint angle in the range.

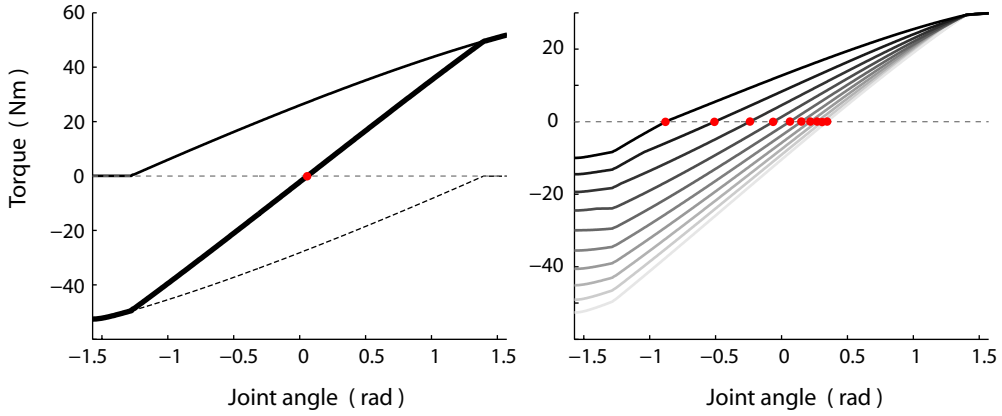

Figure 3.21: Net torque curve of joint at full isometric activation for tendon model (left). Right: extensor activation fixed to 0.5 and flexor ranging from 0 to 1.

3.3.4 Transient dynamics

So far we have only looked at the steady-state behaviour of the antagonist system, i.e. the states at which it comes to rest (EP) and their local properties (stiffness). Of equal interest is the system's transient behaviour, that is the kinematic features of the actual movement as it leads to the EP.

Passive load response

For the same desired movement, the main factor influencing kinematics in the Hill-type muscle model is the viscosity implemented by the force-velocity relationship. Figure 3.22 compares muscle models with and without this viscosity in response to a transient load of 10 N and changing co-contraction. Not surprisingly, the effect of the viscous element is the damping of the perturbations. Also, this damping is stronger for increasing co-contraction. The lack of viscosity, on the other hand, leads to underdamped oscillations around the equilibrium point. It is worth noting that the equilibrium point of the musculoskeletal system now also depends on the load. The equilibrium hypothesis acknowledges that control signals can not directly encode the actual EP, but that the latter emerges from the interaction between an internal, or virtual, EP and external loads.

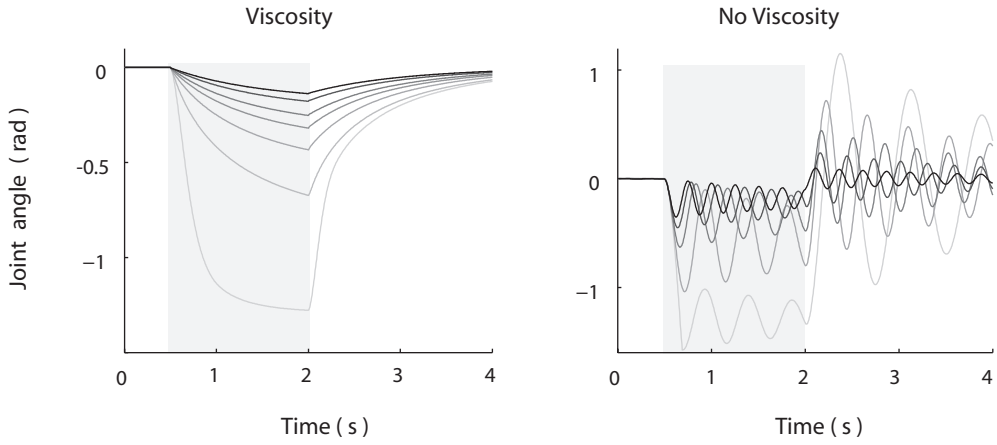

Figure 3.22: Response of joint actuated by antagonist muscles to transient loads of 10 N. Left: the model with viscosity term produces damped movements towards the equilibrium point, now also determined by the load. Right: without viscosity movements are highly underdamped.

It should be noted that the model described above does not include passive damping or joint friction. While it has been shown that passive viscosity can contribute significantly to overall joint dynamics in insects (Zakotnik et al., 2006; Dudek and Full, 2006), its effect in humans is likely small compared to active muscle viscosity and reflex contributions[4]. As Hooper et al. (2009) suggest, this difference might result from a general scaling effect. While muscle passive force varies with muscle cross-sectional area, limb mass varies with limb volume. In large limbs passive forces are hence dominated by inertia and gravity. Since most studies using Hill-type muscle models omit passive viscosity terms (compare, for example, Gribble et al. 1998), the same was done here. While one could speculate that the addition of passive damping could improve stability slightly where oscillations occur at the final position of a movement, this was not investigate in this thesis.

[4]Winters and Stark (1985), for example, report a value of 0.2 Nms/rad

Central control of viscosity

More interesting than the passive properties of the antagonist system when responding to a load is whether joint velocity can be controlled independently from position and whether the observed kinematics bare resemblance with biological data. Intuitively, it would seem that in order to control the velocity of a movement the control system would have to modulate the time course of muscle activations. In this section however, we will ask if movement velocity can also be influenced only by choosing different static open-loop activations. In the following experiments, the simplest model that successfully produced the desired steady-state behaviour (linear muscle length, constant moment arm) is used and the kinematics recorded while the joint produces movements with an amplitude of 100 degrees. All movements are aimed at the same position, but activation of the muscle pair is varied along the EP isocurve. Therefore, the same EP is reached but with different amounts of co-contraction. The resulting time course of joint position and velocity is shown in figure 3.23. It is easily seen that movements caused by higher co-contractions tend to be faster than those with low co-contraction. The absolute value of peak velocity increases and is reached earlier. Consequently, movement duration decreases with co-contraction. This demonstrates that it is possible to control joint velocity without changing the position of the equilibrium. Also, it can be seen that the damping property changes, as lower co-contraction produces more oscillation around the equilibrium point. Overall, the velocity profiles exhibit a bell shape with slight asymmetry when approaching the EP. The system seems slightly overdamped near zero velocity, especially for the highest levels of co-contraction. Interestingly, such deviations from perfectly symmetric velocity profiles are indeed observed in human movements (Bullock and Grossberg, 1988).

Parameters shaping the damping characteristic

The factors that determine the kinematics of a movement are those influencing the force-velocity curve, i.e. the damping parameters shaping the convexity of the curve for shortening, and the asymptote for lengthening velocities. Figure 3.24 and table 3.3.4 summarise the effect of variation in those parameters. Movement kinematics are characterised by three measurements: i) peak velocity v_{peak}; ii) time to peak velocity $t_{v_{peak}}$: the time between the instant that the joint reaches 5% of the total distance to be covered, and the instant at which peak velocity is reached; iii) movement duration T: the time needed to move the joint from 5% to 95% of the total distance to be covered.

Two important observations can be made. Firstly, the asymptote for muscle lengthening velocities modulates the asymmetry of the bell shaped velocity profile. This is due to a steeper slope of the force-velocity curve around zero velocity. With a value of 1.4 and high activations the profile is very close to a perfect Gaussian, while at lower activations the asymmetry when approaching rest becomes more pronounced. With an asymptote of 1.8 however, the asymmetry is very strong even at high activations. Secondly, also due to the steeper slope of the force-velocity curve, damping is increased with a higher asymptote. As a result, peak velocity drops, and movement duration increases. While the asymptote affects damping in the lengthening muscle, parameters a, b shape the damping of the shortening muscle. With higher values the curve becomes more linear. Consequently, the slope of the force-velocity curve is reduced and less damping is observed. Higher values for a, b thus lead to faster movements. But although the resulting movement kinematics can

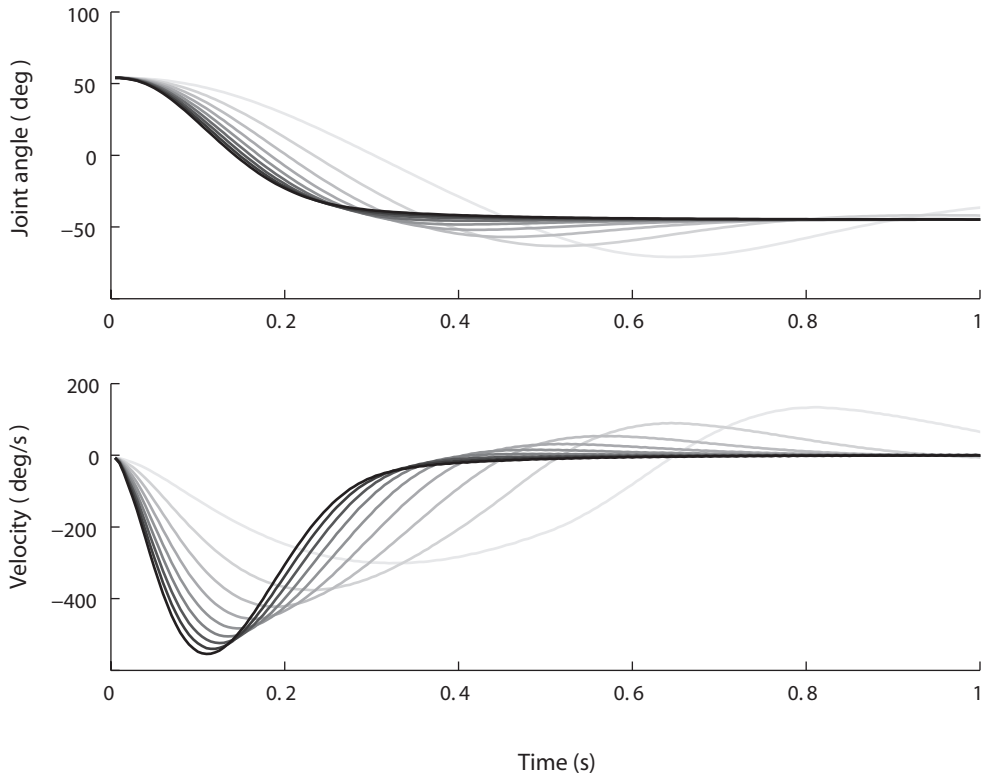

Figure 3.23: Movement kinematics for different muscle activations that lead to the same EP. Darker plots correspond to higher co-contraction and stiffness. With increasing stiffness, peak velocity increases, occurs earlier and movement duration is shorter. The lower the joint's stiffness, the less damped the movements. Damping parameters are: $a = b = 1.0$, and asymptote $a' = 1.4$.

be tuned using these parameters, they do not correspond well to human data. Kistemaker et al. (2006) reports mean peak velocities of 975 degree/s, time to peak velocity of 0.077 s and movement duration of 0.118 s for movements over 100 degrees. Clearly, the movements produced in simulation with open-loop control only are too slow when compared to human data. In chapter 4 other forms of control are explored that have the potential to produce more realistic kinematic data.

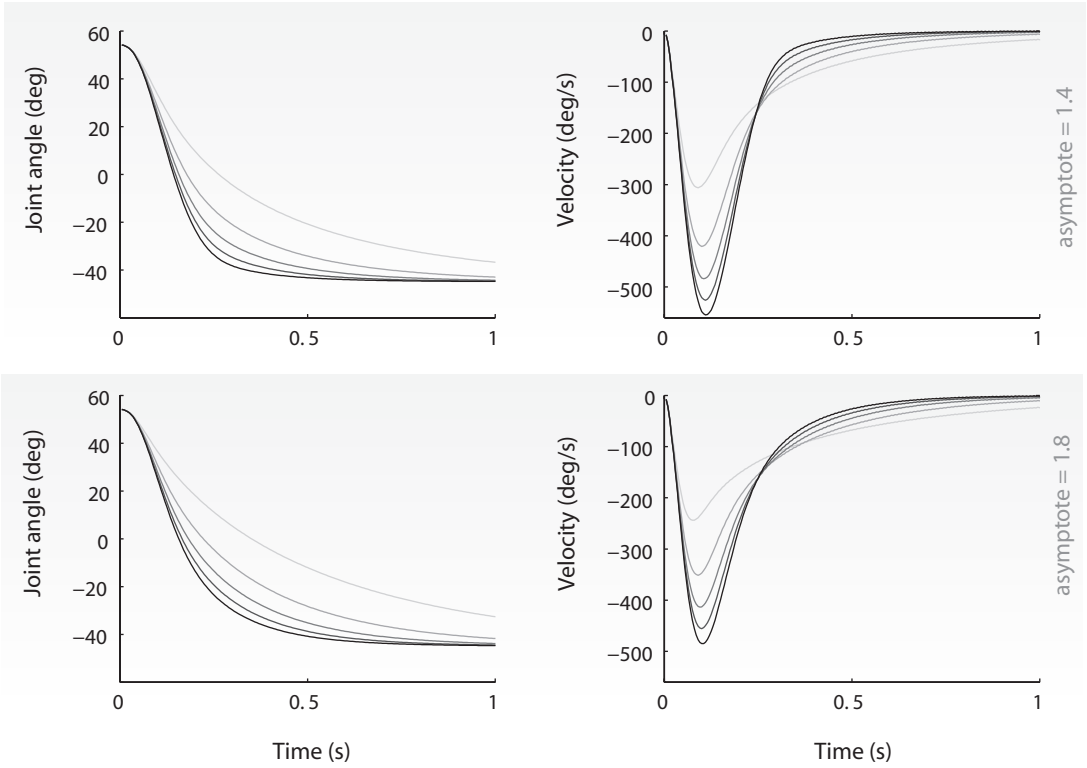

Figure 3.24: Movement kinematics for different damping parameters $a = b \in \{0.2, 0.4, 0.6, 0.8, 1.0\}$. The top row uses an asymptote for muscle lengthening velocity of 1.4, the bottom row uses a value of 1.8. Damping increases with larger asymptote and decreases with larger values of a, b.

ah, bh	$T(s)$	$t_{v_{peak}}(s)$	$v_{peak}(deg/s)$	asymptote
0.2	1.135	0.035	310.51	
0.4	0.670	0.060	425.57	
0.6	0.480	0.060	491.13	1.4
0.8	0.370	0.060	532.26	
1.0	0.290	0.065	561.92	
0.2	1.325	0.025	248.88	
0.4	0.815	0.040	356.55	
0.6	0.610	0.050	420.39	1.8
0.8	0.495	0.050	461.87	
1.0	0.430	0.060	491.81	
human	0.118	0.077	975	human

Table 3.1: Kinematic features of joint movements over 100 degrees for different Hill-type damping parameters.

3.4 Results: Open-loop control

Before moving on to feedback control in the framework of the EP hypothesis, the following sections demonstrate the usefulness of non-linear muscle properties in an open-loop control scheme.

3.4.1 Pulse-step muscle activation

The damping characteristics of muscles have interesting consequences for the optimisation of control signals. To illustrate this point, we implemented a simple control strategy that activates each of two antagonistic muscles using rectangular pulses of amplitudes $a_{1,2}$ and durations $d_{1,2}$, with a parameter t_2 specifying the onset latency of antagonist activation (see figure 3.25). Pulse control has been used in several studies to reproduce various types of human movements (Barto, 1999; Barto et al., 1999; Karniel and Inbar, 1999).

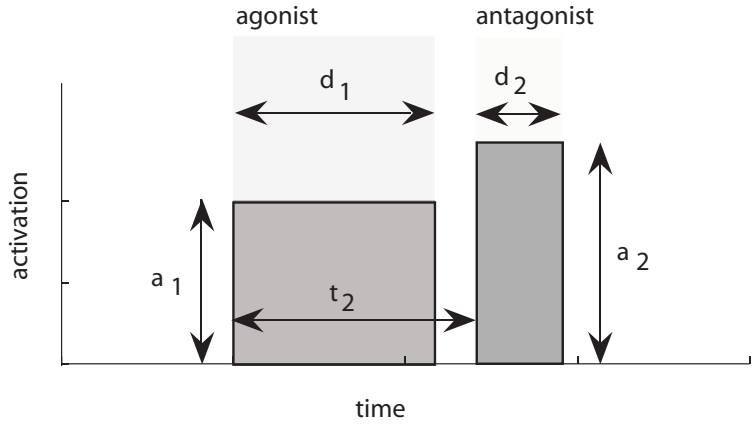

Figure 3.25: Parameters used to describe open loop pulse activation: amplitudes $a_{1,2}$, durations $d_{1,2}$, and antagonist latency t_2.

The relatively small number of control variables allows for an exhaustive evaluation of all possible control strategies against an optimality criterion or *fitness function*. The resulting search space, hereafter referred to as *fitness landscape*, can then be analysed in terms of features like ruggedness or linearity of the regions of best performance. Also, an evolutionary algorithm can be used to identify the globally optimal control strategy in this fitness landscape. The particular evolutionary search algorithm used in this thesis is described in the following section.

3.4.2 Evolutionary algorithm

A simple, spatially distributed genetic algorithm (GA) was used to evolve the parameters of muscles, reflex models and other control mechanisms, such as the pulse-step commands in the following experiments. The algorithm is simple. From a given neighbourhood in a two dimensional array of real-valued genomes, three are randomly chosen and ranked in a tournament according to their fitness. The two best ones create an “offspring” through recombination and mutation. This new genome then replaces the loser of the tournament with a probability for elitism. At maximum elitism the loser is replaced only if the fitness of the new offspring exceeds its own. With

decreasing elitism the probability of the losing genome to be replaced irrespective of its fitness increases. Recombination is realised with a two-point crossover operator, and mutation as a random Gaussian vector displacement of the real-valued genomes. Both, the probability of mutation for an individual gene, as well as the maximum displacement, are parameters of the GA. Components subject to mutation are clipped to values within the interval $[0, 1]$.

An incremental approach to evolution is used in some experiments. Firstly, muscles and control systems were sometimes evolved to produce solutions to a series of increasingly complex evaluation tasks. For example, the task might initially require the production of movements of only one amplitude and speed. Once this is achieved, the task is then expanded to include several different amplitude and speed conditions. Equally, a system can be optimised for single-joint movements first, and then evolved further for multijoint movements. Secondly, some evolutionary parameters (mutation probability and amplitude) were automatically decreased over the course of an evolutionary run to allow for the population to converge on and optimise the best solution it had found so far. The parameters of the genetic algorithm and their ranges are listed in the appendix 3.6.

3.4.3 Flexibility

Figure 3.26 shows a fitness landscape in which the performance criterion consisted of reaching for and stopping at a target position of 45 degree flexion at any point during a 2 s trial. In order to show the whole search space, we somewhat arbitrarily fixed the amplitudes $a_{1,2}$ to values of 0.2, after initial experiments showed that such a setup still provides for a range of successful control strategies.

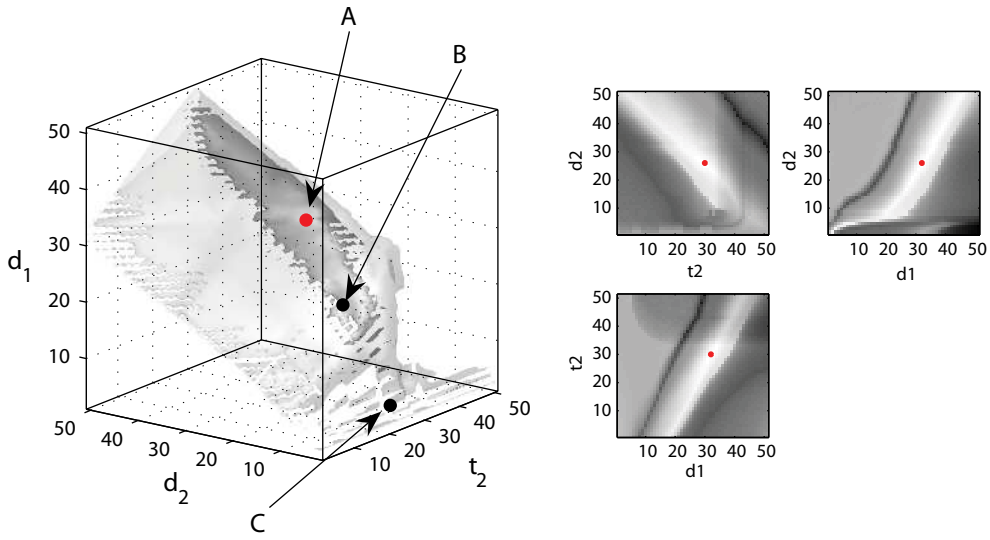

Figure 3.26: Left: isosurface of fitness landscape at fitness levels of 95% (dark) and 80% (bright). Point A shows the overall peak of the surface. B corresponds to a movement that maximizes velocity, while C minimizes energy. Right: slices through the peak of the same fitness landscape.

Several interesting observations can be made from this case of unconstrained goal-directed movement. Firstly, the region of good performance spans a considerable range in each of the three

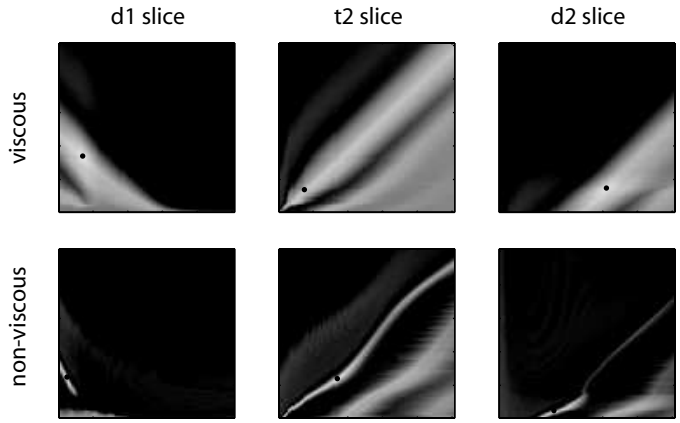

Figure 3.27: Slices through peaks of fitness landscapes for maximising velocity while minimising overshoot. The top row includes viscosity, the bottom row does not. Horizontal and vertical axes both measure time in the interval 0–50 ms. Asymmetries, as observed in the t2 slice for example, are artefacts of the experimental setup and physics engine. For strong accelerations the joint was able to bounce off one of its limits and preserve enough energy to still reach the target (after already having passed it once). Since the fitness function did not punish such behaviour, these control strategies show up as local maxima in the fitness landscape.

remaining dimensions. One can pick almost any value for one of the parameters and will find a combination for the other two that produces a good strategy. In other words, there is a continuum of valid strategies all of which will move the joint towards the desired position, but each having different kinetic or kinematic properties. Movements will differ in terms of velocity, stiffness or energy required. For example, the point marked B corresponds to the fastest movement in this space, while point C marks the one using least energy (measured as the integral over muscle activation). Thus, compared to the stereotypical behaviour of, for example, a PD controller, by using this model one gains flexibility with respect to the details of a movement, while introducing only few additional parameters to be chosen (by either a controller or a more constrained optimisation procedure). Secondly, although the model is highly non-linear in all its properties, good performance within the fitness landscape is found along near linear regions. This simple relationship between parameters would make it easy to create a controller that can find and move along the range of all optimal strategies.

3.4.4 Robustness

In terms of control signal optimisation, the viscous property of the Hill-type muscle model also shows as increased robustness to noise or increased "searchability" of the fitness landscape, a property of interest for evolutionary robotics for instance. Figure 3.27 compares the fitness landscapes of the muscle model with and without the viscosity term for an optimisation that maximises velocity while minimising overshoot. The slices shown were produced by finding for each model the global peak in 5-dimensional parameter space $(a_{1,2}, d_{1,2}, t_2)$ and subsequently fixing two of the parameters (amplitudes $a_{1,2}$) to the values found at the optimum. The resulting slices therefore show the fitness landscape around the optimum in the remaining three dimensions.

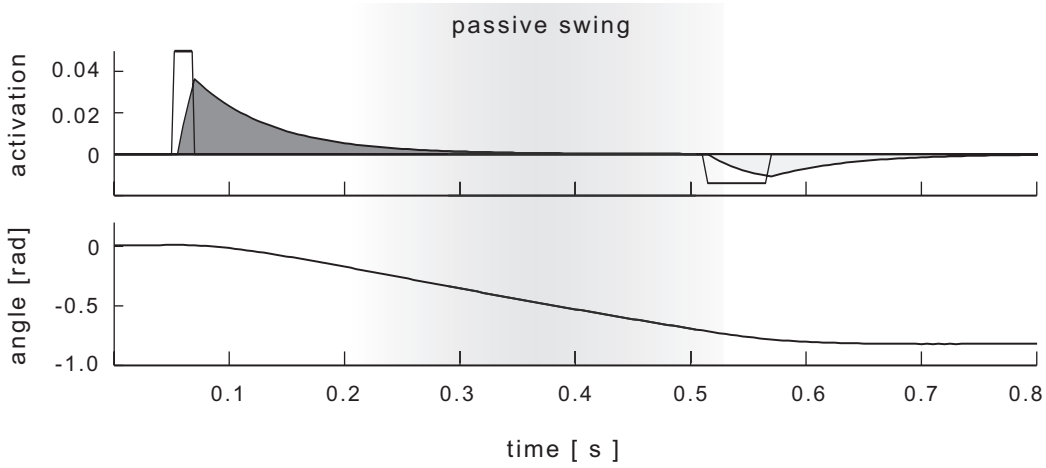

Figure 3.28: Trajectory resulting from typical control signals evolved to minimise energy. Top: input pulses and resulting muscle activations (filled areas). Bottom: joint position. In the highlighted range, muscles are inactive and the joint swings passively.

As can easily be seen, without viscosity the regions of good fitness are much narrower. For the optimisation procedure this means increased difficulty of finding the global optimum. It can also be interpreted as robustness to noise in the control signal. In the viscous model a slight perturbation away from the optimum will still produce relatively good results, while in the non-viscous case performance is easily lost completely. Intuitively this is easy to understand. In the non-viscous case, the antagonist activation has to be precisely timed and scaled such that at the target position forces cancel out exactly and the joint comes to a halt. Any remaining forces not counteracted completely by the antagonist will move the joint away from the target. In the viscous model however, because of its damping effect, small remaining forces will fade quickly and the joint will come to a stop near the target position.

3.4.5 Efficiency

Motorised actuators have to be powered throughout a movement. Even compliant actuators will have to make motors move to simulate a zero force trajectory, i.e. a purely passive swing. Muscles, however, allow for more efficient movement through bi- or triphasic pulse patterns. Minimal muscle activations are sufficient to accelerate and decelerate the joint towards a desired position. This is possible, however, only because antagonistic muscles don't work like springs. That is, in their passive state they don't have to work against each other's resistance. Figure 3.28 is an example of control signals optimised for minimal energy use. Clearly, throughout a large part of the movement neither muscle produces any force and the joint is passively swinging towards its desired position.

3.4.6 Multijoint movements

The movements and open-loop control signals presented so far are clearly oversimplified when compared to natural movements involving many interacting joints. It is striking though, that simple pulse activations, appropriately scaled and timed, allow for well-behaved movement trajec-

tories when combined with non-linear muscle properties. In order to investigate if the increased robustness and flexibility also translates to more complex scenarios, we used the same approach of control signal optimisation to generate motions of two joints (elbow and shoulder). We also enabled gravity and included a static activation level in the control signals that could compensate for its effect. Figure 3.29 presents optimised trajectories in two different conditions. The elbow joint is always required to produce a flexion of 45 degrees. However, in scenario 1 the shoulder moves in the opposite direction, while in scenario 2 it moves in the same direction.

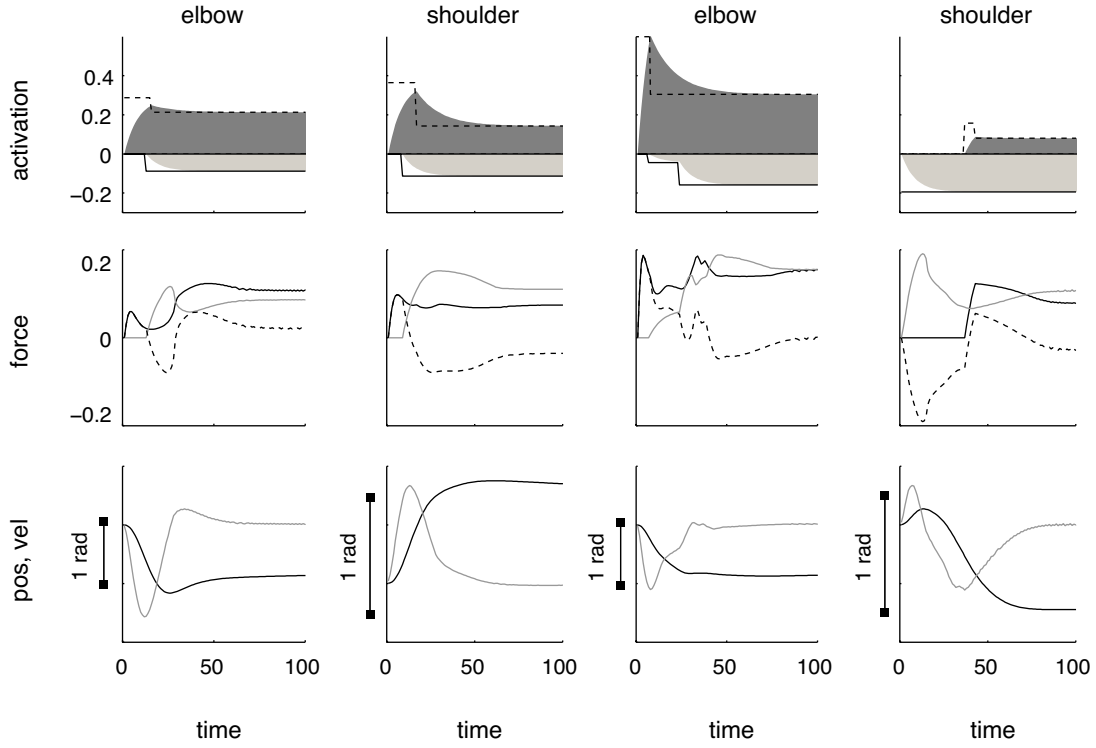

Figure 3.29: Shoulder and elbow trajectories optimised for maximising velocity while minimising energy. The first two columns correspond to scenario 1 (synergistic), the last two columns to scenario 2. Top: pulse-step commands and muscle activations. Middle: muscle forces (solid) and net force (dashed). Bottom: position and velocity.

Both cases were easily evolved and produced trajectories whose final positions corresponded to the desired targets. The figure shows that in the first case the velocity profiles resemble smooth bell-shapes, while they are more jerky in the second case. The reason for this effect are the interaction torques arising from the mechanical coupling of the two joints. In the first scenario movement of the shoulder creates interaction torques in the elbow that are 'synergistic', i.e. support the intended movement, while in the second case the torques counteract movement in the desired direction. It is thus clear that the simple scheme of open-loop control employed here is insufficient for multijoint movements. In fact, it is one of the big open questions in motor control whether the (human) central nervous system uses an internal model of the body to calculate control signals that account for its dynamics, or if a well-designed neuro-musculoskeletal system itself could perform the necessary 'morphological computations'. Chapter 4 will look at equilibrium-point control in the form of the λ-hypothesis to evaluate whether the latter is possible in the case of both single- and

multijoint movements.

3.5 Discussion

In this chapter it was demonstrated that a musculoskeletal model, controlled in open-loop mode with static input signals, produces a dynamical landscape in which an equilibrium of joint position emerges. The stable equilibrium point can be shifted across the range of the joint through differential muscle activation, and its stiffness can be modulated by varying the level of co-activation. It was further shown that the same type of inputs allow for control of the damping properties of the system. Changes in the viscosity affect the system's stability when responding to external perturbation as well as the velocity of movement towards the equilibrium. Thus co-activation of antagonistic muscles simultaneously leads to an increase of stiffness and to faster movements, a strategy also found to be used by humans (Gribble et al., 2003).

The muscle model implemented in this chapter consisted of two symmetrically arranged antagonistic muscles acting on a one degree-of-freedom hinge joint. Although this setup is simpler than the configuration of muscles in a real elbow joint, the resulting dynamics can be considered a subset of the behaviours a more realistic model could produce. Simplifications, such as the exclusion of a tendon element, calcium-dynamics, and non-linear moment arms, were justified by comparing the dynamics of the resulting systems to those of the complete model. In going beyond previous work in the field, it was shown that the qualitative features described above are not dependent on the presence of these components. However, various relationships between motor command and steady-state behaviour were demonstrated to be non-linear when they are included. In the simpler model, EP isocurves and stiffness along those isocurves vary linearly. This could be exploited by a simple control scheme in which a single number, the flexor-extensor activation ratio, determines joint position, while their absolute values determine joint stiffness. The question then arises as to how position and stiffness are controlled when these relationships are non-linear, as is likely the case in more complex, asymmetrical multi-muscle systems. The traditional explanation would be that the brain learns to represent these non-linearities using internal models, which can then be used to adapt the motor commands appropriately. Another possibility is that spinal reflexes are organised such that these relationships are effectively linearised from the perspective of higher levels of the control system. Schemes for using reflex connections to ensure independent control of position and stiffness in the presence of muscle asymmetries or changing moment arms have been demonstrated in the past (Feldman, 1993; Bullock and Grossberg, 1991).

Qualitatively, the results of this chapter confirm findings by other researchers for both natural human movements (see e.g. Gribble et al., 2003) and simulated muscle models. Kistemaker et al. (2007a), for example, studied open-loop control using a Hill-type muscle model that differs from the one studied here in details of the implementation of the constitutive relationships, and includes the simulation of not only mono- but also bi-articulate elbow muscles. Also, parameters describing the lumped muscle models in that study were chosen with the aim of matching the combined effect of specific human muscles. Despite this difference, their results regarding the existence of stable equilibria and the relationship between co-activation and stiffness are very similar. Only the shape of the net-torques and EP maps differs between the models, but not their range. Stable control

of joint position through statically co-activated opposing muscles was also shown analytically in (Giesl and Wagner, 2007). Here, the authors used a Hill-type model that is of comparable complexity to the one presented in this chapter, but modified to be twice differentiable. They determined the basin of attraction of stable equilibria in joint space and found large ranges of self-stabilisation. The experiments conducted in this chapter extend the aforementioned studies by identifying model components that are not required to generate the qualitative behaviour, and by showing how steady-state behaviour varies with changes in moment arm and muscle length functions.

Comparing the simulations in this chapter to the range of models found in the wider field of biological motor control, they are at the same time more complex than lumped muscle models and less complex than those aiming for higher levels of biological accuracy. For example, Contreras-Vidal et al. (1997) have studied independent control of joint position and stiffness using a muscle simulation that only incorporates a quadratic force-length relationship and joint friction, but neither passive (parallel or serial) elasticity, nor Hill's equation for velocity-dependent force production. An equally simple model was used by Barto et al. (1999) to study predictive motor control based on delayed sensory feedback. Here the authors simulated muscles as spring-like actuators with non-linear damping in the form of a fractional power law, which was intended to approximate the combination of non-linear muscle properties and spinal reflex mechanisms. On the other extreme one finds high-fidelity studies such as the one presented in (Garner and Pandy, 2001). Here, three-dimensional reconstructions of muscles and bones were derived from Computed Tomography images and cadaver data to model the complete human upper limb, including seven bones, thirteen degrees of freedom and 42 muscle bundles. Also, in-vivo force measurements were used to estimate the parameters of a full Hill-type model for each muscle group simulated. The goal of this study was anthropometric fidelity itself, that is, to match human data as accurately as possible. Studying movement control at an intermediate level of detail, as chosen in this thesis, can be beneficial because it ensures that observed features are neither due to oversimplification, nor specific to human anatomy and physiology.

While qualitative features like the range of stiffness and bell-shaped velocity profiles were successfully reproduced in this chapter, this is not true for the kinematic details of movement transients. This should not come as a surprise, as it is known that natural movements are not the result of static muscle activations. Motor neurons are always modulated by spinal reflex circuits and are usually silent at the end of a movement. EMG recordings also show that antagonistic muscles show triphasic burst patterns, whereby a joint is accelerated, decelerated and stabilised by three consecutive transient activations. The next chapter will therefore explore whether muscles and simple reflex dynamics can interact to produce more realistic motion.

An interesting finding in this chapter was the sensitivity of musculoskeletal dynamics to assumptions about the moment arm of the muscles modelled. It was found that for certain functions relating moment arm to joint angle the system would exhibit unstable dynamics. Such models were not further considered here or in the following chapters. However, it is an interesting question whether evolution has shaped the attachment of muscles to the skeleton such that only stable equilibria will ever emerge. There is some evidence that this is not the case (Akazawa and Okuno, 2006). An interesting avenue to be explored in future work are the implications of unstable dynamics at the

muscle level for control systems at a higher level.

On the conceptual side, the emergence of a controllable equilibrium point is relevant for hypotheses about the mechanisms of coordination in complex systems like the human body. If posture and movement are seen as the result of joint level EPs and the shifting thereof, then control *arises from* the dynamic organisation of the system rather then being *enforced upon* it. One could say that through musculoskeletal dynamics a new level of description (and control) comes into existence in the domain of motor behaviour. There is no special mechanism at work, such as a feedback controller, and no representation of goal states. But while on the level of muscles one can only talk about individual muscle forces, in the combined system movement can be described by shifts in equilibrium position. In effect, a new controllable variable is created that reduces the degrees of freedoms to be considered during coordinated motion (in this case from two force variables to one positional variable). This is what Bernstein referred to as *synergies* or *coordinative structures*. Kelso explains:

> "During a movement, the internal degrees of freedom of these functional groupings are not controlled directly but are constrained to relate among themselves in a relatively fixed and autonomous manner. The functional group can be controlled as if it had many fewer degrees of freedom than comprise its parts, thus reducing the number of control decisions required" (Kelso and Tuller 1984, p. 325).

Central commands, in this view,

> "serve an organising function by biasing lower-level systems toward producing a class of actions, but the lower level system can adjust autonomously to varying contextual conditions" (Kelso and Tuller 1984, p. 330).

Thus, rather than controlling low-level actions directly, central influences are thought to set up and modulate a dynamic organisation, the result of which is the autonomous evolution over time of the system's behaviour. This synergy is functional, i.e. dynamically created for a given task at hand, rather than fixed once and for all. Only when co-activated, for example, does the antagonist system create an EP. Without co-activation the system is loose and could be controlled with individual pulse signals, as was demonstrated in this chapter. The tuning of synergies provides flexibility in the execution of an action with minimal amount of additional control. The increase of co-activation, for example, changes the system's behaviour around the EP such that perturbations are more efficiently rejected, without explicitly calculating the correct response to a given perturbation. Finally, equifinality, the property of a system to reach the same position with varying trajectories from different initial conditions, is the result of the lower-level musculoskeletal system having formed an attractor. In this way it provides trajectory "planning" for free, without burdening a central controller with this problem.

In summary, this chapter has demonstrated that many qualitative features of the steady-state behaviour of single-joint movements can be reproduced with a minimal muscle model that incorporates the most fundamental non-linear characteristics of force production. As the model exhibits the desired equilibrium behaviour as well as a sufficient level of biological plausibility (correctly reproducing, for example, levels of joint stiffness as a function of co-contraction), it is considered appropriate for studying the assumptions and implications of the EP hypothesis in the next chapter.

3.6 Appendix: Genetic Algorithm parameters

The following table summarises the parameters of the spatially distributed genetic algorithm and their ranges. For an overview of the algorithm see section 3.4.2.

	min	regular	max
number of generations	100	1000	2500
population size	25	100	225
mutation rate	0.1	0.5	1.0
mutation amplitude	0.001	0.1	0.25
recombination rate	0	0.05	0.1
elitism probability	0	0.5	1

Table 3.2: Parameters of the genetic algorithm and their ranges. Where the term "rate" is used, this is equivalent to a probability, i.e. a value in the range [0, 1].

As a rule of thumb, experiments with a larger number of genetically encoded values used larger populations and were evolved for longer. Also, optimisation occurred in three stages: a short initial exploration with maximum mutation rate and amplitude (1.0 and 0.25 respectively), followed by a long period with "regular" mutation rate and amplitude (0.5 and 0.1), and finally a short period during which the GA was allowed to converge to the peak of the best solution it had found so far (0.1 and 0.001). The initial exploration and final convergence phases typically lasted for 10% of the maximum number of generations. Where an experiment diverts from the above values, this will be stated in the corresponding section.

Chapter 4

Feedback control

This chapter analyses the dynamics of the muscle model developed in the previous chapter when coupled to a model of the stretch reflex based on the λ-formulation of the EP hypothesis. In particular, it is studied whether such an EP model can reproduce the kinematics of natural (human) arm movements under varying speed and amplitude conditions. We specifically investigate the ability of the coupled system to deal with feedback delays, to produce triphasic muscle burst patterns despite simple monotonic inputs, and to produce smooth multijoint movements. Also, the relative importance of various feedback modalities is examined.

4.1 Introduction

It is clear that if muscles were pure force generators, complex muscle activations would be needed to create the torques that propel a limb to a desired position. Any central command aiming to specify these torques directly would have to take into account the dynamic properties of the various muscles involved in the movement, the dynamics of the pools of motor neurons innervating those muscles, as well as the inertial properties of the limb and any external forces acting on it (the latter of which depend on the orientation of the limb in space, to complicate the matter further). It has long been recognised though, that the viscoelastic properties of muscles and reflexes can serve so as to allow for a different mode of operation, in which muscle dynamics are exploited to simplify the inverse dynamics problem (Feldman, 1966; Nichols and Houk, 1976). As shown in the previous chapter, muscle stiffness and length-dependence create an equilibrium position (EP) at the point where the forces of antagonist muscles cancel each other out. This property has lead to the formulation of the equilibrium-point hypothesis, which in its simplest form implies that the central nervous system (CNS) can encode posture, i.e. joint angles, in a single ratio of agonist to antagonist activation. Several types of equilibrium-point controllers have been suggested as models for movement production that exploit the viscoelastic properties of muscles.

4.1.1 Servo-hypothesis

Based on the neurophysiology of the tonic stretch reflex (see figure 4.1), Merton (1953) proposed one of the first motor control hypotheses. He suggested that the CNS uses the γ-system to implement a servo-mechanism controlling muscle length. In his servo scheme, descending signals were thought to modulate the activity of γ-neurons that innervate stretch sensitive muscle spindles. Spindles are proprioceptors which convey sensory information about muscle length and velocity by firing at a rate proportional to the stretch of the intrafusal muscle fibre that their sensory endings spiral around. This muscle stretch proportional feedback is then transmitted via Ia-interneurons to the α-motorneurons of the receptor bearing muscle. Activity of α-neurons in turn leads to contraction of muscle fibres, which generate force and thereby counteract the stretch that originally activated the spindles. The closed loop of the tonic stretch reflex therefore acts as a negative feedback system that minimises muscle stretch. Now, the role of the γ-neurons is to modify the sensitivity of the muscle spindle, i.e. to increase the probability of action potential firing. γ-neuron activity therefore has an effect similar to actual stretch of the muscle. Merton suggested that central modification of spindle sensitivity via γ-neurons acts to effectively set a resting length towards which the tonic stretch reflex will drive the muscle. Crucially, Merton assumed this system to work as a perfect servo in which *any* external load would be balanced by an increase in muscle force, such that muscle length would not change at all. Although attractive for its simplicity, the theory had to be abandoned after experiments failed to support two of its assumptions. Initially, it predicted that γ-activity should precede that of α-neurons. It was shown however by Vallbo (1971) that both are activated simultaneously. As a result, an extension of the model was proposed in which co-activation of both pathways meant that movement was initiated via direct control of α-neuron activity, while the responsibility of the γ-neuron was to keep spindles from becoming slack, i.e. to maintain sensitivity while the muscle contracted, and to counteract perturbations (this version is also known as servo-assist). Nevertheless, in order to perfectly reject external loads, the model relied on a very high feedback gain of the stretch reflex. It was shown however that this was not the case (Matthews, 1970; Vallbo, 1970).

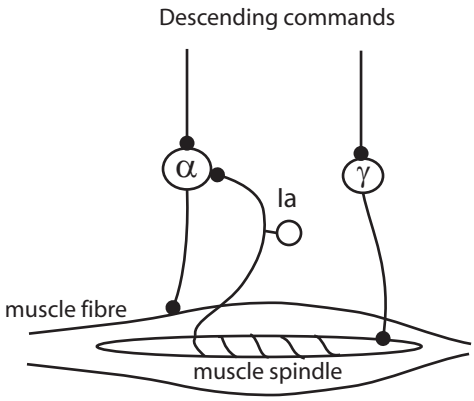

Figure 4.1: The tonic stretch reflex. Shown are the α-motoneuron that activates the muscle fibre, the γ-motoneuron modifying spindle sensitivity, and Ia afferents responding to muscle stretch well as its rate of change.

4.1.2 α-model

Based on the observation that deafferented monkeys deprived of ongoing visual feedback could still produce goal-directed arm and head movements, even in the presence of initial perturbations, the hypothesis of *final position control* suggested that the CNS specifies directly and exclusively the final position of a movement, while the details of the trajectory are the result of the inherent dynamics of the muscles and limb (Polit and Bizzi, 1979). More specifically, given that the movements were carried out without peripheral feedback, i.e. in the absence of a functioning stretch reflex, it was suggested that the final position was defined by setting the spring constants of antagonist muscles via direct control of α-motoneurons. Further experiments (Bizzi et al., 1984) revealed that the shift in equilibrium position was not in fact instantaneous. Instead, the CNS was found to specify a continuous *virtual equilibrium trajectory*, such that interrupted movements would be driven towards intermediate positions. According to this α*-formulation of the EP hypothesis*, a central planner directly controls reciprocal and co-activation of α-motoneurons, the final common pathway, in order to specify an EP along with a stiffness about that position. Even though the α-formulation of the EP hypothesis avoids some of the pitfalls faced by the servo-theory, it is not completely satisfactory either. Although monkeys and humans are able to produce pointing movements without proprioceptive feedback, motor performance is significantly degraded, with trajectories becoming much more erratic than in normal subjects. Also, subjects were highly trained to operate under the deafferented condition, and even then only large amplitude movements of moderate speed and low accuracy were considered. It is therefore clear that reflexes should play an important role in any model of motor control.

4.1.3 λ-model

While the α-model emphasises the mechanical properties of muscles in establishing an equilibrium position, the λ-model recognises the importance of reflex contributions. It is based on observations by Matthews (1959) and Feldman (1966), which showed that a fixed level of descending input to the spinal cord is associated not with a a corresponding level of muscle activation, length or force, but rather with an invariant force-length relationship (IC), i.e. a continuous, load-dependent curve of stable equilibria. Different descending signals, according to these findings, establish a threshold length at which muscle activity is initiated. In the supra-threshold range of muscle lengths, activation increases non-linearly with the difference between threshold and actual length. In contrast to the α-model, this non-linear relationship is not attributed solely to muscles however, but to the combination of muscles and the tonic stretch reflex.

The physiological basis for threshold control is illustrated in figure 4.2. Each α-MN receives both descending inputs as well as afferent feedback related to muscle length (also see figure 4.1), and is recruited when its membrane potential exceeds its electrical threshold. When a muscle is stretched, the resulting afferent influence will lead to an increase in membrane potential until the muscle reaches a length at which the threshold is exceeded and the motoneurons starts firing. The resulting activation produces muscle shortening and thus tends to move it closer to the threshold length. If central facilitatory input is added, either directly or through interneurons and the γ-pathway, that threshold will be reached at a shorter muscle length. Through this integration with muscle-length

dependent feedback at the membrane, descending signals therefore become spatial variables; they specify a change in muscle threshold length λ. It is important to stress the difference between the α- and λ-model here: while the former suggests that central controls change motoneuron *output activity*, the latter suggests the modulation of motoneuron *excitability*.

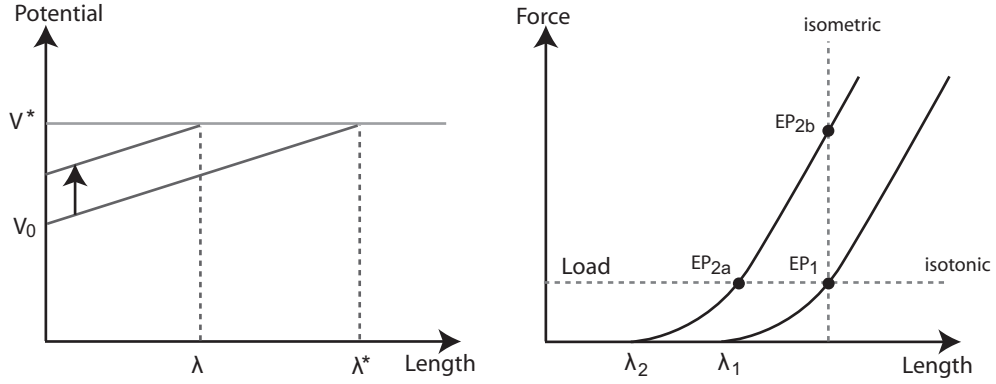

Figure 4.2: Left: neurophysiological basis of changes in threshold length λ. Central input to the α-MN means that its potential V reaches its threshold V^* not at muscle lengths λ^*, but at the shorter length λ. Right: changes in λ shift the invariant characteristic (IC). At the same load level the system reaches a different equilibrium (EP_{2a} instead of EP_1). If muscle length is held constant (isometric condition), the system reaches EP_{2b} instead.

The effect of threshold control on the steady-state of the muscle-reflex system is illustrated in 4.2. The system is in equilibrium when muscle force equals external load. Any temporary perturbation (stretch) of muscle length will be rejected by the reflex and muscle properties that are responsible for instantiating the IC curve. If the external load changes while the threshold length remains constant, both muscle force and length will settle on a different equilibrium point along the IC, producing involuntary movements as a result. Voluntary movements on the other hand are produced by a shift in the threshold length required to elicit the stretch reflex. After such a shift, the previous EP is now a deviation from the newly established EP, and the same mechanism responsible for stabilizing posture will move the muscle towards a new position.

In the case of multiple muscles, the λ-model proposes a central command that consists of two components: a reciprocal part R that shifts the reflex threshold of antagonistic muscles in the same direction (in joint space) to control EP position; and a co-contraction part C that shifts the thresholds in opposite directions so as to increase or decrease stiffness at the EP. It is important to note that these two commands do not uniquely specify desired position and stiffness (Feldman and Latash, 2005). Both can be modulated further by non-centrally specified components of the stretch reflex. Also, a shift of threshold length can imply both a change in position as well as a change in force output, if external loads are taken into account (e.g. isometric contraction).

The EP-hypothesis proposes that smooth movements are produced through simple monotonic (usually ramp-shaped) shifts of threshold lengths. This is one aspect of the model's attractiveness when compared to direct force control. The complex torque patterns needed for certain movements are thought to be the result of inherent muscle and reflex dynamics and need not be taken into account in the control of movements. If the required EP shifts were of complex shape,

not much was gained over alternative hypotheses which claim that the brain uses internal models of the body to control muscle forces directly. Several studies have attempted to refute the EP-hypothesis based on reconstructions of the equilibrium trajectory from experimental data (Latash and Gottlieb, 1991; Gomi and Kawato, 1996; Bellomo and Inbar, 1997) or from considerations of optimal control strategies (Hogan, 1984). While some studies concluded that complex N-shaped equilibrium shifts are necessary to account for empirically observed patterns of multijoint movement, their results are questionable as they used over-simplified musculoskeletal models. In fact, when non-linear muscle behaviour is taken into account, simple ramp-shaped control signals are sufficient to produce fast and smooth movements in line with empirical measures (Gribble et al., 1998). As muscle non-linearities can contribute significantly to movement dynamics (Brown and Loeb, 2000; van Soest and Bobbert, 1993) other studies using simplified linear models (Popescu et al., 2003) can equally be disregarded as criticism of the EP-hypothesis.

Several clarifications and extensions of the λ-model have been proposed over the years to account for a range of experimentally observed movement dynamics. The formulation by Feldman (1986), for example, includes velocity feedback to improve damping in the system. A co-contraction command was added to allow for control of stiffness, which also affects movement speed (Gribble et al., 1998). In order to explain the fastest arm movements, a velocity reference signal was proposed (de Lussanet et al., 2002; McIntyre and Bizzi, 1993), such that the error between a desired velocity input and actual velocity was added to the threshold offset (similar to the proportional term in a PID controller). Kistemaker et al. (2006, 2007b) have shown that a detailed muscle model (including non-linearities and a tendon component) in conjunction with the mentioned extensions to the λ-model (as well as use of intermittent feedback), is able to produce fast goal-directed arm movements with stiffness in the range of experimentally observed measures. In this chapter we compare Kistemaker's model to increasingly simple abstractions, in order to find the minimal set of features necessary to reproduce fast movements. The different models are evaluated along three dimensions: the exploitation of inherent dynamics in feedback control; the simplicity of control signals required; and their biological plausibility.

4.2 Methods

In order to compare different muscle-reflex models with experimental data, reference trajectories are created that match kinematic markers extracted from human data (Kistemaker et al., 2006), such as duration of movement or peak velocity. The assumption used to decide on the form of the reference trajectory is that movements should be smooth and exhibit the classic bell-shaped velocity profile observed in human movements (see chapter 2). Consequently, the *minimum jerk* criterion (described below), a well established concept in optimal control theory, is employed as a reference for the optimisation of muscle model parameters and feedback gains. The optimisation proceeds as follows: first, a desired movement of given amplitude and duration is chosen and a corresponding minimum jerk trajectory generated. A muscle-reflex model is then evolved using a simple GA (see section 3.4.2), in which the difference between minimum jerk and actual trajectory serves as the fitness criterion. To test whether simple control signals are sufficient to match human data, a simple linear ramp is used to input the desired joint angles. The minimum jerk trajectory is used only as the desired output, not as input to a controller. A given model is evaluated on a

series of different movements to avoid overfitting and individual performances are combined into an overall fitness.

4.2.1 Minimum jerk

In (Hogan, 1984) dynamic optimisation was used to find the input to an EP-controller that would produce the smoothest motion from an initial to a final equilibrium position. Smoothness H of a trajectory $x(t)$ was defined by integrating the rate of change of acceleration (jerk) of the motion over the desired duration T:

$$H(x(t)) = \frac{1}{2}\int_{t=0}^{T} \dddot{x}^2 dt \tag{4.1}$$

The function which corresponds to the minimum of this measure was then used as the input trajectory for an EP-controller. Given initial position x_0, final position x_f, and assuming that at these positions the system is at rest, the minimum jerk trajectory was found to be:

$$x(t) = x_0 + (x_f - x_0)(10(t/T)^3 - 15(t/T)^4 + 6(t/T)^5) \tag{4.2}$$

The corresponding velocity profile can be found via simple derivation:

$$v(t) = 30d\frac{t^2}{T^3} - 60d\frac{t^3}{T^4} + 30d\frac{t^4}{T^5} \tag{4.3}$$

with substitution $d = x_f - x_0$. In Cartesian space, when calculated for individual spatial components, such trajectories form straight-line paths with bell-shaped velocity profiles. For the purpose of experiments in this chapter, however, minimum jerk-trajectories were used only to maximise smoothness on the joint level, as we are not concerned with the inverse kinematics problem. Also, in contrast to (Hogan, 1984), minimum jerk trajectories are used only as a reference for the optimisation of muscle-reflex parameters, not as the actual input trajectory. As simple control signals are desired, input to the EP-controller is always a monotonic ramp shift of given amplitude and duration.

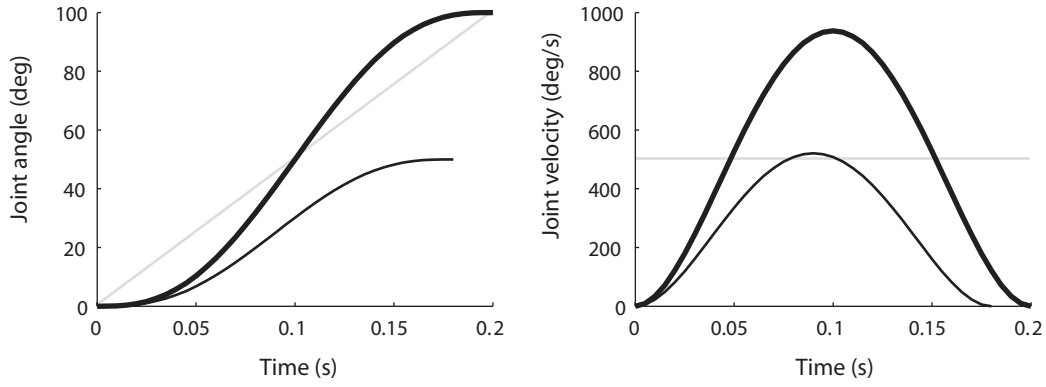

Figure 4.3: Minimum jerk trajectories for two movements of 100° and 50° lasting 0.2 and 0.18 s respectively. Position is shown on the left, and velocity on the right.

4.2.2 Optimisation algorithm

A simple genetic algorithm[1] is used to optimise muscle parameters (shape of the damping function, maximum isometric force), feedback gains, and the onset of the input ramp relative to the minimum jerk trajectory. The muscle model used in this chapter is the simplest found in the previous chapter, which still allowed for EP and stiffness control; namely one with a linear muscle length mapping, constant moment arm, and without calcium dynamics.

Most experiments in this chapter evaluate a muscle-reflex model on at least two movements of different amplitude: one covering 100 degrees over a duration of 0.2 seconds, and another of 50 degrees over 0.18 seconds (as measured experimentally by Kistemaker et al. (2006) in subjects instructed to produce fast movements). The quality, or fitness F, of a muscle-reflex solution was calculated from the difference between actual and desired (minimum jerk) trajectory, scaled into the range $[0,1]$: $F = 1 - |x - x_d|/\pi$. This measure was then averaged over all movements to be optimised in that experiment.

Each experiment was carried out at least five times with different initial conditions to ensure sufficient confidence in the reliability of acquired data. In each experiment the GA was run for 100-1000 generations, during the last 10% of which a lower mutation rate was used to let the algorithm converge on the peak of the best solution found so far. The maximum number of generations was determined heuristically by running the experiment a few times without restricting the duration of the optimisation. In all experiments reported here, fitness would eventually plateau around the same level across repeated runs (with a standard deviation on the order of 10^{-4}% of maximum fitness), and evolved parameters would show similarly low variation. The number of generations at which this plateau was reached, plus an additional hundred generations, was then chosen as the limit for repeated runs that contributed toward statistical results. Since the optimisation procedure reliably plateaued in the same small area of the fitness landscape, it was assumed that running it for longer would not have affected the result. This is important when comparing results from two different experiments. If, for example, two different kinds of models evolve different levels of fitness, we can say with some confidence that this is due to the nature of the controllers themselves, and not a function of how long the controllers were allowed to evolve (though it is possible that the fitness landscapes had different properties, such that one was easier to optimise than the other). The same argument applies to those cases where a satisfactory solution was not found at all. It can not be ruled out that a solution exists in a part of the fitness landscape that the algorithm failed to explore. However, the kinds of control models evolved in this thesis are often very similar to each other, at least in those cases where results are compared directly. They usually differ in only few terms, such as the form of damping employed, or the amount of feedback delay present. Since they were also evaluated using the same fitness function, one can reasonably expect that the resulting fitness landscapes should have similar properties (though this was not explicitly confirmed here). Differences in the ability to find a fitness optimum are therefore implicitly attributed to the form of the evolved controllers in the following experiments. The reader should nevertheless be aware of the above caveats (local minima, differences in fitness landscape properties).

[1] See sections 3.4.2 for an overview and 3.6 for parameter values.

4.2.3 Feedback model

In the EP-controller implemented here, muscle activations are determined from a weighted sum of different open-loop and feedback components. It incorporates the α-model, i.e. direct input to α-motoneurons, the λ-model, and the addition of a desired velocity signal. By clamping the weights of individual components to zero, each of these models can be studied in isolation. Allowing for optimisation of all weights, on the other hand, should find the best combination of these components. The full model was defined as

$$A(t) = a_{ol} + [k_p(L^M(t-\delta) - \lambda) + k_v(\dot{\lambda} - v^M(t-\delta)) - k_d v^M(t-\delta)]_0^1 \tag{4.4}$$

where a_{ol} is the open-loop command, L^M muscle length, v^M muscle velocity, λ the EP threshold offset, δ the feedback transmission delay, and k_i the different feedback gains. The term in square brackets constitutes the reflex contribution and contains the classic λ-model $(k_p(L^M - \lambda) - k_d v^M)$ as well as the error in desired velocity.

Alpha Model

The first and simplest model serves as a control experiment. Muscles are activated using static activations a_{ol} only. The levels of activation required to achieve a desired endpoint are determined using the mapping between differential activation of antagonists and EP positions found in the previous chapter. A controller of this type therefore relies on the existence of such an inverse map. As also observed, activation levels are underdetermined by EP position, as co-contraction (and hence stiffness) has to be chosen as well. This was done using the stiffness maps also produced in the previous chapter. In the case of the muscle model used in this chapter these relationships turned out to be linear. A given EP could easily be found at a unique ratio of agonist to antagonist activation, while the sum of activations determined its stiffness. It is worth noting that this inverse look-up would be much less trivial for muscle models that don't exhibit linear relationships. When more than two muscles are considered, the problem of redundancy would have to be solved as well (Loeb et al., 1999).

Energetically this α model would be suboptimal, as it necessitates constant non-zero activations at the final position to achieve stability. It would also not be in accordance with the observation that EMG levels (and hence muscle activations) are usually zero at the resting pose. Therefore, an exponential decay was applied to activation levels at resting positions, so that force output is zero before and after the actual movement.

Lambda Model

For the reflex contribution, λ thresholds were determined by an inverse look-up of the muscle lengths that correspond to the current point (joint angle) on the virtual EP ramp. The complexity of this inverse mapping depends on the function that describes muscle length as a function of joint angle and the current force output. As in this chapter a tendon-less model was chosen, and a linear angle to muscle length function, this again was simple. In a different model, more complex computation might be needed, but the problem is fundamentally the same. The redundancy in muscle activations was solved by picking the pair with the lowest resulting stiffness. Where a desired velocity reference was employed, it was calculated as the derivative of the corresponding

λ threshold. Conduction delays (0–0.025 s) were added to muscle length- and velocity-feedback with durations depending on the experiment.

The reflex component of the controller on its own, when compared to pure open-loop control, would energetically be more efficient. It avoids the constant muscle activations at the resting pose. It introduces a new complication, however, namely potential instability resulting from long signal delays and large feedback gains (see section 4.3.1). When the reflex component is used along with the open-loop component, the former can be interpreted as the reciprocal R command in the multi-muscle λ-model, while the latter implements the co-contraction command C.

4.3 Muscle-reflex EP control

In the following section the dynamics of antagonistic muscles (as developed in the previous chapter) are studied when driven by equilibrium-point controllers based on the λ-model. The next chapter will then compare this muscle-reflex system with a more abstract model, in which muscles are replaced with a single non-linear spring-damper.

4.3.1 Feedback delays

It is well known that transmission delays can limit the performance of feedback systems by creating oscillations when feedback gains are large. Hidler and Rymer (2001), for example, used a model of the stretch reflex to show the destabilising effect of high motoneuron threshold, gain, and neural transport delays on the ankle. While robotic actuators can be built such that feedback delays are negligible, in humans the limited speed of action potential propagation and the number of synapses connecting central motor commands to final motor output can add up significantly — St-Onge et al. (1997) estimate 14–18 ms. In this section, a muscle-reflex system with feedback delays will be studied for its ability to produce fast movement without such oscillations. The full reflex model is used, including open-loop static activation, error proportional, error derivative and velocity proportional terms. Muscle and reflex parameters were optimised for both the 100° and 50° amplitude movements of a single joint. The system was evaluated eight times with different amounts of feedback delay. For each level, the experiment was repeated five times to produce reliable results.

Figure 4.4 summarises the effect of increasing feedback delay on the relative strength of individual reflex terms. The first thing to notice is that standard deviation is low for all measured quantities, confirming that the optimisation process reliably picked the same optimal solutions. Secondly, performance does not drop immediately for relatively small delays. Although it drops eventually, performance stays within the 99% range for delays of up to 0.025 s. In fact, optimal performance is not found at zero delay, but rather at 0.005–0.01 s. Thirdly, a strong correlation can be observed between the different feedback gains and the length of the delay. The longer the delay, the lower the actual feedback gains, but the higher the level of co-contraction. For increasing feedback delays, the system relies more and more on the inherent open-loop dynamics of the muscle rather than the reflex action.

Figure 4.5 plots the actual joint trajectories for different feedback delays. It confirms that the drop in performance for larger delays is indeed due to oscillations around the EP. The slightly better

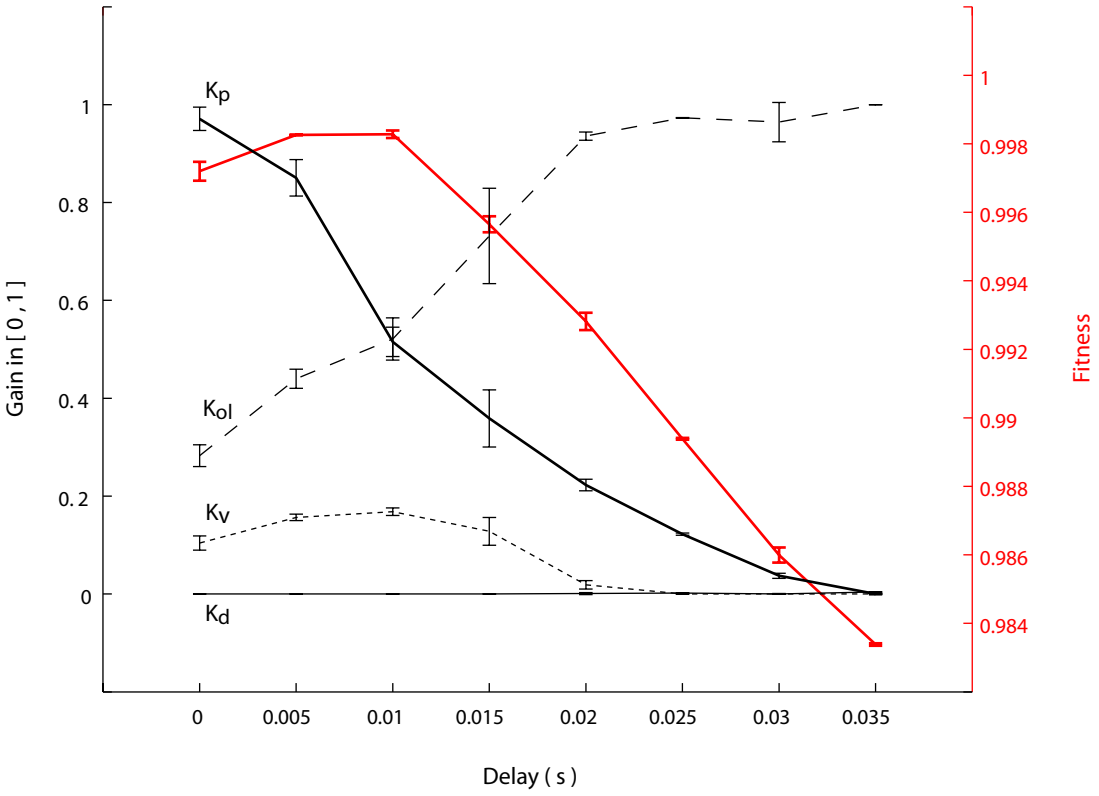

Figure 4.4: Effect of delayed feedback on performance and resulting feedback gains. Proportional gain k_p, derivative gain k_d, velocity reference gain k_v and open-loop gain k_{OL} as well as fitness are shown for increasing feedback delays. Each point corresponds to the mean value over the best individuals from 5 evolutionary runs. A single standard deviation is shown as errorbars at the top and bottom of the gain data points. In case of fitness, two standard deviations are drawn. Feedback gains are expressed as proportions of their upper limit.

performance with small delays, on the other hand, seems to be the result of reduced overdamping close to the target. Without delay, strong muscle damping around zero velocity (see section 3.2.8) leads to an approach towards the target that is slower than that described by the minimum jerk trajectory. The addition of feedback delay, however, implies that the perceived error between target and actual position is greater than that of the non-delayed controller when approaching the target. As a result, more accelerating force is produced for longer (for the length of the time delay), and the same level of reflex damping is arrived at a little later. When tuned just right, the delay thereby counteracts the strong viscosity of the muscle without producing undesired oscillations.

The results suggest that feedback delays, to a certain degree, can be “assimilated” into the musculoskeletal dynamics without impairing, and to some extent even improving performance. Eventually, however, oscillations are unavoidable and the only way to compensate for this effect is to reduce feedback gains and rely on the muscle’s instantaneous attractor dynamics. Similar results have been observed in a model of the spine (Franklin and Granata, 2007). The authors found that reflexes allowed for stability at levels where intrinsic stiffness was insufficient, while also noting that increasing delays required lower reflex gains and greater co-contraction.

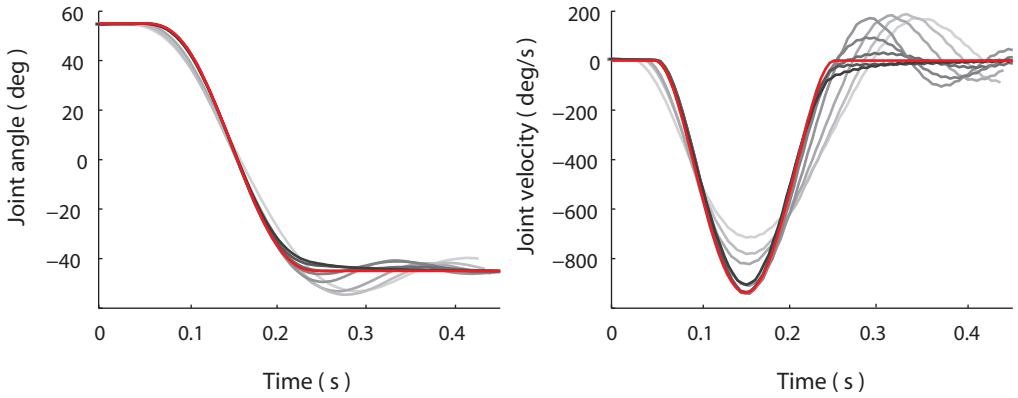

Figure 4.5: Feedback delays. Joint trajectories (left) and velocity (right) of best evolved hybrid controllers for varying feedback delays. Lighter plots correspond to larger delays. Best performance is found with a delay of 0.01 s, with larger values leading to increasing oscillations around the EP.

4.3.2 Feedback modalities

It is still an open question what type of feedback control human spinal reflexes implement, if that's indeed their role at all (see McCrea, 1992, for a review of the controversy concerning reflex circuitry and functionality). Although muscle spindles produce a signal that mixes positional and velocity information, for example, it is not known how this information is employed in the closed loop system as a whole, and whether velocity or error in velocity are significant factors. In this section, experiments are carried out to assess the contribution of the positional λ term, velocity-dependent damping, velocity-error feedback and open-loop signals in the production of fast and smooth movements. To this effect, three different types of controller are defined that differ in the combination of reflex components they employ. The closed-loop λ controller only contains the λ- and simple damping terms. The λ^+ controller extends this model by adding velocity-error feedback. This is functionally different from basic viscosity in that damping forces are only produced if the actual movement is too fast when compared to the desired movement. Fast movements are not necessarily opposed when high speed is desired. Finally, a *hybrid* closed- and open-loop controller adds the co-contraction component and therefore constitutes the complete model. All controllers were optimised for both, small and large, amplitude movements. In a first set of experiments no delay was used and upper limits for the feedback gains were chosen after running a few initial tests with the hybrid controller. A model with only velocity reference, but without simple velocity term, was not considered, as in the initial tests the velocity proportional term consistently evolved a zero gain. The upper limits for feedback gains chosen were $k_p = 6.0$, $k_d = 2.0$, $k_v = 2.0$, and $k_{ol} = 1.0$.

The performance of the three different controllers is summarised in table 4.1. The first thing to observe is that an open-loop co-contraction command significantly improves the speed of movement and hence the matching of the minimum jerk reference. The performance measure shows that the hybrid model produces the best fit, followed by the lambda model with velocity reference and finally the pure lambda controller. No experiments were carried out using a lambda plus co-contraction controller, so it can't be determined whether co-contraction or velocity reference yield greater improvements. In terms of kinematic indices, the hybrid controller approaches, but does

	hybrid	λ^+	λ	open-loop	min. jerk	human
Fit_{max}[%]	99.73	98.94	98.10			
Fit_{avg}[%]	99.72	98.94	98.18			
Fit_{std}[%]	$0.14 \cdot 10^{-3}$	$0.05 \cdot 10^{-3}$	0			
T [s]	0.145	0.175	0.175	0.265	0.125	0.118
$t_{v_{peak}}$ [s]	0.065	0.065	0.095	0.065	0.06	0.077
v_{peak} [deg/s]	906	732	650	555	937	975

Table 4.1: Performance and kinematic features of joint movements over 100 degrees for different types of controllers. Kinematic indices are presented for the best evolved controller. Corresponding values from the idealised minimum jerk trajectory and measured human data are also shown for comparison.

not perfectly match the features of the minimum jerk trajectory or experimental data. It reaches 97% of the reference peak velocity for example, while the λ^+ and λ controllers only reach 78% and 69% respectively. The standard deviation (of fitness as well as evolved parameters, see below) suggests that the same solutions were found across repeated runs. Since there is no indication that the fitness landscapes created by the three types of controllers would be qualitatively different, the fitness peaks are assumed to reflect the potential of the models, and not a difference in their "evolvability".

	k_p	k_d	k_v	k_{ol}	$hill_{a,b}$	$hill_{asymp}$	F_0^M [N]	t_0 [s]
hybrid mean	5.83	0	0.2	0.28	0.63	1.6	1368	-0.009
λ^+ mean	6	0	0.53	-	0.18	1.53	1500	-0.0119
λ mean	6	0.34	-	-	0.4	1.55	1500	-0.0500
hybrid std	0.1427	0	0.03	0.02	0.18	0.35	81.5	0.002
λ^+ std	0	0	0.02	-	0.09	0.3	0	0.002
λ std	0	0.0001	-	-	0.0029	0.1550	0	0

Table 4.2: Means and standard deviation of best evolved parameters for each controller.

Table 4.2 lists average parameters evolved across five evolutionary runs. Not surprisingly, both positional reflex gain and maximum isometric muscle force tend towards their respective maxima allowed in this experiment. As we optimised for very fast movements, this is what would be expected from a PD-like system. In the absence of feedback delay, nothing constrains the range of these parameters. More surprisingly, for both controllers with velocity-error feedback, the linear damping term consistently evolved towards zero. A more detailed study of the relationship between the two forms of damping and the resulting dynamics would be necessary to explain this observation fully. However, velocity reference on its own allowed for sufficiently fast movements while still preventing endpoint overshoot (see figure 4.6 below). Any addition of absolute damping would inevitably lead to slower movement and hence reduced performance. The hybrid controller, however, relied less on velocity feedback. Instead, it made use of the muscles' intrinsic damping

by ensuring a sufficient level of co-contraction.

Figure 4.6 plots joint angle and velocity for the different controllers in the case of large amplitude movement. As the data has already shown, the hybrid controller closely resembles a perfect minimum jerk trajectory, though not quite reaching the desired peak velocity and being slightly overdamped around the endpoint (likely the result of relatively high muscle damping coefficients; see table 4.2). Comparing trajectories to those of the pure open-loop system (dashed line) suggests that at least part of the hybrid controller's advantage lies in the contribution of co-contraction to a low latency in the onset of motion. The other two controllers in comparison seem unable to reach the desired velocity and are not sufficiently damped at the endpoint. I.e. no compromise could be found within the limits of the allowed feedback gains, between the required speed and the damping necessary to prevent oscillations.

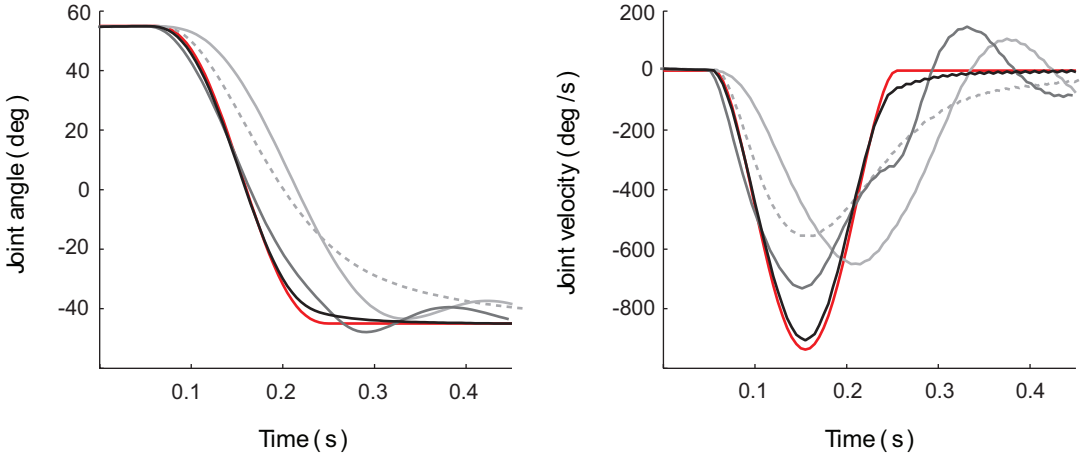

Figure 4.6: Trajectories of fast movements produced by different feedback controllers. Red curves indicate the minimum jerk trajectory and dashed lines the open-loop controller. The λ-controller is shown in light grey, λ^+-controller in medium grey and the hybrid controller in black. Only the latter provides a good fit for the minimum jerk trajectory.

Because in the previous experiment optimisation converged on the upper limit for the positional error gain, the same experiments were repeated while allowing for larger limits. In order to prevent gains from becoming unrealistically high, a feedback delay of 0.01 s was introduced. This should lead to a performance hit for very large feedback gains by leading to endpoint oscillations.

	hybrid	λ^+	λ	open-loop	min. jerk	human
Fit_{max}[%]	99.83	99.28	98.56			
T [s]	0.125	0.165	0.155	0.265	0.125	0.118
$t_{v_{peak}}$ [s]	0.065	0.065	0.11	0.065	0.06	0.077
v_{peak} [deg/s]	940	824	744	555	937	975

Table 4.3: Performance and kinematic features of joint movements over 100 degrees for different types of controllers and 0.01s feedback delay. Different maximum feedback gains are used.

Kinematic indices and evolved parameters for these experiments are presented in table 4.3 and table 4.4. The λ controller, despite making strong use of the extended limits on feedback gains ($k_p = 19.7$ compared to $k_p = 6$), showed no major improvement, reaching a fitness of 98.56% as compared to 98.10% in the previous experiment (and peak velocity increasing from $v_{peak} =$ 650 deg/s to $v_{peak} = 744$ deg/s). The λ^+ controller also produced larger feedback gains, leading to an increase in its fitness of 0.034%. Both controllers co-evolved slightly weaker muscles, however, and different muscle damping characterstics, explaining why the large feedback gains did not lead to oscillations large enough to impede performance. Also, the λ controller, which evolved the largest feedback gain, does not employ velocity-error feedback, suggesting that the remaining feedback components are more resilient to transmission delays. The hybrid controller alone did not increase its feedback gains. Instead, it compensated for the delay by shifting from proportional feedback to more open-loop co-contraction. Although this did not significantly change the movement kinematics as measured by the indices, it seemed to stabilize the joint at the endpoint (trajectories not shown).

	k_p	k_d	k_v	k_{ol}	$hill_{a,b}$	$hill_{asymp}$	F_0^M [N]	t_0 [s]
hybrid max	3.15	0	0.34	0.53	1.0	1.52	903	-0.0044
λ^+ max	8.02	0	0.7	-	0.12	1.48	1103	-0.0016
λ max	19.7	0.56	-	-	0.03	1.23	1446	-0.0301

Table 4.4: Best evolved parameters for each controller including feedback delay of 0.01 s and adaptive maximum feedback gains.

In summary, although none of the models were able to exactly match experimental data, the hybrid model's kinematics came very close as measured by the different movement indices. It should not be surprising that a difference remains, as real elbow movement involves up to six different muscles, arranged in a complex manner. Here on the other hand, only two symmetric muscles without tendon were modelled in a simple symmetric setup.

4.3.3 Inherent triphasic muscle bursts

EMG measurements of antagonistic muscle activity during fast limb movements are often characterised by a triphasic alternating burst pattern. In a rapid elbow flexion for instance, one would typically expect to see an initial burst in biceps activity, followed by a burst in the triceps, and often, but less reliably, a smaller final burst in the biceps. Since these bursts are translated into forces by the muscles, the functional consequence is an initial acceleration of the limb towards the target position, followed by a deceleration that halts the movement. If necessary, such when the decelerating burst turned out too strong, a third pulse can prevent a reversal and thereby arrest the motion. Like other invariants observed in voluntary movements (e.g. straight trajectories in Cartesian space), the existence of this burst pattern has lead some to suggest that it has to be the result of a centrally computed motor program. In this section we will show that this is not necessarily the case. A triphasic burst pattern does instead readily emerge from the dynamic interaction between neural reflexes and the musculoskeletal system.

Bullock and Grossberg (1992) have shown in a spinal reflex model which incorporates α-γ-coactivation, reciprocal inhibition of antagonists and Renshaw-interneurons, that triphasic bursts occur when the ramp shift in desired position is significantly faster than the actual motion (by a factor of ∼2), and when the gain for velocity feedback is significantly larger than the positional feedback gain (by an order of magnitude). In the following experiments, different rates of threshold shifts are compared and individual reflex components analysed for their relative contribution to the production of a triphasic burst pattern. To this end, three optimisations of the hybrid controller with 0.01 s feedback delay were undertaken for a high amplitude movement of 100°. The rates of the threshold shifts were varied such that the resulting ramps had durations of 0.2 s, 0.1 s and 0.0 s.

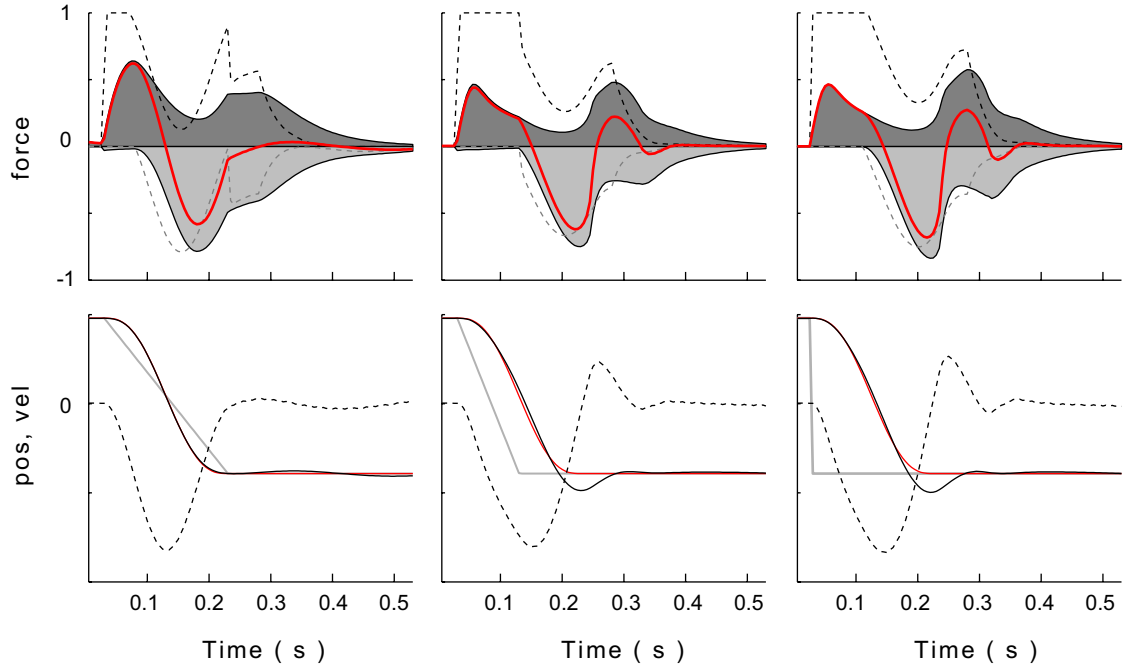

Figure 4.7: Kinematics and reflex response for evolved 100 degree movements with 0.01 s feedback delay. The ramp input signal (from left to right column) has a duration of 0.2 s, 0.1 s and 0.0 s respectively. The top row depicts reflex response (muscle activation) as dashed lines, muscle force as filled areas, and net force (sum of antagonists) in red. Dark curves represent the flexor, lighter colours the extensor. The bottom row presents joint angle (solid black), desired minimum jerk trajectory (red), the commanded ramp signal (grey) and velocity (dashed).

The kinematics of the best evolved controller for each of the three conditions are shown in figure 4.7. Note how all ramp durations, even a simple step signal, produce a reflex response that shows three maxima leading to acceleration, deceleration and stabilisation of joint motion. The best performing controllers achieved a fitness of 99.83%, 99.4% and 99.14% respectively for ramps of 0.2 s, 0.1 s and 0.0 s. Their kinematics differ in that input ramps which are faster than the actual movement lead to overshoot, while a ramp of length comparable to the desired movement duration appears critically damped. Beyond a certain rate of the ramp-shift, however, no significant difference is found. Evolved parameters showed a clear pattern. Compared to the 0.2 s ramp, controllers using a 0.1 s ramp evolved smaller velocity error gains (by 57%), but larger muscle

intrinsic damping (the convexity of the force-velocity relationship for shortening decreased by 90% and the asymptote for lengthening increased by 50%). The controller with step-signal input was similar to the short ramp, but with a 10% increase in open-loop co-contraction. Together, these changes signify a shift from reflex control to intrinsic muscle dynamics as the rate of the threshold shift increases. When the duration of the ramp signal was allowed to evolve as well, it tended towards the length of the desired movement, and not shorter. This is in contrast to other studies which suggested shorter threshold ramps (Bullock and Grossberg, 1992; Gribble et al., 1998).

In order to explain how the bi- and triphasic burst pattern emerges from a simple ramp-shaped input signal, we analysed the relative contribution of positional and velocity error feedback to overall muscle activation. Figure 4.8 compares these contributions for ramps shifts of 0.2 s and 0.1 s duration. As a first observation, note how the symmetrical setup of the antagonistic muscles produce symmetrical error signals for both position and velocity. Because one muscle is supposed to shorten as much as the other needs to lengthen, the error signals are equal in amount but of opposite sign. However, in the λ-model muscles become activated only if the overall input to α-motoneurons exceeds its threshold, i.e. when net reflex output is positive. As a result, the symmetry of error signals is broken, and flexor and extensor muscle activations differentiate.

Inspecting the controller driven with a 0.2 s ramp, the first pulse occurring in the flexor is comprised mostly of the velocity error signal, especially in the beginning, with a smaller and gradual addition of positional error. This is explained by the fact that the ramp signal implies a gradual shift in desired position, but an abrupt change in desired velocity. At this stage, only the flexor is active. In order to reduce the initial error (due to a change in desired position), the extensor would have to actively lengthen, but the λ-model respects the fact that muscles can only shorten actively. As the initial burst accelerates the limb, flexor position and velocity error become smaller, eventually "self-terminating" its activation. The limb soon reaches a velocity greater than desired, which eventually results in extensor velocity feedback overcoming its negative positional error. This marks the beginning of the second burst, which decelerates the limb as it approaches the target. As limb velocity falls below the desired value towards the end, a final smaller burst in the flexor ensures that the motion is not unnecessarily overdamped. In summary, the reflex controller produces a triphasic burst pattern mostly as the result of limb velocity first lagging, then leading, and finally lagging again the desired velocity. In conjunction with the muscle's low-pass filter, as well as stiffness and damping properties, these discrete burst are transformed into a single continuous minimum jerk trajectory.

By comparing the left and right column in figure 4.8, it becomes clear that a shift in desired position significantly faster than the desired motion produces a different triphasic burst pattern. First of all, the steeper ramp produces a larger initial error in position. Hence the first burst is not constituted mainly of velocity error anymore. Secondly, the resulting step signal in desired velocity is now not only shorter, but also larger than the velocity that the limb can achieve. This results in the first burst not terminating as quickly, because the velocity error does not reverse sign until the ramp ends and desired velocity returns to zero. For the same reason the decelerating extensor burst is delayed until that same point in time. The resulting overshoot finally leads to a small burst in the flexor that arrests the motion.

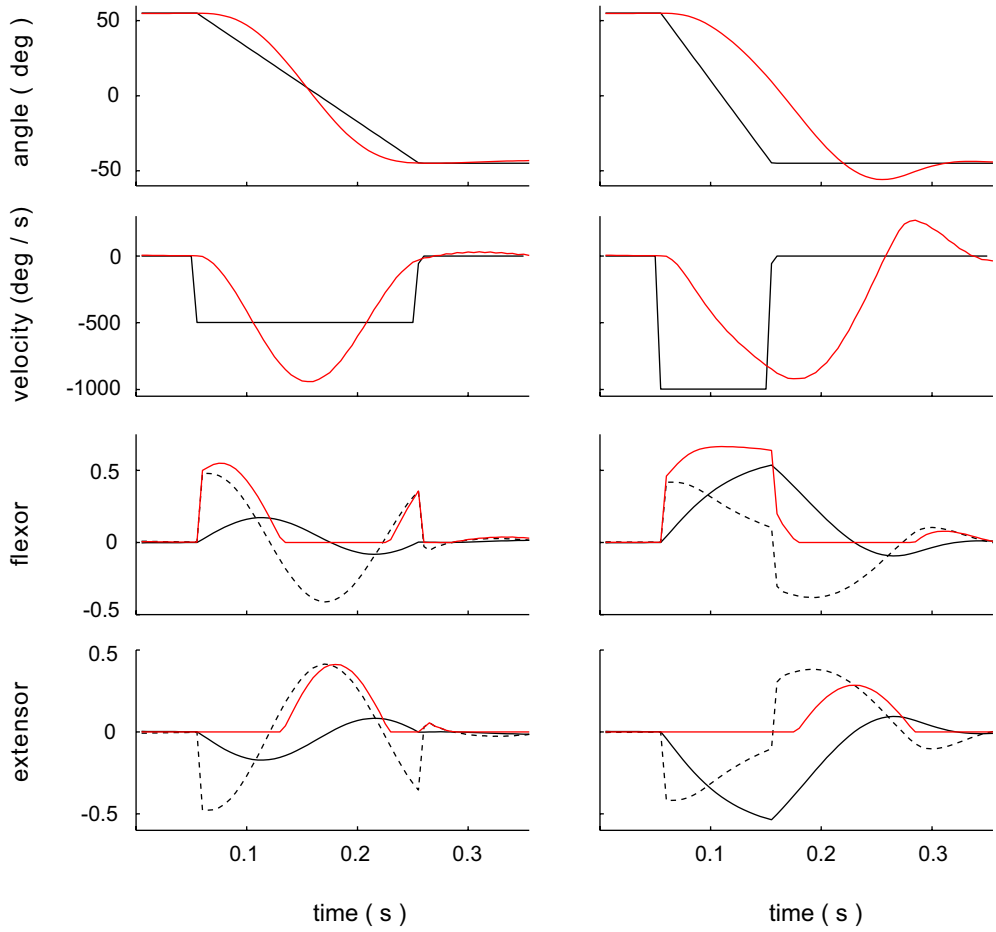

Figure 4.8: Emergence of triphasic burst pattern. Left column: ramp shift of 0.2 s duration. Right column: ramp shift of 0.1 s. Top row: commanded joint angle (black) and actual angle (red). Second row: desired velocity (black) and actual velocity (red). Third and fourth row plot flexor and extensor reflex components: position error feedback (solid black), velocity error feedback (dashed black) and sum of both errors, clamped to positive values $[k_p(L^M - \lambda) + k_v(\dot{\lambda} - v^M)]_0^1$. The latter corresponds to the combined reflex contribution of the controller, i.e. without the added co-contraction.

In conclusion, a model of the stretch reflex based on the λ-model can be tuned to produce fast and smooth movements with a natural triphasic burst pattern using a simple linear shift in threshold length. This result confirms similar findings obtained with explicit neural models of the stretch reflex (Bullock and Grossberg, 1992), and suggests that triphasic bursts are not necessarily pre-programmed. The burst pattern emerges from the system's dynamics in different ways across a range of threshold ramp durations. Overshoot in the range found here can be observed in the fastest movements produced by human subjects. Hence this finding is not sufficient to decide which ramp duration better reflects reality.

4.3.4 Control of movement distance and velocity

One goal of the EP-hypothesis is a simplified motor control process. St-Onge et al. (1997), therefore, suggested that movements of different amplitude and speed could be controlled simply by varying the duration and rate of a monotonic shift in the stretch reflex threshold. According to this

model, distance is encoded by the duration of a fixed rate equilibrium shift, while speed of movement depends on the slope of the ramp shift. This control scheme reproduced empirically found kinematic and electromyographic (EMG) features of fast perturbed and unperturbed movements when equilibrium shifts were of short duration. Specifically, the time course was chosen such that the shift ended near peak velocity, i.e. a significant time interval existed between the end of the EP shift and the end of the movement. In (Gribble et al., 1998), the authors used a similar setup, with a ramp shift about half the duration of the movement. Other formulations of the λ-model, in contrast, use EP shifts that are closer to the intended duration of the movement (e.g. Kistemaker et al. 2006). In addition to the EP shift, St-Onge et al. (1997) varied the gain of the reflex damping term as well as muscle co-contraction over time. The damping profile followed the same time course as the EP shift (i.e. ramp-shaped), while co-contraction increased linearly to a plateau, and towards the end decreased slowly to simulate a gradual falloff in tonic EMG level (relaxation). It was found that damping gain and co-contraction level influenced peak velocity and helped to reduce terminal overshoot. Overall levels were chosen according to the desired movement.

For movements of different amplitude, a salient feature of the model proposed by St-Onge et al. (1997) was its production of position and velocity traces which were similar during the initial phase and then diverged at a point that depended on the desired movement distance. Similar patterns were observed by Gottlieb (1998). Measuring EMG activity during voluntary single-joint movements in human subjects, it was found that kinematics and agonist muscle activity were independent of distance up to peak acceleration (while the area of the agonist burst increased with distance).

Distance control with fixed rate EP shifts

In a first set of experiments we tested whether movements of different amplitude could be produced with fixed rate equilibrium shifts of different duration. Different reflex models and rates of EP shift were studied for their ability to produce kinematics and EMG patterns that initially follow the same time course for different amplitudes, in line with the experimental observations described above. Three different movement amplitudes (55°, 75° and 100°) were optimised using two different reflex models (with and without open-loop co-contraction) and two different rates for the EP shift (300 deg/s and 600 deg/s). In all cases the duration of the minimum jerk trajectory was allowed to evolve for each movement (as the desired movement duration was unknown) but was constrained to 100–200% of the duration of the threshold ramp. The onset of exponential muscle relaxation (to 10% of maximum activation) was also evolved. Feedback transmission delays were set to a value of 0.015 s, a value in the range reported by St-Onge et al. (1997) .

Figure 4.9 compares the kinematics produced under three different conditions. The hybrid model with a relatively slow EP shift (left column) produced trajectories most resembling the minimum jerk case. Trajectories for movements of different amplitude diverged relatively quick however. This can be explained by the fact that the open-loop muscle activation depends on the final desired position. Hence, the further the target (i.e. the larger the amplitude of movement), the greater the open-loop contribution, and consequently the initial acceleration and velocity. This also explains why the ramp shift did not terminate before the end of the actual movement in all cases. For the largest amplitude movement the open-loop activation was sufficient to propel the limb such as to

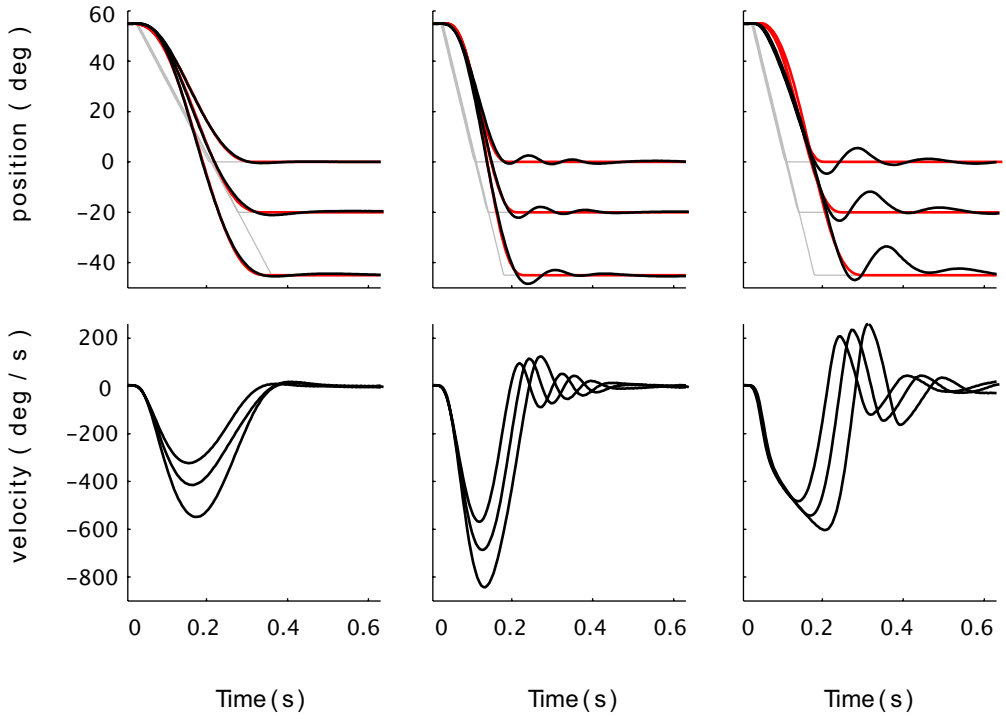

Figure 4.9: Fixed rate λ shifts of varying distance (55°, 75° and 100°). Left: hybrid model with slow EP shift (300 deg/s). Middle: hybrid model with fast EP shift (600 deg/s). Right: λ^{+} controller with fast EP shift.

lead the EP shift.

The same reflex model driven by a faster EP shift (middle column) produced slight oscillations around the end point (within the range observable in human experiments). Because position and velocity errors are larger initially for faster ramps, the reflex contribution towards overall muscle activation must be larger too. Thus, while actual trajectories diverge too for this controller, they do so mostly in response to the desired trajectories diverging. The points of divergence can be located where the corresponding EP shift reaches its final position plateau.

The final model (right column) lacks open-loop muscle activation. Therefore force production is fully determined by reflex activity. As all feedback gains and muscle parameters are constant across the different movement amplitudes, the corresponding trajectories can only diverge when the input to the reflex controllers are different. This in turn can only be the case when either the desired velocity changes (it drops to zero at the end of the ramp), or the desired position changes (it reaches a plateau for one movement at the end of the ramp, while continuing to ramp down for others). In the case observed here, reflex gains evolved such that divergence occurred only when a trajectory overshoots its target and the positional error reverses sign as a result (positional feedback gain was significantly larger when compared to the other two models). As a result, position and velocity traces were bundled together as observed in (St-Onge et al., 1997) and (Gottlieb, 1998). Also, EP shifts ended before the movement reached its peak velocity. However, the large positional gain, combined with relatively low damping, produced oscillations that are too large when compared with experimental or model data reported in these studies.

In summary, movement distance can be controlled by varying the duration of a constant rate shift of the reflex threshold, without necessitating the modification of feedback gains. Kinematics and muscle activities for movements of different amplitude are observed to be more similar initially the greater the relative contribution of reflex activity. The fastest EP shifts produced undesirable oscillations in the model lacking open-loop co-contraction. This difference is likely due to the fact that in (St-Onge et al., 1997) co-contraction and damping gains depended on movement amplitude, while here they were not allowed to change between movements. Furthermore, not only did the overall level of feedback gains differ from movement to movement, they were also dynamically controlled throughout a movement (ramped up and down). Here, in contrast, gains remained fixed at a given level for the duration of a movement. This was assumed to be more in line with the goal of using the simplest possible control signals. With respect to the minimisation of jerk, the best trajectories were produced by the hybrid model with a comparatively slow EP shift.

Velocity control with variable rate EP shifts

The previous section has shown that movement distance can be controlled by varying the duration of a constant rate EP shift. In follow-up experiments we investigated whether the velocity of movement is also controllable. In aiming for the simplest control process, it would be reasonable to hope that a change in the rate of the shift would suffice to achieve different speeds, without any additional changes in reflex gains. To test this hypothesis, we optimised a hybrid reflex controller to produce three 55° minimum jerk movements with durations of 0.18 s, 0.27 s and 0.36 s. A single set of reflex and muscle parameters was evolved for all three movements. Only the duration of the EP shift was allowed to vary across movements (the amplitude was fixed, hence duration translated directly into rate).

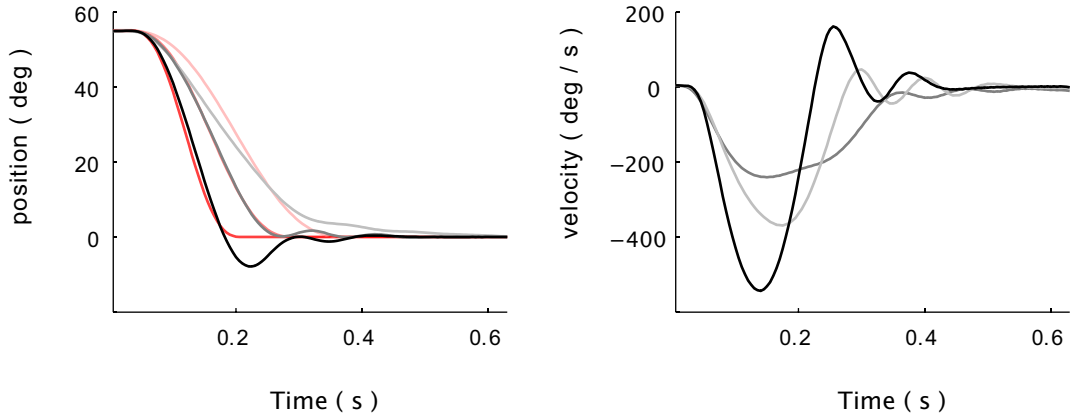

Figure 4.10: Variable rate EP shifts over 55° lasting 0.18 s, 0.27 s and 0.36 s. Red traces are the desired minimum jerk trajectories. Black lines plot the fastest, grey the moderate, and light grey the slowest movement. Joint angle trajectories are shown on the left, velocities on the right. Note the rather large overshoot during the fastest, and asymmetric velocity profile during the slowest movement.

The resulting trajectories are shown in figure 4.10. A clear pattern is easily observed. The fastest EP shift leads to motion which initially lags the desired trajectory and produces significant overshoot with quickly decaying terminal oscillations. The slowest shift, in contrast, results in the limb initially leading the desired position. The deviation is then corrected by the feedback controller

in a way that is overly damped. The resulting velocity profile does not resemble the typical bell shape. Only the moderately paced EP shift produces the desired minimum jerk trajectory (albeit not without small oscillations either). Clearly, the optimisation process has not found a single set of reflex gains that would be optimal for movements of different velocities. The best controller identified constitutes a trade-off that performs well in the average case, but cannot ensure correct speed and damping for slower or faster movements. The fact that this result is repeatable over several runs (with the evolutionary algorithm starting from different initial conditions), and that fitness reliably plateaued in the same region of the fitness landscape, indicates that the failure to find a solution is a property of the controller and not an artefact of the optimisation procedure. It can not be ruled out, of course, that the same submaximal local optimum was encountered in each of the repeated runs. But the fact that this was never observed in previous experiments, which should have had similar fitness landscapes, supports the conclusion that the speed of movement in this model can not be controlled by changing reflex gains alone.

Simultaneous control of distance and velocity

Combining the control strategies described above, a final set of experiments was aimed at identifying the minimal set of changes that need to be applied to a reflex controller to achieve simultaneous control of both, movement distance and velocity. A hybrid reflex controller was therefore optimised to produce four different movements that covered high and low velocities as well as small and large amplitudes. It was quickly confirmed that a single set of muscle and reflex parameters was not sufficient to achieve the desired flexibility. As the position-velocity phase plots in figure 4.11 illustrate, fast movements produced undesired oscillations, while slow movements were significantly overdamped. This was to be expected after the previous experiment had demonstrated the difficulty of finding a trade-off in reflex gains that would produce critical damping for movements of different speed.

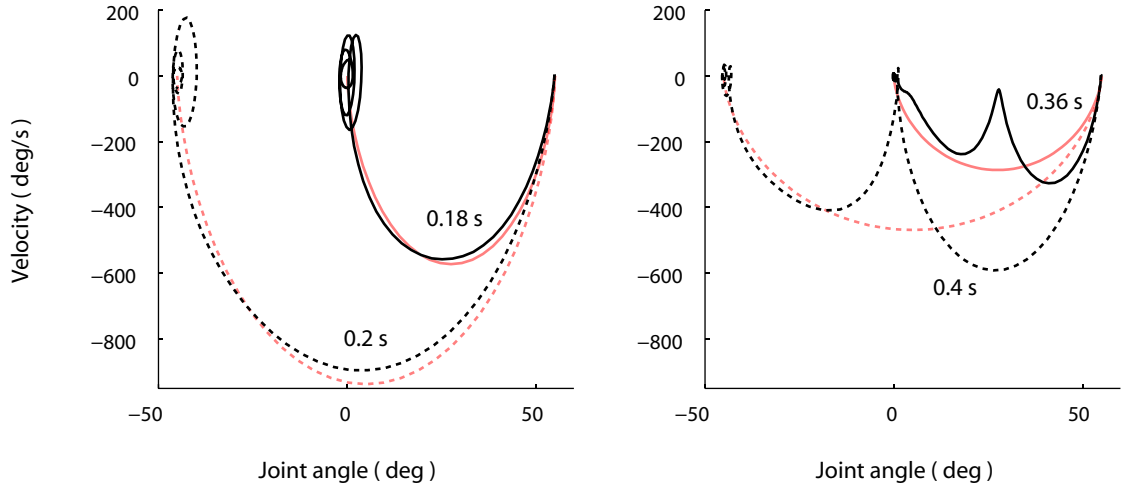

Figure 4.11: Phase plots of single gain set controller for fast and slow movements. For fast movements (left) the controller produces undesirable oscillation, while slow movements (right) are significantly overdamped. A compromise for the damping characteristics of fast and slow movements was not found with a single set of fixed reflex gains.

Consequently, a broad set of experiments was conducted in which different subsets of reflex gains were systematically chosen and allowed to evolve depending on the desired type of motion. From the subsets of controllers that successfully evolved minimum jerk trajectories for large and small amplitude movements at different speeds, those with the smallest number of necessary parameter changes were then identified. The trajectories produced by three such controllers are shown as phase plots in figure 4.12.

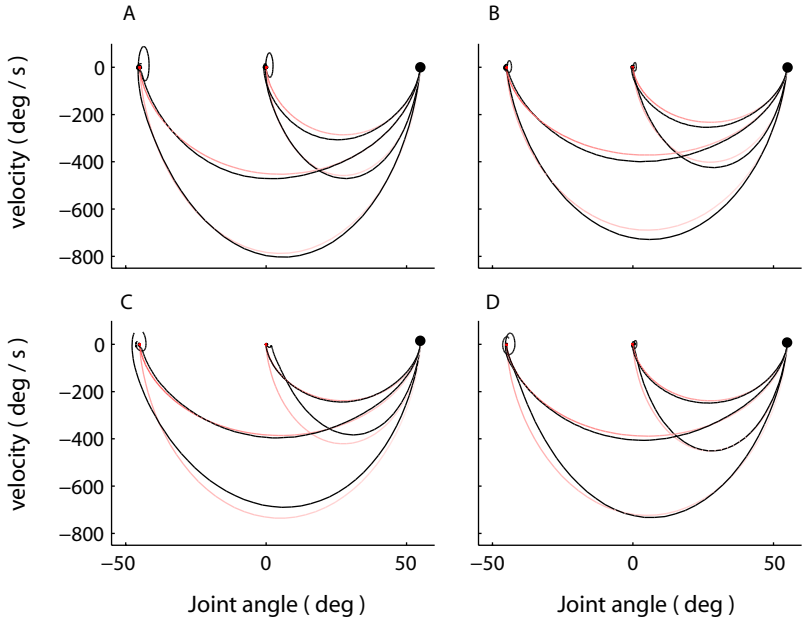

Figure 4.12: Phase space plot of movements generated by different reflex gain models. A: four different open-loop gains (background co-activation). B: as A, but with ramp shifts being 20% slower. C: only two different open-loop gains; one for fast one for slow movements. Also uses ramp-shifts that are 20% slower than maximum. D: two open-loop gains and two velocity proportional (k_v) gains.

The first controller (A) uses a different open-loop gain for each movement, i.e. a different level of muscle co-contraction for each combination of desired distance and velocity. The remaining reflex- and muscle parameters on the other hand are the same for all movements. The produced trajectories have minimum jerk profiles (99.68% fitness), with slight terminal oscillations. When the intended movements are slowed down by 20% (B), these oscillations are visibly reduced (99.66% fitness). Minimum jerk trajectories can also be produced using only two different open-loop gains, one for fast and another for slow movements (C), albeit with slightly less precision (99.62% fitness). A different but equally successful strategy was found (D), in which two open-loop gains are combined with two different damping terms for slow and fast movement (99.71% fitness).

To summarise, simple monotonic threshold shifts of different duration and rate can be used to control both the distance as well as the velocity of movement. However, along with this simple strategy the viscoelasticity of the system has to be tuned to produce critically damped movements at different speeds. A means to achieve this is the ability to vary the muscle-inherent damping characteristic by choosing an appropriate level of co-contraction. This seems to be a strategy also utilised by human subjects (Suzuki et al., 2001). Alternatively, or in addition, the reflex contribution to the system's viscoelasticity can be adapted through selection of appropriate feedback

gains.

4.3.5 Multijoint movement

In the previous sections it was shown that a variety of single-joint movements can be produced using simple monotonic EP shifts, and that the resulting kinematic features (such as triphasic bursts, bell-shaped velocity profile, level of joint stiffness) were similar to those recorded in human experiments. Additional complications could arise however when more than a single joint is considered. During multijoint limb movements, interaction torques arise at one joint as a result of the motion of limbs around other joints in the chain. Lifting one's arm at the shoulder, for instance, also generates rotational forces that tend to extend the elbow. Equally, torques flexing the elbow lead to equal and opposite torques at the shoulder. This begs the question of whether such torques are automatically compensated for as an intrinsic part of the muscle-reflex dynamics (given a plausible level of joint stiffness), or whether control signals need to be predictively adjusted to counteract the effect of these internal loads.

In the most optimistic formulation of the equilibrium-point hypothesis, no information about limb dynamics should be necessary at all to smoothly move from one position to another. Kinematics alone (joint angles and velocities, or their muscle equivalents) should suffice. To test whether this is indeed the case, reflex controllers were evolved for simple targeted movements about two joints (elbow and shoulder). Analogously to the single-joint experiments, simple monotonic EP shifts were used as input to two separate reflex models (of the hybrid type), each of which was controlling an antagonistic muscle pair. The setup therefore treated each joint in isolation without any interaction between the corresponding reflex controllers. The time course of the two EP shifts was enforced to be synchronous. Each of the two muscle-reflex systems was described by its own set of parameters. They were optimised using two different movements that varied in the relative direction of elbow and shoulder motion, and hence produced interaction torques of opposite sign. The first movement involved flexion of both shoulder and elbow, while the second one consisted of shoulder extension and elbow flexion. The latter therefore constituted a "synergistic" case, in which the resulting interaction torques assisted the intended motion, while in the former case the interaction torques created resistance in the other joint.

The joint trajectories of the best evolved controllers are shown as phase plots in figure 4.13. It is easily seen that the simple strategy of independently but synchronously driving the two joints is inadequate. Whether feedback delays are present or not, interaction torques generate more perturbation in the joints than either of the two muscle-reflex systems can compensate for (given a biologically plausible level of maximum stiffness). It should be repeated here, that caveats about the possibility of stagnation in local minima applies to this as it did to the previous experiments in which no satisfying solution was found. However, the fitness function and model equations (and hence the resulting fitness landscapes) are very similar to those used in experiments that succeeded in identifying the desired controllers. It would therefore seem unlikely that the algorithm should always have succeeded in one set of experiments, while always failing in another. We hence conclude that the inability to compensate for interaction torques is a property of the control strategy, and not a reflection of the optimisation procedure used.

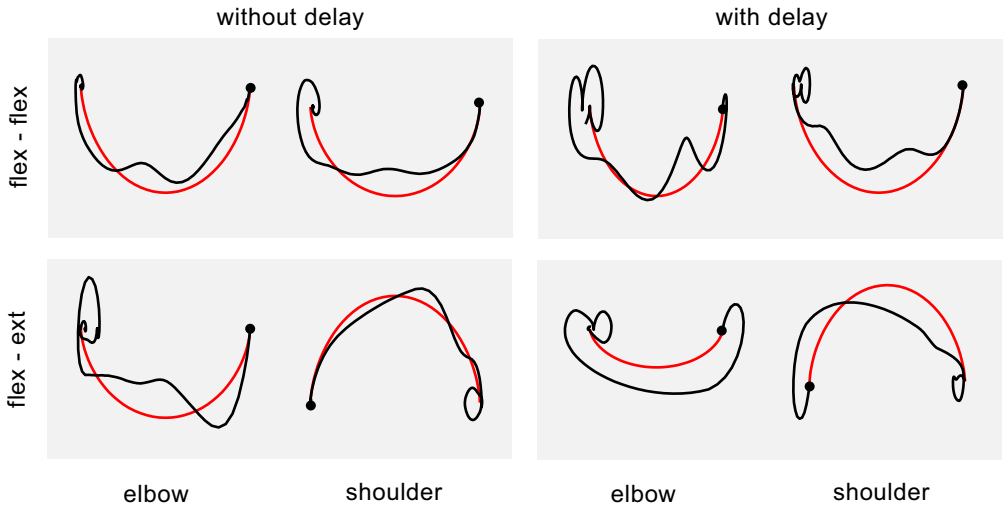

Figure 4.13: Phase space plot of multijoint movements with simple synchronous λ-ramps. Desired trajectory in red, actual in black. Initial positions are indicated by a dot. Whether feedback delay is present or not, interaction torques disrupt the ability to produce smooth movements with bell-shaped velocity profile.

This result is consistent with experiments that have shown that during multijoint arm movements muscles spanning one joint are activated depending on the motion in another joint. Gribble and Ostry (1999) for example found that EMG activity in shoulder muscles scaled with the magnitude and sign of the interaction torque created in that joint by motion of the elbow. If the interaction torque opposed shoulder movement, muscle activity was stronger than when it assisted movement. Since interaction torque in the non-focal joint is proportional to the movement of the focal joint, it follows that a relatively simple strategy seems to be at work during such multijoint movements. Muscles of the non-focal joint are activated proportionally to muscles of the focal joint. Indeed, in (Gottlieb et al., 1996) a near linear relationship between non-focal and focal joint torques was found to be a sufficient rule of coordination to explain observed kinematics during elbow and shoulder movements. Torques at the two joints varied with load and speed, but always in close synchrony. This linear synergy was also found to be robust to load perturbations (Debicki and Gribble, 2004), and to apply even when the non-focal joint was mechanically fixed (Debicki and Gribble, 2005), in which case no torque would be necessary at all to counteract interaction torques.

So although it seems that the nervous system takes limb dynamics into account when adjusting control signals to muscles to compensate for interaction torques, a simple mechanism of coordination might be responsible. While a number of researchers have suggested that this “predictive” compensation of limb dynamics is based on internal models (e.g. Wolpert and Ghahramani, 2000), others have shown that adaptation to external and internal loads can be explained within the equilibrium-point framework (e.g. Flash and Gurevich, 1997). In (Gribble and Ostry, 2000), a simple adaptive mechanism was used in which EP shifts were adjusted in direct proportion to the positional error between actual and desired movement. After few iterations of this learning scheme, trajectories produced by the modified EP shifts matched empirical data, without necessitating inverse dynamics calculations or coordinate transformations between positional error and corrective forces.

4.4 Discussion

A comparatively simple muscle-reflex model, only incorporating the basic non-linearities, was demonstrated to produce single-joint movements the kinematics of which are comparable to human data. Small delays can be accommodated into its dynamics, while larger delays can cause terminal oscillations as is common to all feedback systems. The combined muscle-reflex system can exploit open-loop stability, however, which makes it more resilient to delays than a pure feedback system. Indeed, open-loop co-contraction was found to be necessary for achieving the highest velocities when faced with feedback delays. Velocity error feedback equally proved necessary to achieve high speeds without oscillations at the endpoint. When this feedback modality was available, absolute velocity feedback (i.e. basic viscosity) seemed redundant or even disruptive and such controllers evolved to minimise the corresponding gain.

The muscle-reflex system studied in this chapter also produces triphasic muscle burst patterns independent of the length of the input ramp, suggesting that this is an emergent feature of the dynamics rather than centrally planned. Even at the lower limit, i.e. with an instantaneous shift of virtual EP position, this pattern was observed, although resulting dynamics in this case showed significantly more overshoot. When the duration of the ramp shift is optimised explicitly, it tends towards the desired duration of the movement. This is in contrast to other experiments which have suggested that the EP shift could be faster, ending at the point of maximum velocity (Bullock and Grossberg, 1992; Gribble et al., 1998).

Movement distance can be controlled simply by varying the duration of a fixed rate EP shift in the model considered here. This is possible without tuning of feedback gains. While open-loop co-contraction was necessary to produce fast movements without oscillations, it also resulted in trajectories that quickly diverge. This is in contrast to the strategy used by human subjects (Gottlieb, 1998) and results based on a different muscle-reflex model (St-Onge et al., 1997). Controlling movement velocity by using different rates for the EP shift turned out to be difficult. A single set of feedback gains that achieves critically damped movements independent of speed could not be found. Trajectories become either underdamped or overdamped for most conditions.

For control of both distance and velocity, the smallest subsets of feedback gains were identified that need to be varied to achieve control of both without losing the minimum jerk quality of the resulting trajectories. It was found that good results could be achieved either when different amounts of co-contraction were used for each combination of desired distance and velocity, or when co-contraction and damping terms differed for slow and fast movements. Such tuning of viscoelastic properties for the task at hand seems to be a strategy also utilised by human subjects (Suzuki et al., 2001).

With respect to multijoint movements it was found that simple synchronous EP shifts controlling two joints can not produce fast and smooth movements within realistic limits for maximum force production and stiffness. Interaction torques are too disruptive to be compensated for by a simple compliant feedback controller. It can therefore be concluded that interaction torques need to be accounted for explicitly during multijoint movements. It is an open question, however, whether internal inverse dynamics models are required or whether a modified adaptive EP model can achieve the necessary compensation.

The muscle-reflex model studied in this chapter differs from other models in its level of complexity. It is arguably the most simple model which still accounts for the non-linear properties of individual muscles (and was chosen for that reason). As shown in the previous chapters, the basic non-linearities in muscle viscoelasticity (force-length-velocity characteristics) are necessary to achieve stability while allowing for flexibility with respect to movement position, stiffness and velocity. Other details, like anthropomorphic muscle paths and moment arms, accounting for muscle pennation angle, or models of different types of muscle fibres (fast and slow-twitch), were not required. Other models found in the literature may include calcium dynamics, a tendon element and bi-articulate muscle pairs (e.g. Kistemaker et al., 2007a), or use anthropomorphic data to model specific human muscles (Garner and Pandy, 2001). While this is expected to increase fidelity in matching experimental data, it was not required to study the phenomena of interest in this chapter. Equally, a simple control model, namely a linear combination of direct state feedback and static activation levels, was sufficient to reproduce human movement features. Neither were complicated time-varying reflex gains needed (as in St-Onge et al., 1997), nor detailed modelling of sensory organs or neural circuitry (Lan et al., 2005). The simplifications used here allowed for easier and more complete characterisation of the system's behaviour (such as maps of joint stiffness at all equilibrium-points) and did not impede the kind of questions asked. The goal was not to provide an anatomically correct arm model, but to study whether experimentally observed movement features, such as triphasic muscle burst patterns, can emerge from the non-linear dynamics of a muscle-reflex system. To this end the level of modelling proved sufficient. Although the model can not predict the precise time-course of muscle forces in human arm movements, it does predict the importance of velocity error feedback (relative vs. absolute damping), the tuning of viscoelasticity for movements of different speeds, and the need for compensation of interaction torques during multijoint movements. Although individually some of these results have been demonstrated in both simpler and more complex models, this chapter has shown that the observed features are neither due to oversimplifications, nor specific to human physiology or anatomy. It was further demonstrated that equilibrium-point control is feasible for movements of different speeds and amplitudes with appropriate adjustments of feedback gains, i.e. not limited to any particular range of movements (Kistemaker et al., 2006; Pilon and Feldman, 2006).

The importance of an open-loop (co-contraction) command for the control of fast movements highlights an often misunderstood concept of the EP-hypothesis. Namely, that it suggests pure feedback control; that it is therefore prone to destabilising feedback delays; and that feedback would arrive too late to contribute to fast movement. But even the lambda signal itself is a feedforward command. It shifts motoneuron thresholds prior to the onset of movement, such that sensory feedback will contribute from the beginning. The co-activation command constitutes another feedforward component. Nevertheless, both components imply that the central control of movement requires a "representation", or map, of the relationship between desired angles and muscle(-tendon) lengths. If such maps were to be understood as internal models, then one could argue that the dichotomy between the EP- and the force-control hypothesis is not as strict as is often presumed. However, the internal maps required by the EP hypothesis are of a very different nature than those postulated by the force-control hypothesis. The former are essentially representations of skeletal geometry, i.e. purely kinematic, while the latter are complete and detailed "simulations" of the dynamics of force production. While the former are easy to acquire, the lat-

ter are hard if not impossible (see chapter 2). Equilibrium-point control therefore is not strictly model-free, but it avoids the pitfalls associated with the inverse dynamics problem.

Several interesting avenues remain to be explored. In this thesis, for example, muscle models were discarded that can lead to unstable dynamics. There is some evidence, however, that unstable dynamics can occur naturally in human arm movements (Akazawa and Okuno, 2006). Further work should aim to identify whether this is a common feature and study the implications of unstable dynamics at the joint level for feedback controllers like the λ-model. Even though an unstable equilibrium might be detrimental to discrete goal-directed actions, for example, a system consisting of a repellor surrounded by two attractors, as identified in the previous chapter, might be beneficial for oscillatory behaviours.

Further work is needed to assess the relative contribution of inherent muscle properties and reflex action on the stability of the coupled system. Of particular interest would be the contribution of muscles to the compensation for feedback delay, as the effect of the muscle "preflex" can provide stability where feedback alone is not sufficient. Giesl and Wagner (2007), for example, have analytically determined the size of the basin of attraction for the equilibrium produced by antagonistic muscles in the absence of reflexes (also see Wagner and Blickhan, 1999). It would be interesting to see whether their technique can be applied in more complicated scenarios. Alternatively one could determine the relative contribution of muscle and reflex stabilising actions numerically, for example through "lesion" studies of the reflex controllers.

Finally, extensions to the EP-hypothesis are needed that can account for the effect of interaction torques during multijoint movements. Chapter 6 proposes two such mechanisms, one of which is based on force-feedback between neighbouring joints, and the other on feed-forward compensation.

Chapter 5

Lumped muscle-reflex model

In the previous chapter it was shown that a detailed simulation of antagonistic skeletal muscles can reproduce the kinematics of simple goal directed movements, albeit not accounting for the interaction torques arising during multijoint movements. For simulations that include many joints or degrees of freedom, it would be convenient, with respect to the complexity of simulation and analysis, if the qualitative dynamics of human movement could be captured in a simpler model. This chapter investigates if individual muscles need to be modelled at all, or whether a simple lumped model with attractor dynamics at the joint level might be sufficient.

It might seem surprising that such a simplified muscle model is suggested here, when in previous chapters it was pointed out that oversimplification is often the cause for misguided criticism of the EP hypothesis. But as chapter 4 has shown, it is not always necessary to pick the most detailed or complicated model available either. It might often be sufficient to pick one that readily produces the phenomenon one wishes to investigate. In chapter 6, for example, we will study possible mechanisms for the compensation of interaction torques. Such torques appear by necessity in any multijointed physical system, not just those controlled by muscles with complex internal dynamics. The model proposed in the following sections will be useful because the reduced number of parameters makes it easier to analyse the dynamics of the movement it produces. At the chosen level of detail such a model will not be able to make predictions about details of animal movements, i.e. those actuated by skeletal muscles. But it will suffice as a tool to investigate potential forms of feedback or feedforward control in abstract.

5.1 Joint model

Many variations can be found in the biomechanics literature for m odelling limb motion on the level of joint attractor dynamics. Most can be described as non-linear extensions of a basic spring, or equivalently PD control, model. In (Barto et al., 1999; Karniel and Inbar, 1999) for example, limb control was modelled by a spring-mass system of the form $M\ddot{x} + B(\dot{x})^{\frac{1}{5}} + K(x - x_{eq}) = 0$, where x is the position of an object of mass M, x_{eq} the equilibrium position, B the damping coefficient, and K the spring stiffness. This model produces trajectories qualitatively similar to human

wrist movement when $M = 1$, $B = 3$ and $K = 30$ (Wu et al., 1990). In the following experiments, different non-linear functions are compared as candidates for a joint controller comprising elastic and viscous forces analogous to the aforementioned spring-mass setup. The resulting systems can be interpreted as minimal equivalent models of the combined effect of nonlinear muscle properties and the stretch reflex mechanism.

Two options are studied for modelling joint elasticity, namely a linear function of position error and an exponential function:

$$F_{lin} = K(\theta - \lambda) \tag{5.1}$$

$$F_{exp} = \begin{cases} Ke^{(\theta-\lambda)-1} & \text{if } \theta >= \lambda \\ -Ke^{-(\theta-\lambda)-1} & \text{if } \theta < \lambda \end{cases} \tag{5.2}$$

Here K is stiffness, θ the actual joint angle, and λ the desired angle. Linear elasticity was used in early models, such as the one proposed by Hogan (1984), who showed that minimum jerk optimisation of such models can accurately predict observed kinematic invariants. Exponential elasticity in contrast was used by several researchers as an approximation of a muscle's invariant characteristic (Gribble et al., 1998; Pilon and Feldman, 2006). Although the combined elasticity of two muscles in an antagonistic setup would have a different form at the joint level, the exponential is distinguished from the linear model by the fact that stiffness (tangent of the force function) is not constant, but increases with the difference between actual and EP position (see figure 5.1).

For viscous forces, a linear model and two different non-linearities are considered:

$$F_{lin} = B\dot{\theta} \tag{5.3}$$

$$F_{asinh} = B\,\text{asinh}(\dot{\theta}) \tag{5.4}$$

$$F_{power} = B \cdot \text{sgn}(\dot{\theta}) \cdot \left|\dot{\theta}\right|^{1/n} \quad n \in [0,1] \tag{5.5}$$

where B is the damping gain, and $\dot{\theta}$ joint angular velocity. Non-linear viscosity as described by a power law was previously found to allow for fast movements that terminate with little oscillations in a model of human wrist movements (Barto et al., 1999). As figure 5.1 illustrates, in such a model effective damping (the slope of the velocity dependent force function) increases sharply as velocity approaches zero. Hence damping is strongest at rest while dropping quickly for faster motion. The inverse hyperbolic sine function (*asinh*) was used, for example, by Martin (2005) for having the same benefit as the power function. It differs however in that damping drops more smoothly for increasing velocity. It also has the advantage of not having a discontinuity at zero velocity (desirable for numerical stability) and of not saturating asymptotically. The similar arc tangent (atan) function was used in (Gribble et al., 1998) as an approximation of the function which describes a muscle's force dependency on lengthening and shortening velocity (see chapter 3). As it is better suited for numerical simulation, while resembling the overall shape of the power law, only the asinh function was considered in the following experiments.

Several studies have proposed relative damping of the form $F_{rel} = B(\dot{\lambda} - \dot{\theta})$ as an improvement over absolute damping of the form $F_{abs} = B\dot{\theta}$ (de Lussanet et al., 2002; McIntyre and Bizzi, 1993). While absolute damping alone was found insufficient for re-producing the fastest human movements ($\approx$ 950 deg/s) at plausible stiffness levels, relative damping increased the maximum speed

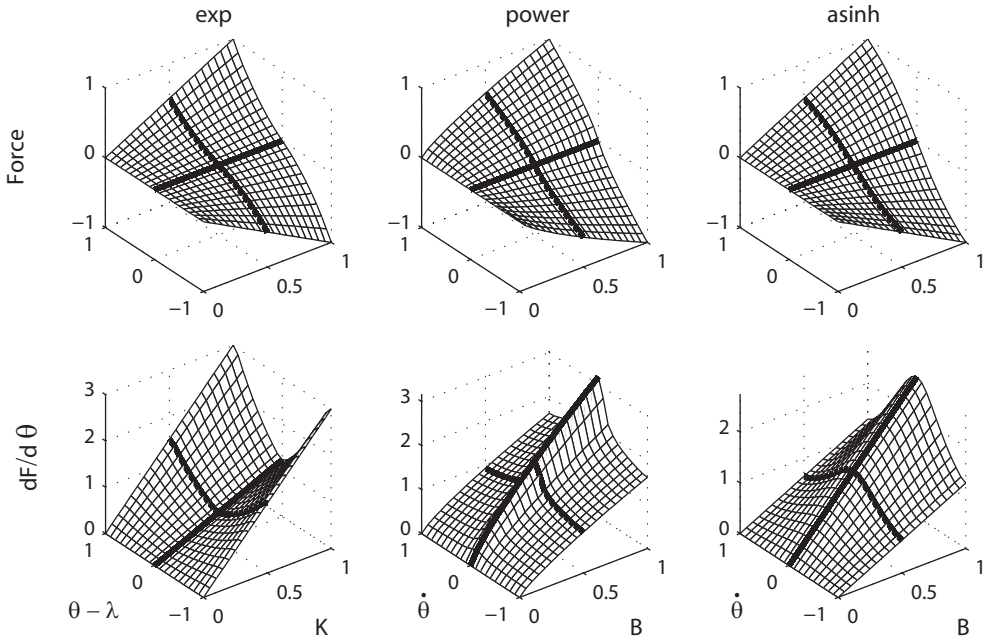

Figure 5.1: Different functions chosen as models of non-linear joint elasticity and viscosity. Horizontal axes measure angular error or velocity [-1,1] and stiffness or damping gain [0,1]. The resulting force F is measured on the vertical axis. The first row shows force itself, and the second row the derivative of force with respect to angular deviation. The linear model is omitted as its resulting surface is flat. For comparison all surfaces are scaled to a maximum force of 1 N.

achievable. In addition to the different controller non-linearities described above, the following experiments therefore also compare the effect of relative and absolute damping and their relative importance in producing fast and smooth movements.

5.2 Single-joint movements

The first experiment was aimed at identifying the combination of elasticity and viscosity models, as well as damping type and duration of EP shift, that achieves naturally smooth minimum jerk trajectories at various speeds. The output of each controller was simply $F = F_{pos} + F_{rel} + F_{abs}$, i.e. the result of adding elastic force (F_{pos}) as well as relative damping (F_{rel}) and absolute damping (F_{abs}) terms. For any given controller, the elastic component was either linear or exponential, while the damping terms were linear or described by the *asinh* function. All possible combinations were studied, leading to eight (2x2x2) different types of controller. In three separate sets of experiments (fast, moderate and slow movement conditions) each type of controller was optimised for both a large and a small amplitude movement using a genetic algorithm[1]. A single set of feedback gains (K, B_{rel}, B_{abs}) was used for both movements, while the duration of the EP shift was allowed to vary between the two. The fastest desired movements had durations of 0.2 s and 0.18 s for amplitudes of 100° and 50° respectively. In the moderate speed condition movements were twice as long (0.4 s and 0.36 s), and three times as long for slow movements (0.6 s and 0.54 s). Each controller was evaluated by driving it with an EP shift of evolved duration, and comparing the resulting

[1] See sections 3.4.2 for an overview of the algorithm and 3.6 for parameter values.

kinematics with the desired minimum jerk trajectory. Performance was measured by the absolute difference between the two, scaled to a value in the range [0,1]. Durations of the evolved EP shift were constrained to vary between 50% and 100% of the minimum jerk duration. Feedback gains were evolved in the range [0,1] and then scaled by a maximum value to prevent unrealistically high stiffness or damping. Measures of natural damping gain and dynamic stiffness, i.e. stiffness during movement rather than at rest, vary considerably in the literature. While older experiments have suggested stiffness values of up to 126 Nm/rad (Lacquaniti et al., 1982), more recent studies have found values as low as 14 Nm/rad (Gomi and Kawato, 1997; Bennett et al., 1992). It was decided to evaluate controllers with relatively low stiffness and the maximum was chosen to be 15 Nm/rad. Maximum damping to stiffness ratios reported in the literature vary between 0.1 and 0.25. This value is implicitly constrained by the optimization process, however, which favors minimum jerk like trajectories and hence penalizes terminal oscillations. It was therefore decided not to constrain damping gains any further, but allow maximum levels of the same strength as elastic forces (i.e. damping to stiffness ratio equalled 1 at most).

5.2.1 Optimality of non-linear reflex response

Each of the eight possible controllers was optimised at least five times for each of the three speed conditions. The performance of the best evolved controllers and the mean performance across repeated runs were then compared for any significant differences between the various linear and non-linear modelling functions. While the best performance found can be considered a reflection of the true potential of the controller (if the genetic algorithm found the global optimum), the mean and variance in performance rather reflects properties of the search space ("evolvability", ruggedness of fitness landscape) and the optimisation algorithm.

Table 5.1 summarises the performance of the best evolved controllers. In order to compare the best performances across the 2x2x2 different controller types an analysis was carried out that is similar to calculation of marginal means in an ANOVA statistic. A mean value was calculated for one factor (type of elasticity/viscosity) by averaging across all levels of the other factors. E.g. to assess the effect of exponential elasticity, the maximum performances of all linearly elastic models are averaged irrespective of the type of damping function, and compared to the average of maxima across all exponential models.

For the fastest movements these "maximum marginal means" in fitness MF are $MF_{lin} = 99.71\%$ and $MF_{exp} = 99.72\%$, which is not considered different given the low standard deviation (see below). The maximum marginal means for linear and non-linear relative damping, on the other hand, are $MF_{lin} = 99.63\%$ and $MF_{asinh} = 99.79\%$, indicating a significant effect. For absolute damping the means were $MF_{lin} = 99.71\%$ and $MF_{asinh} = 99.71\%$. Thus, considering only the best evolved controllers, it can be concluded that only the non-linearity in relative damping has a significant effect on the performance of fast movements. A full ANOVA statistic was also carried out, the results of which are found in the Appendix of this chapter (means are shown in table 5.3 and bar plots of true marginal means in figure 5.5). The mean performances are virtually identical to the maximum performances (greatest standard deviation $std = 0.0001$). Both a one-way ANOVA (with each of the eight model combination as separate factors) and a 2x2x2 ANOVA showed a clear effect of relative damping with a significance of $p = 0$.

Model			Speed			
F_{pos}	F_{vel}	F_{dmp}	fast	mod	slow	mean
lin	lin	lin	99.62	99.33	99.70	99.55
		asinh	99.63	99.39	99.67	99.56
	asinh	lin	99.79	99.47	99.71	99.66
		asinh	99.79	99.47	99.67	99.64
exp	lin	lin	99.63	99.70	99.77	99.70
		asinh	99.62	99.23	99.81	99.55
	asinh	lin	99.79	99.75	99.77	99.77
		asinh	99.80	99.47	99.81	99.70

Table 5.1: Best fitness percentage (across 5 runs for fast and slow movements, and 10 runs for moderate speed) for all elasticity and viscosity models as well as speed conditions.

For the slowest movements a different significant effect was found. Here the maximum marginal means for elasticity models were $MF_{lin} = 99.69\%$ and $MF_{exp} = 99.77\%$; for relative damping $MF_{lin} = 99.74\%$ and $MF_{asinh} = 99.74\%$; and for absolute damping $MF_{lin} = 99.74\%$ and $MF_{asinh} = 99.74\%$. Hence exponential elasticity seems beneficial for slow movements while the other non-linearities have no influence on performance. A 2x2x2 ANOVA confirms that the elasticity function is a significant main effect ($p = 0.03$), while the other main- and interaction effects are not significant ($p > 0.26$).

For moderately fast movements maximum marginal means were $MF_{lin} = 99.39\%$ and $MF_{exp} = 99.52\%$ for elasticity; $MF_{lin} = 99.39\%$ and $MF_{asinh} = 99.54\%$ for relative damping; and $MF_{lin} = 99.54\%$ and $MF_{asinh} = 99.39\%$ for absolute damping. I.e. controllers perform slightly better with exponential elasticity, non-linear relative damping and linear absolute damping. A 2x2x2 ANOVA confirms a significant main effect for relative damping ($p = 0$), and a marginally significant effect for elasticity ($p = 0.03$).

In summary, for fast and moderate movement speeds non-linear relative damping significantly improves performance. Non-linear elasticity significantly improves only slow movements, while moderate movements benefit little. Non-linear absolute damping, in contrast, did not show any significant effect on movement performance. We chose the model that performed best across the different speed conditions (exponential elasticity, non-linear relative damping and linear absolute damping) for further examination in the following sections.

5.2.2 Controlling movement velocity

In the previous experiments, reflex controllers were optimised independently for each of the three different speed conditions. While allowing different feedback gains to evolve depending on the required movement means that the system's dynamics can be optimally tuned for the task at hand, it also introduces additional control parameters. Since the aim of equilibrium-point approaches is the simplification of the control process, it would be desirable if there existed a simple relationship

between desired movement and feedback gains. Table 5.2 compares how each parameter depends on the intended movement speed for the best (non-linear) and worst (linear) controllers.

model	speed	K	V	B	T_1[%]	T_1[%]
best	fast	0.927	6.15	0	58	66
	mod1	0.11	2	0	60	65
	mod2	15	0.44	1.57	57	50
	slow	9.6	0	1.5	58	50
worst	fast	0.225	3	0	68	65
	mod1	0.02	1.57	0	68	66
	mod2	11.4	0.78	0.78	62	57
	slow1	11	0	1.5	55	50
	slow2	10.5	0	0.015	97	100

Table 5.2: Average evolved parameters for fast, moderate and slow movements. The first controller (best) has exponential elasticity, non-linear relative damping and linear absolute damping, while the second controller (worst) comprises only linear terms.

The non-linear model relies mostly on relative damping to achieve the highest desired speeds, with a small contribution of elasticity but no absolute damping. For moderate movements the optimisation process found two different strategies. The first consists of a reduction in both positional gain and relative damping to slow down the movement. The second, in contrast, relies more heavily on elasticity, but very little on relative damping. Absolute damping is used instead to avoid overshoot and oscillations. For the slowest movements, relative damping is completely replaced with significant elastic forces and absolute damping. The optimal duration of EP shifts is about half the desired movement duration across all speed conditions. The model consisting of purely linear elastic and viscous forces shows analogous tendencies. Compared to the non-linear model, optimal gains are significantly smaller, while the duration of EP shifts for fast movements is longer. Another strategy for slow movements was also found in which the duration of EP shifts is increased two-fold, while elastic and viscous forces are reduced.

To gain a more detailed picture of the relationship between optimal feedback gains and desired movement speed the best non-linear model was optimised again for a single 50 degree movement of durations ranging from 0.15 to 0.85s. To minimise the number of varying parameters, the duration of the EP shift was constrained to be 60% of desired movement time (i.e. in the optimal range found in previous experiments). The results are summarized in figure 5.2 (left). Minimum jerk trajectories were successfully reproduced across all desired movement durations. The average performance was 99.81% with a standard deviation of 0.05%. In contrast, a simple linear model without relative damping (effectively a PD) was able to produce the desired trajectories only for movements slower than 0.45s (compare figure 5.6 in the Appendix). The change in feedback gains for different velocities shows a pattern similar to the one found in the previous experiment. The shorter the movement duration, the more heavily relative damping is used, while for slower movements elastic and damping forces alone are sufficient. The relative contributions of each vary non-linearly with desired speed. While the damping gains exhibit nearly monotonos change,

elasticity quickly increases to a peak around 0.4-0.5s and then slowly drops. This adds significant complexity to the EP model under consideration. Not only would the central nervous system have to chose the optimal duration of EP shift, it would also need to acquire a mechanism for tuning reflex gains to the desired movement speed and amplitude.

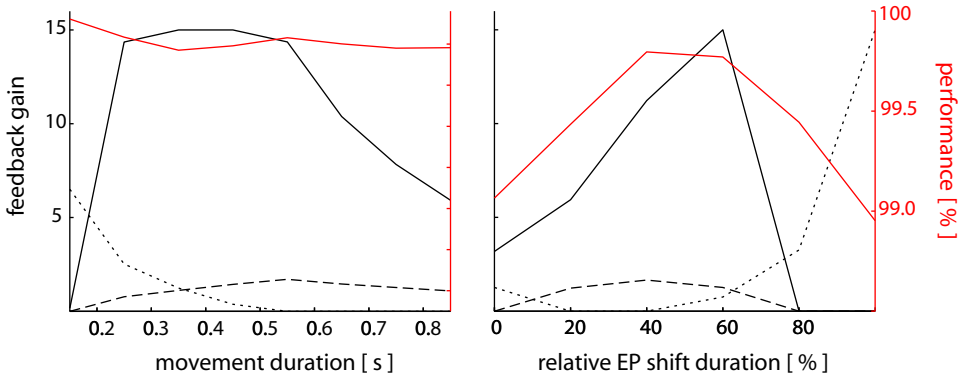

Figure 5.2: Optimal feedback gains. Left: as a function of movement duration with EP shift fixed at 60% of movement time. Right: as a function of relative EP shift duration, with a desired movement of 0.4 s. Black lines correspond to feedback gains: solid for elasticity, dotted for relative damping and dashed for absolute damping. Red lines trace performance (fitness).

In a second set of experiments it was tested whether assumptions about the duration of the EP shift would affect predictions regarding the amount of stiffness and damping necessary for smooth movements. The best non-linear controller was repeatedly optimised for a single movement of 50 degrees lasting 0.4 seconds, while varying the duration of the EP shift from 0 to 100% of desired movement time. Performance and evolved feedback gains are shown in figure 5.2 (right). First, results confirm that the optimal EP shift for this type of controller ends about halfway through the actual movement. This is in contrast to the full muscle-reflex model, which performed best with an EP shift of the same duration as the desired movement. Second, optimal feedback gains vary dramatically with the duration of the EP shift. For very fast shifts the system relies mostly on elastic forces, while for the slowest shifts elastic forces are minimized and replaced with relative damping. Hence, when simple EP models are used to predict properties of natural muscle-reflex dynamics, it is important to be aware of the significant effect that the assumed duration of the EP shift has on predicted feedback gains.

5.2.3 Effect of non-linear reflex response on joint kinematics

The superior performance of the non-linear model ($F = 99.79\%$) when compared to the linear model ($F = 99.62\%$) is reflected in measured kinematic indices. For the fastest large amplitude movement (100° over 0.2 s) the linear model reaches a peak velocity of 730 deg/s after 0.145 s ($T = 0.15$ s), while the non-linear model reaches 950 deg/s after only 0.11 s ($T = 0.14$ s). For reference, the target minimum jerk trajectory has a peak velocity of 937 deg/s only 0.06 s into the movement ($T = 0.125$ s). Clearly, considering only the fastest movements, the linear model is incapable of producing the forces necessary to achieve the desired speed. The non-linear model performs significantly better, but both reach peak velocity later than the minimum jerk trajectory.

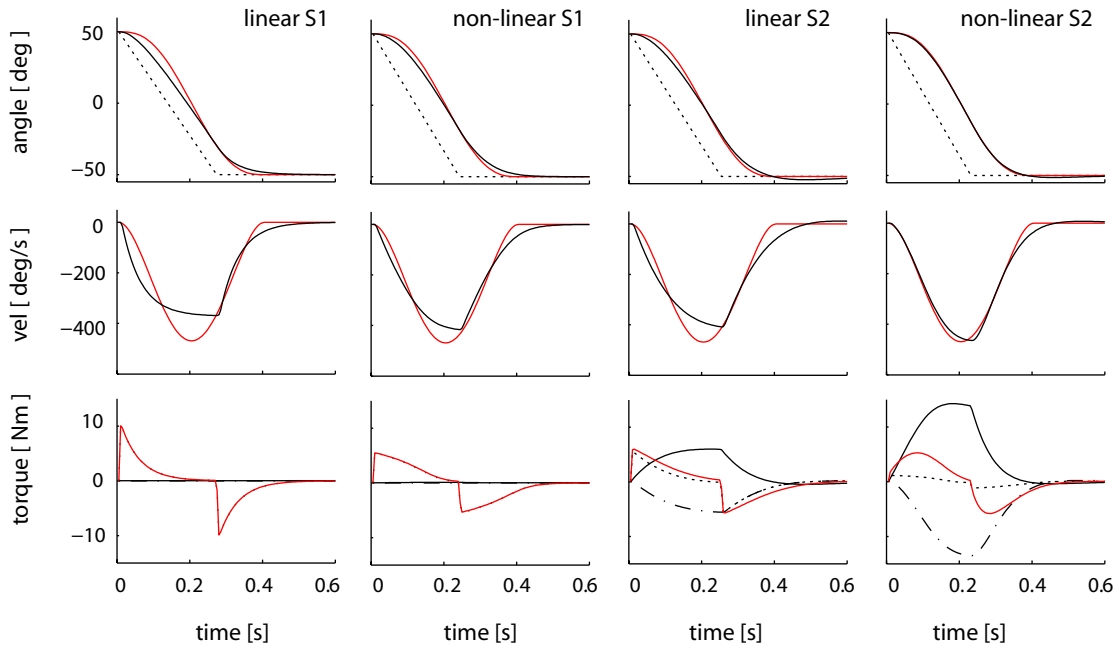

Figure 5.3: Kinematics and reflex response for two movement strategies (S1, S2) used by the linear and non-linear models. The top row shows desired trajectory (red), EP shift (dotted) and actual trajectory (sold black). The second row plots desired and actual velocity profile in red and black respectively. The bottom row shows individual reflex responses (black) and net torque applied to the joint (red). The solid curve represents elastic force, while absolute damping is drawn slash-dotted and relative damping as a dotted curve.

For slower movements the differences between the two models are more subtle. Figure 5.3 plots the kinematics and reflex response of the two models for movements of moderate speed. The two different strategies identified above are shown (compare table 5.2). The first strategy (S1) relies solely on relative damping to produce the desired trajectory, while the other two feedback gains are virtually zero. The second strategy (S2), in contrast, makes use of both elastic and viscous forces. In both cases the non-linear model improves upon the linear model. It prevents the actual position from leading the EP during the initial phase, and allows for less damped motion during the fastest interval, thereby producing higher peak velocity. The combined effect is a velocity profile that better resembles the desired bell shape.

5.3 Multijoint movements

In a final test of the validity of joint-level EP controllers as models of human motor control mechanisms, the non-linear model was optimised for the production of multijoint movements. Only the arguably simplest extension to the single joint case was considered; namely two hinge joints, each being driven by a separate controller, and no communication between the two. Control was implicitly coupled, however, by using synchronous EP shifts of the same duration and velocity. In order to observe the effect of interaction torques, each controller was optimised for two movements that differed in the direction of motion of the two joints. In the first case elbow and shoulder joints moved in the same direction, while in the second case the direction of the shoulder was re-

versed. Analogous to the multijoint experiments using explicit muscle models, the latter condition constitutes a synergistic case, in which interaction torques assist the motion, while in the former condition torques oppose the intended movement.

Several approaches were considered for mapping and constraining the individual feedback gains to be optimised. Options included independent and unconstrained optimisation of all parameters; constraining of the shoulder stiffness to twice the level of the elbow (as it needs to lift a stronger load); constraining all viscous forces to be at most half of the maximum elastic forces (empirically, damping forces are significantly lower than stiffness in humans arm movements); allowing all feedback gains to be twice as high as in the single-joint case (because higher stiffness could potentially counter interaction torques); enforcing minimum stiffness and maximum damping to prevent relative damping from dominating the dynamics (this should encourage strategy S2, which was found to be a better match for human kinematics above); and using a single fixed (but optimised) ratio between elbow and shoulder gains (desirable as a simple control strategy). As the intention was to test whether simple feedback control is possible without accounting for interaction torques, all experiments used a single set of feedback gains to control the two movements.

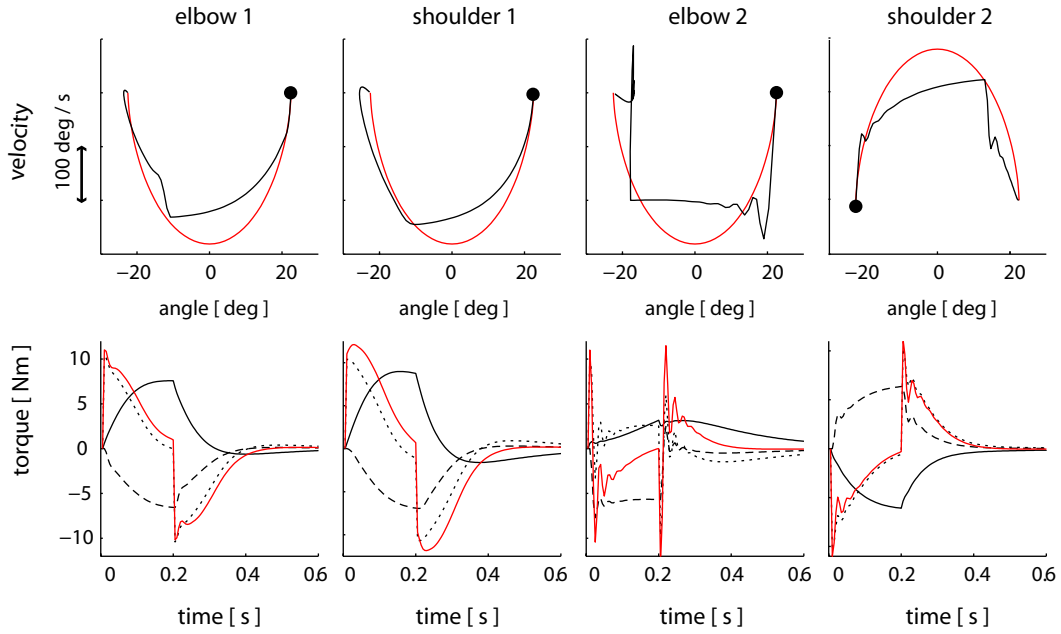

Figure 5.4: Angle-velocity phase plot (top row) and reflex response (bottom row) of an optimised multijoint EP controller. The first two columns show elbow and shoulder activity when both joints move in the same direction (assisting interaction torques), while in the last two columns movement is in opposite directions (opposing interaction torques). Initial position and velocity are marked by a dot.

Although a few of the resulting controllers differed quantitatively in both performance and kinematics, all of them failed to qualitatively reproduce natural minimum jerk trajectories. A typical controller is shown in figure 5.4. It is obvious that the interaction torques arising in one joint due to movement in the other prevent the system from producing smooth, natural trajectories. When movement direction is such as to create movement-opposing interaction torques (first two columns) the actual position lags the desired trajectory in both joints. When interaction torques as-

sist the movement (last two columns), actual position initially leads the equilibrium shift. Tremor-like oscillations can also be observed during acceleration and deceleration of the arm in the latter case. Furthermore, follow-up experiments were carried out to investigate whether the inability to compensate for interaction torques was simply due to the optimisation process having to find a trade-off in feedback gains between the two different directions of movement. However, even when optimised for a single direction only, perturbations caused by interaction torques are not sufficiently rejected. These results confirm the same limitation found in the explicit muscle-reflex model.

5.4 Discussion

This chapter has shown that a joint-level EP control model with non-linear elastic and viscous forces produces more natural single-joint movements than a linear model (as measured relative to a minimum jerk profile). It was found that the optimal duration of the EP shift for this type of controller is about half that of the intended movement time. This is in contrast to the full muscle-reflex model, which performed best with an EP shift of the same duration as the desired movement. When other EP shift durations were chosen, optimal feedback gains changed significantly. This means that the assumed time course of (currently non-observable) control variables such as the EP shift duration influences predicted reflex gains. This is important to bear in mind when comparing models of equilibrium-point control that make different assumptions about the time-course of the control variable; and when comparing predicted reflex gains to stiffness and damping levels measured in humans. The experiments further highlighted the necessity of tuning EP controllers for movements of different velocity (confirming results from the previous chapter). The relative contribution of individual reflex components varied non-linearly with desired speed. The added complexity of treating reflex gains as non-trivial control variables undermines the EP hypothesis only in so far as its simplicity is concerned. While reference to the body's complex dynamics can still be avoided, it implies that the central nervous system would need a mapping between desired position and speed on one hand, and the appropriate reflex gains on the other. A more significant limitation of this simple model is exposed when multijoint movements are considered. Here it failed to qualitatively match natural human performance. At realistic stiffness and damping levels, interaction torques create perturbations that can not be sufficiently rejected by the controller. It therefore confirms the results obtained using the explicit muscle model. For multijoint movements, a control strategy more complex than synchronous EP shifts must be necessary to produce the smooth trajectories observed empirically. Two potential mechanisms are investigated in the next chapter.

5.5 Appendix: ANOVA results

Model			Speed			
F_{pos}	F_{vel}	F_{dmp}	fast	mod	slow	mean
lin	lin	lin	99.62	99.23	99.42	99.42
		asinh	99.62	99.24	99.42	99.43
	asinh	lin	99.77	99.45	99.52	99.58
		asinh	99.78	99.46	99.42	99.55
exp	lin	lin	99.62	99.41	99.61	99.55
		asinh	99.62	99.22	99.52	99.45
	asinh	lin	99.78	99.51	99.62	99.63
		asinh	99.78	99.45	99.81	99.68

Table 5.3: Mean fitness percentage (across 5 runs for fast and slow movements, and 10 runs for moderate speed) for all elasticity and viscosity models as well as speed conditions.

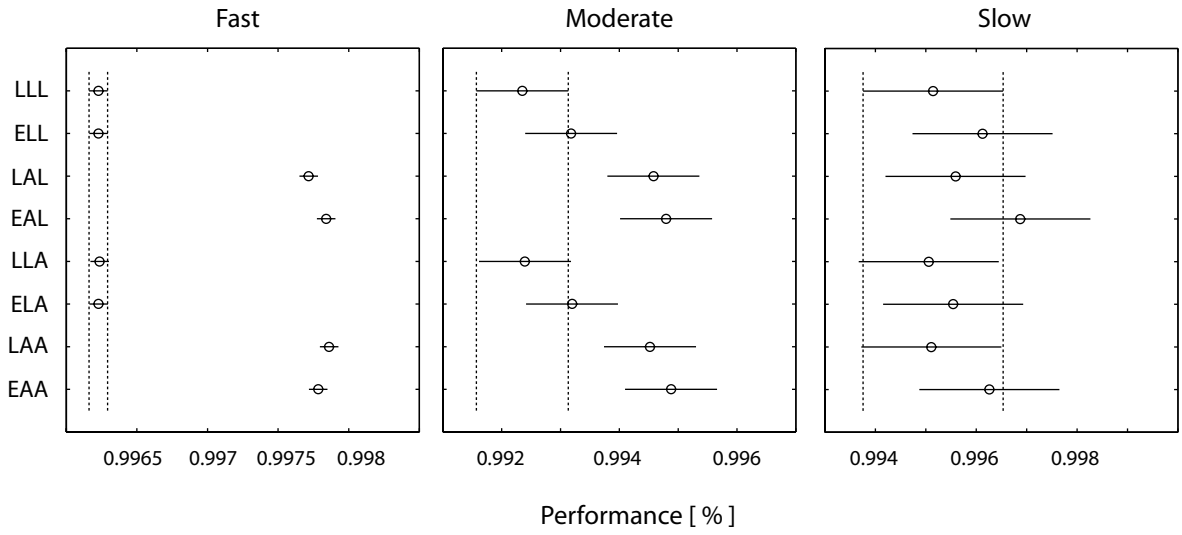

Figure 5.5: Multiple comparison test of 2x2x2 ANOVA results. Shown are all group means with 95% confidence intervals. Two means are significantly different if their intervals are disjoint. Groups names are comprised of three initials indicating the function used for elasticity (L=linear, E=exponential), relative damping (L=linear, A=asinh) and absolute damping (L=linear, A=asinh) respectively.

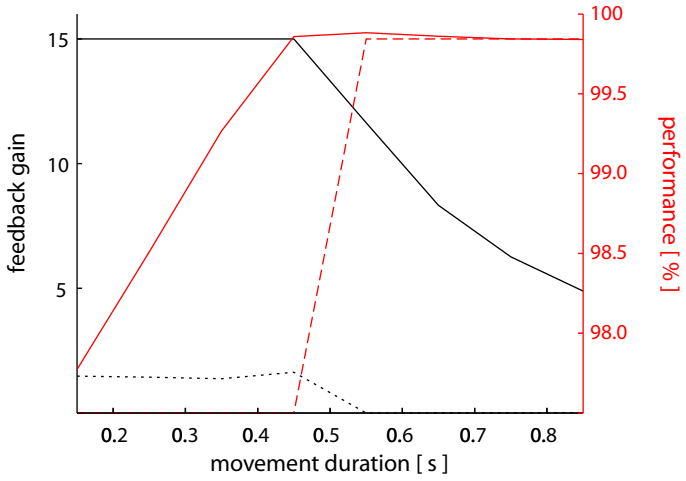

Figure 5.6: Feedback gains as a function of movement duration for a simple PD like controller. Strength of elasticity (solid black) and absolute damping (dotted black) is shown, as well as the relative duration of the EP shift (dashed red). The latter is measured as a percentage of desired movement duration. Performance (fitness) is also displayed (solid red). Note how for fast movements optimal performance can not be achieved at the given level of maximum stiffness (15 N/rad). For slower movements, the evolved strategy consists of decreasing elastic forces along with increasing duration of the EP shift.

Chapter 6

Compensation for interaction torques

In the following sections we use the lumped muscle-reflex model developed in the previous chapter to explore two different strategies for compensating interaction torques during multijoint movements.

6.1 Introduction

Both muscle-reflex models considered in the previous chapters, as well as the model of muscles driven with feedforward pulse-step signals, are able to reproduce the kinematics of human single-joint reaching movements. While explicitly modelling individual muscles more faithfully reproduces, for example, the typical bell-shape velocity profile, all approaches fail to cope with the interaction torques arising during multijoint movements. This calls into question the validity of the equilibrium-point hypothesis' claim that movements can be controlled without explicitly taking into account the dynamics of the body. Indeed, it would suggest that the central nervous system needs to predict the interaction torques resulting from an intended movement and appropriately adapt the movement "plan" so as to cancel out such perturbations preemptively. For any such prediction to be accurate, an internal model of the body's dynamics would be required. Many researchers therefore conclude that the force-control hypothesis alone, that is forces/torques as control variables driven by internal models, can explain the production of natural movements. This does not follow logically. Equally valid would be the suggestion of a position control model in which the desired position is corrected by predicted interaction torques, and inverse dynamics calculations that map the required counter-torques onto correcting position offsets. A similar strategy was proposed by Gribble and Ostry (2000). In a model based on equilibrium-point control, the authors devised an iterative learning scheme which uses position error to adjust initial control signals in a manner that eventually restores desired trajectories in the presence of interaction torques. Even though the system did not require explicit inverse dynamics calculations, it effectively learnt an internal model in the form of an inverse map from desired position to required control signals.

In this chapter we argue that an even simpler option might exist. The morphology of human limbs

does not usually change[1], and their joint chains are relatively short. The arm consists of only shoulder, elbow and wrist joint, the latter of which plays a lesser role in dynamics because the mass of the chain below it (the hand) is relatively small. Crucially, for human arm movements near linear relationships have been identified between the direction of joint movement, the interaction torques resulting from it, and the actively generated muscle torques in connected joints (Gottlieb et al., 1996; Gribble and Ostry, 1999; also see section 4.3.5). This suggests that the central nervous system could acquire a simple heuristic for controlling the movement of joints in a limb. A potential control scheme could take the form of a kinematics-based shift in desired position (as was used in previous chapters) on which is superimposed a transient corrective position offset derived according to simple rules from the desired direction of movement. Such a heuristic would most likely not be accurate. However, the equilibrium point created by the muscle-reflex system would ensure that the desired position is eventually reached, even if the modified transients are temporarily deviating from the desired position or the monotonic shift thereof. Based on this idea, we propose two strategies for addressing the problem of interaction torques in the framework of the equilibrium-point hypothesis. The first uses force feedback as an approximation of arising interaction torques. This is then used in a simple proportional control scheme at neighbouring joints. The second strategy does not rely on this hypothesised role of force feedback, but uses instead an approximate "prediction" of the upcoming interaction torque that is based on the desired movement direction and amplitude. Thus the former represents a feedback and the latter a feedforward compensation scheme.

6.2 Feedback compensation

Experiments in which EMG and torque pulses at the elbow and shoulder were measured have identified a simple strategy used by human subjects to coordinate the motion of these joints during pointing movements. It was observed that the torque produced at the shoulder is proportional to that produced in the elbow and that both follow the same time profile (Gottlieb et al., 1996). As confirmed by Gribble and Ostry (1999), such a *linear synergy* helps reducing the effect of intersegmental dynamics. If torques at the shoulder vary in proportion with torques at the elbow, then according to physical laws they must also vary with the interaction torque produced. This is because the interaction torque experienced at the shoulder joint itself is proportional to the original torque applied at the elbow. The question then is how the final torque is controlled so that it is proportional to the interaction torque, particularly in the EP hypothesis, which postulates position- and not force-control. The simplest approach is to offset the desired position negatively proportional to the upcoming interaction torque. If, for example, the direction of the interaction torque is such as to lead to flexion of the elbow, then the desired position at that joint can be offset in the opposite direction, that is towards extension. In a first set of experiments, we tested whether such an approach is feasible. As an approximation of the interaction torque at one joint we used the torque output of the other joint. In short, for each muscle-reflex controller we added to the monotonic shift in desired position the weighted torque output of the other joint's controller.

[1] Except for the duration of development, during which changes in, for example, limb lengths are slow compared to the time-scales involved in learning to reach.

6.2.1 Methods

As the problem of interaction torques arises in any articulated rigid body system, not just those powered by muscle-like actuators, the simpler lumped muscle-reflex model presented in the previous chapter is used in the following experiments. This model is in effect a non-linear proportional-derivative (PD) controller with added velocity error feedback (also called "relative damping"). For further details see section 5.1.

In the first experiment, controllers were evolved using a GA[2] to produce smooth minimum jerk trajectories with amplitudes of $2\frac{\pi}{8}$, $2.5\frac{\pi}{8}$ and $3\frac{\pi}{8}$ rad at both joints (45°, 56.25°, and 67.5°). For all amplitudes, the rate of change of the desired EP shift was 225 deg/s, leading to ramp durations of 0.2, 0.25 and 0.3 s. For each amplitude condition two trials were performed: one in which shoulder and elbow joint rotate in opposite directions, and one in which the direction of movement is the same. Consequently, in the former trial resulting interaction torques support the desired motion, while in the latter trial they oppose it. Different feedback gains (stiffness K, velocity error V, and velocity proportional B) were evolved for the two joints, but the same set was used for all six trials. Previous experiments found that different viscoelastic properties are necessary only for different movement speeds, but not amplitudes.

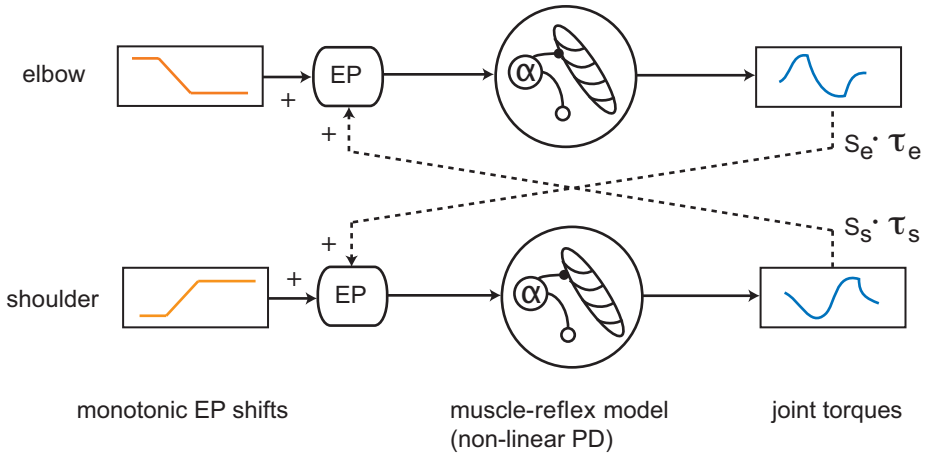

Figure 6.1: Torque feedback control scheme: each joint is actuated by a lumped muscle-reflex model, in effect a non-linear PD controller with relative damping. The controller receives as input the desired position of the joint, i.e. the virtual EP, and outputs a time-varying torque that is applied to the arm model ($\tau_{e/s}$ for elbow and shoulder). The desired position of each joint is the result of adding a central command that monotonically shifts from initial to final position, and the gain-scaled feedback of torque produced in the other joint ($s_{e/s} \cdot \tau_{e/s}$).

The control scheme for this experiment is illustrated in figure 6.1. Each controller receives as input a desired joint angle that monotonically shifts from initial to final position. As described above, the two joints do not act in isolation, however, but are coupled through the torque feedback they receive from each other. To be precise, the torque produced in one joint is scaled by a feedback gain and added to the central signal controlling the other joint. Each virtual EP trajectory is thus

[2] See sections 3.4.2 for an overview of the genetic algorithm used, and 3.6 for parameter values.

the result of adding a simple ramp-shaped control signal and a potentially complex time-varying torque feedback.

For each trial and joint a different torque feedback gain was evolved as it was not known a priori how it would depend on the desired amplitude or speed of movement. Both positive and negative torque feedback gains were allowed. In addition, for each of the three different amplitudes the duration of the minimum jerk trajectory (against which actual trajectories were evaluated) was optimised. This was because previous experiments had found that the relationship between the rate of change and duration of the monotonic shift in desired position on the one hand, and the duration of the produced minimum jerk trajectory on the other, is not always linear. The range of the desired duration was constrained to 100–200% of the ramp duration to avoid cases in which the same movement dynamics evolve independent of the input ramp. The particular range was chosen because experiments in the previous chapter found that the ramp shift is optimal at approximately half the duration of the desired movement. All in all, each genome encoded for six "ordinary" reflex gains, twelve torque feedback gains, and three minimum jerk trajectory durations.

Once the controllers had succeeded on this first task, the resulting system was incrementally evolved for a higher resolution of amplitudes (now including $1.75\frac{\pi}{8}$, $2.25\frac{\pi}{8}$ and $2.75\frac{\pi}{8}$ rad), as well as for different speeds (25% faster and 25% slower). Finally, a test for generalisation was carried out with the best evolved system in which amplitudes varied between $1\frac{\pi}{8}$ and $3\frac{\pi}{8}$. Also, for comparison, a control experiment was conducted in which a muscle-reflex system was evolved on the initial range of movements but without the addition of torque feedback.

6.2.2 Results

The control experiment demonstrates again the failure of simple feedback systems to deal with interaction torques. Figure 6.2 presents the trajectories and velocity profile of the reflex-controller without torque feedback. In neither the supporting nor the opposing interaction torque condition does the system exhibit natural dynamics. The velocity profiles are not generally bell-shaped and feature a non-continuity at peak velocity, which coincides with the desired position reaching its plateau.

Compare these trajectories with those produced by the controller featuring torque feedback, shown in figure 6.3. Although velocity profiles are not perfectly smooth, they much better resemble the desired minimum jerk trajectory (shown in red). Several interesting features are worth noting in this data.

Firstly, when intersegmental dynamics support the desired motion (first two columns), overall torques applied are significantly smaller than when they oppose the intended motion (last two columns). Thus, the system seems to *exploit* the existence of interaction torques when possible, and otherwise generates larger forces to *counteract* them. Interestingly, the same pattern is observed in human subjects (Gribble and Ostry, 1999). The effect is particularly striking for the elbow in the trial with supporting interaction torques (leftmost column). First, note that the experimental setup is such that positive torques move a joint towards more negative angles. Now, as the figure demonstrates for the trial in question, the elbow generates torques that would move the joint not in the desired, but exactly the opposite direction. This means that the interaction torque

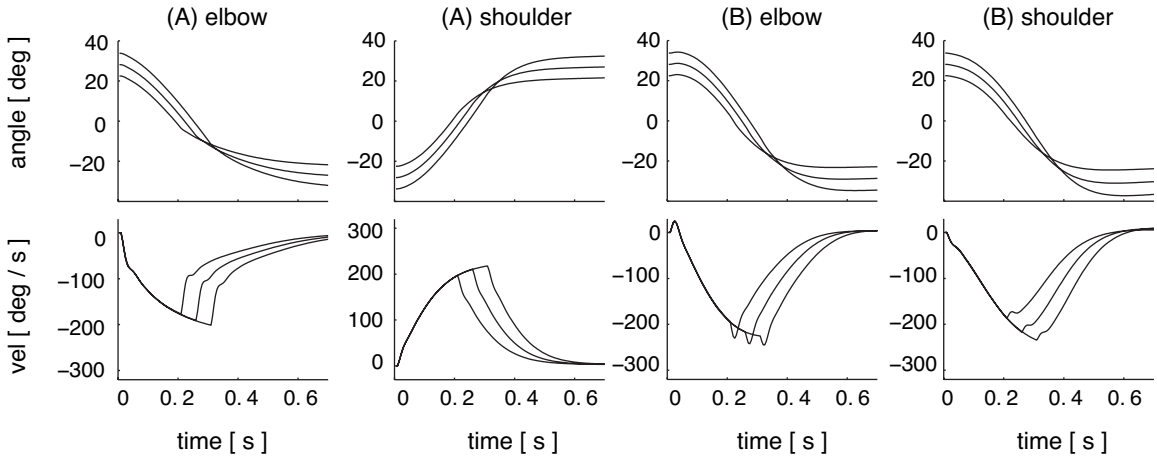

Figure 6.2: Kinematics of the control model (without torque feedback). Shown are angular position (top) and velocity (bottom) of elbow and shoulder joint during three movements in opposite directions (A, left) and the same directions (B, right). Amplitudes are 45°, 56.25°, and 67.5°, and EP shift durations 0.2, 0.25 and 0.3 s, respectively.

produced by the shoulder is already driving the elbow in the right direction so strongly that it needs to actively oppose it, that is, produce a breaking force instead of accelerating in the desired direction.

Secondly, torque feedback gains have evolved such as to modify the input trajectory (dashed line in the first row) only in certain cases. To be more specific, the virtual EP trajectory of the elbow is modulated by torque feedback only when interaction torques are supportive. The shoulder's input trajectory on the other hand is modulated only for opposing interaction torques. In all other cases torque feedback gains evolved towards zero. Furthermore, the role of torque feedback seems to differ in the two cases where it is employed. For movements in opposite directions, the input trajectory for the elbow is equal to the sum of the linear ramp shift and the negative of the torque produced at the shoulder. The resulting input trajectory initially accelerates more slowly than the unmodified ramp, but then temporarily overshoots the actual target. The effect of this modification can only be understood when the other feedback modalities are taken into account. When comparing the contributions of the different modalities to the overall force production (bottom left in figure 6.3), it becomes clear that the result of the input modification is an equalisation of the proportional and derivative components. The time course of the proportional term is now so similar to that of the damping term (but of opposite sign) that their sum, and therefore the overall torque produced, becomes very small. The contributions are in fact shaped such that a small breaking force is created instead of an acceleration, as described above. Compare that to the unmodified input trajectory (third column). The seemingly minor differences in shape of the proportional and derivative components here lead to significant acceleration rather than deceleration.

Torque feedback at the shoulder joint has a different functionality. Here, the addition of elbow torque to the shoulder's input trajectory leads to greater acceleration of the virtual EP when compared to the original input ramp (top of rightmost column). This is followed not by an overshoot, but by a reversal of direction away from the target position, to which the virtual EP then gradually

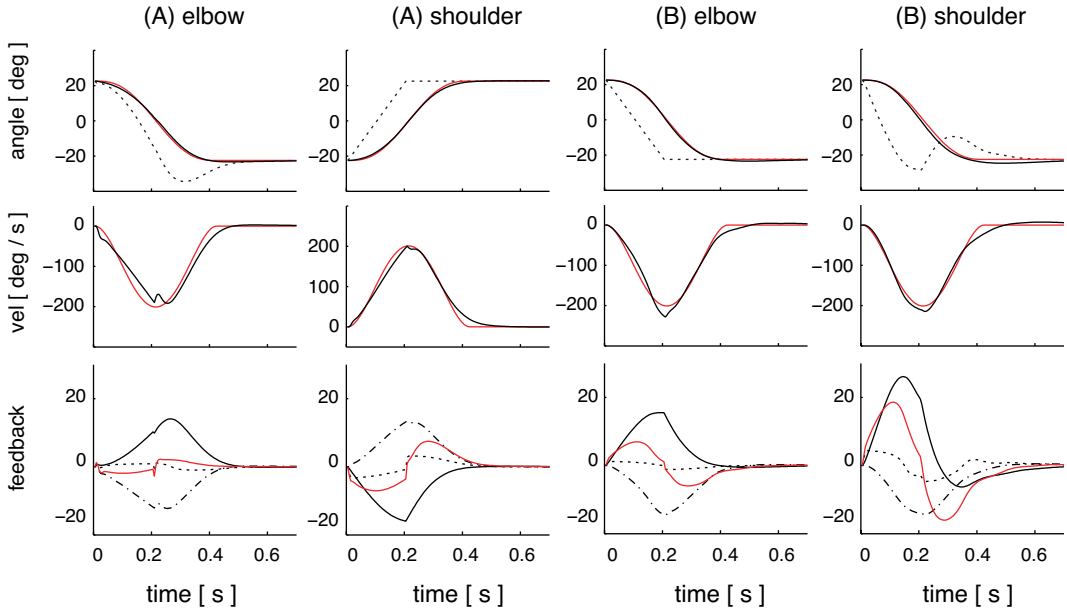

Figure 6.3: Multijoint kinematics of torque feedback model at moderate speed and medium amplitude. Shown are angular position (top) and velocity (middle), as well as feedback response (bottom). Red lines indicate the minimum jerk trajectory in the first two rows, and the dashed line plots the input signal (desired position ramp plus torque feedback). In the last row, solid black lines correspond to the positional error term, dashed to velocity error, and dash-dotted to the damping term. The red line plots final torque output.

relaxes. The effect on individual reflex components is equally reversed. Instead of equalising the proportional and derivative terms, the positional error is exaggerated. The result is a greater force production than is the case with a normal input ramp (second column). The greater accelerating torque is then matched by an equally amplified decelerating impulse, which is the result of the reversal in direction of the input trajectory at that point. Of course, the amplification of torque applied at the shoulder is exactly what is required to counteract the opposing interaction torque resulting from elbow motion.

Where torque feedback is used to adjust the original control signal, the resulting virtual EP trajectories show similarities with those produced by the learning scheme described in (Gribble and Ostry, 2000). Generally, they also find a difference in strategy between movements in the same and those in opposite directions. In particular, both an overshoot followed by reversal of direction, as well as unmodified monotonic shifts can be observed in both models. But while the learning scheme seems to produce the latter only at the shoulder in the case of assisting interaction torques, they also occur here at the elbow for opposing torques. Visual inspection indicates that the learning scheme failed to create trajectories as smooth as those produced here with torque feedback. The authors report that better results could be achieved if their learning algorithm was applied for more iterations. It would be interesting to know whether the control signals would be more similar if their trajectories were further optimised.

The results indicate that it would be too simple to view feedback controllers such as the one demonstrated here merely as damped non-linear springs. Closing the loop between the two joints leads to a complex dynamical system, which through the interaction of its various subsystems is

capable of "choosing" different strategies to cope with both supporting as well as opposing interaction torques. Furthermore, a simple non-linear feedback controller with added torque feedback achieves just that without the need for learning an internal model or inverse dynamics calculations.

However, although the resulting trajectories are compensated for intersegmental dynamics qualitatively, they do show some deviations from the desired minimum jerk trajectory. Even though not visible in plots of angular position, the velocity profile shows a noticeable kink around peak velocity. This can be explained as follows. The input trajectory of the joint unaffected by torque feedback is non-smooth (non-differentiable) where it changes from a ramp to a plateau. The desired velocity input to the controller (not drawn), which is the piecewise derivative of the desired position ramp, therefore features a non-continuous step change. It forms a rectangular function which changes from zero to the constant velocity of the position ramp and then back to zero again. Both these abrupt changes show up in the different components of the reflex controller and in its final torque output. Through torque feedback, this effect can then further spread to the other joint, where it becomes particularly apparent when overall torque output is low (leftmost column). It is worth emphasising here again that the simple feedback model is not meant to perfectly model human muscles and reflexes or match experimental data, and it is expected to differ in details such as the one described. While additions to the model could arguably help to re-produce natural kinematics more faithfully (e.g. a low-pass filter on "muscle activation"), the current complexity of the model seems to be sufficient for studying general principles such as the compensation for intersegmental dynamics.

The torque feedback model exhibits another interesting feature. Actively produced torques indicate a synergy between the two controlled joints. The time profile of torque at the elbow is effectively a scaled version of the shoulder torque (red lines in bottom row of figure 6.3). This is the case independently of the direction of interaction torques, hence even where the elbow produces breaking instead of accelerating forces. This seems to be in line with findings of a linear synergy during goal-directed arm movements by Gottlieb et al. (1996). Figure 6.4 shows the close time synchrony of the two joints more clearly by superimposing the normalised torque waveforms (left) and plotting elbow torque against shoulder torque (right).

Even though the torque waveforms are not as smooth as those extracted from experiments with human subjects, they qualitatively reproduce the near-linear and figure eight curves reported in (Gottlieb et al., 1996). These results hint at the possibility that the observed linear synergy constitutes yet another movement feature that emerges from the dynamics of the muscle-reflex system. Thus, instead of reflecting a strategy used by higher centres to directly plan the torques at each joint, as proposed by Gottlieb et al. (1996), the results can be interpreted as evidence for an underlying organisation of the motor apparatus that allows higher levels to control multijoint movements without regard for intersegmental dynamics.

Finally, the proposed torque feedback mechanism seems to be functional across a range of different amplitudes and speeds. Figure 6.5 presents kinematic data from the generalisation test, in which amplitudes vary from 22.5° to 67.5° and speeds are considered that are 25% faster and slower than the moderate condition.

As the figure shows, smooth movements are produced in almost all cases. Several observations can be made, though. Firstly, the kink at peak velocity described above is visible again in the first of

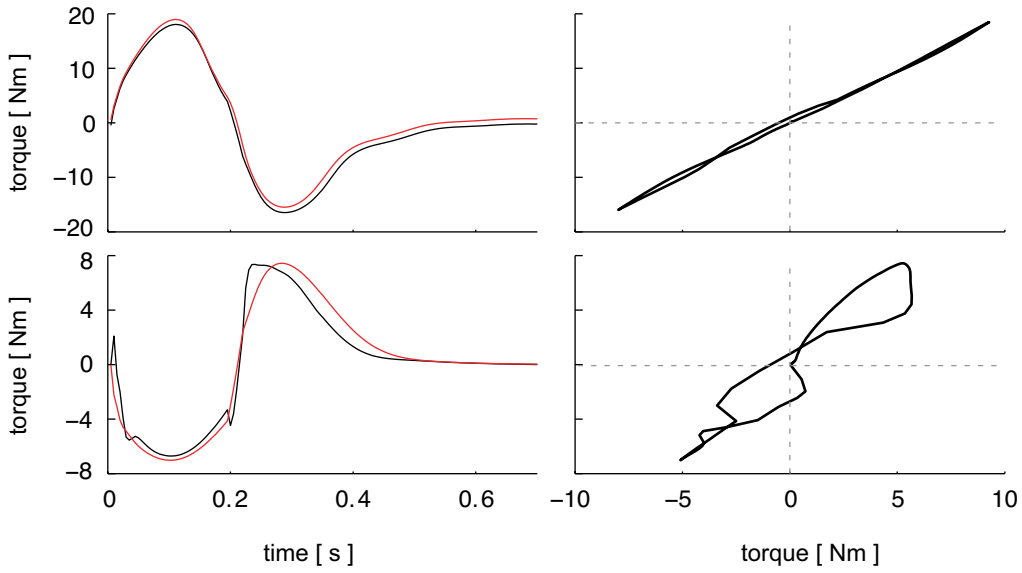

Figure 6.4: Linear synergy in multijoint movements with torque feedback. On the left, shoulder (red) and elbow torque (black) are superimposed after normalisation for amplitude and offset for clarity. The top row corresponds to movements in the same direction, and the bottom row in opposite direction. In the right column shoulder torque is plotted against elbow torque.

the two trials for all amplitudes. Secondly, for some of the larger amplitudes, the velocity profile is unnaturally flattened near peak velocity. This is most likely due to the fact that, apart from torque feedback, all other feedback gains were held constant across the different amplitude conditions. Even though this proved sufficient for single-joint movements in the previous chapters, in the case of multijoint movements the resulting viscoelastic properties do not seem to be always appropriate. This is connected to another observation. For a constant rate of change of the virtual EP, the evolved durations for the minimum jerk trajectory (against which the performance is compared) vary non-linearly as a function of movement amplitude. In other words, for larger amplitudes the optimal movement duration becomes shorter relative to the input ramp, meaning that the system "prefers" to move faster the larger the distance to the target. The velocity profiles for different amplitudes consequently show different peak velocities despite being caused by the same constant rate shift in desired position. It would therefore be reasonable to assume that better performance could be expected if the system was allowed different stiffness parameters for different amplitude and speed conditions. This was in fact observed in previous chapters.

Lastly, the observed kinematics (with exception of the anomaly just mentioned), qualitatively match those of human subjects instructed to move accurately and rapidly to target positions at variable distances (Gottlieb et al., 1990). In what the authors coined the *speed-insensitive strategy*, they found that the initial rate of rise in torque and velocity at the shoulder and elbow are uniform across different amplitudes. This is evident here in velocity profiles that initially superimpose almost perfectly, and diverge only past their peak values. They also found that greater distances cause these variables to rise for longer intervals, and therefore to larger peak values. In other words, humans prefer to move faster to cover larger distances when not instructed to move at any particular speed. This, as already mentioned, is reproduced here in the different peak veloc-

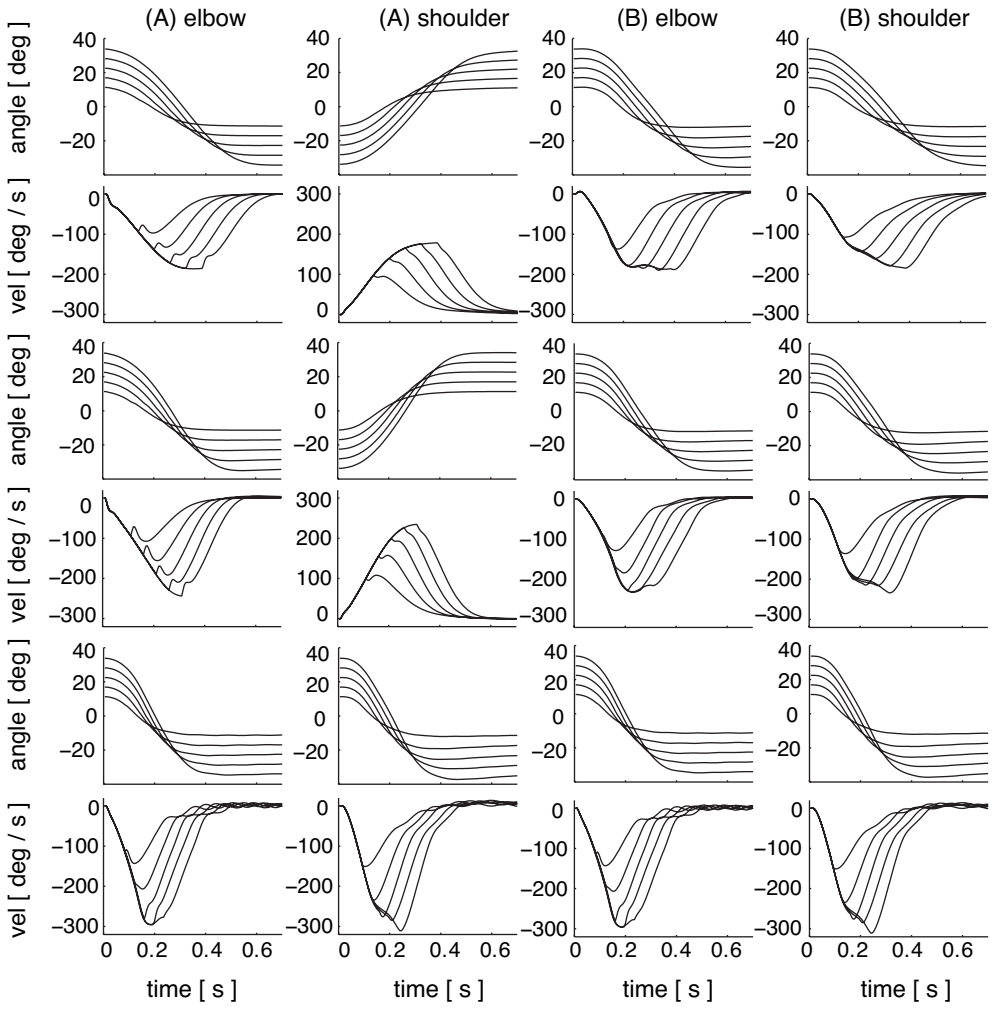

Figure 6.5: Multijoint kinematics of the torque feedback model for a range of amplitudes (22.25°–67.5°) and three different velocities (rate of EP shift is 168.75, 225, and 281.25 deg/s). The first two columns show the kinematics (position and velocity) of the elbow and shoulder joint during movements in opposite directions. The last two columns display the same data for movements in the same direction. The first two rows correspond to slow, the rows in the middle to moderately paced, and the last two rows to fast movements.

ities observed at different amplitudes. Gottlieb et al. (1990) suggested that this speed-insensitive strategy is implemented through central control of amplitude invariant motoneuron patterns that vary in duration and timing. The model proposed here suggests instead that the observed strategy reflects an adaptive organisation of spinal motor circuits that allows for control of movement distance via simple shifts in joint equilibrium position at a constant rate.

With regard to the complexity of adjusting interjoint torque feedback for a desired type of movement, it can be noted that the corresponding feedback gains evolved to be constant across different movement amplitudes. In fact, the gains were also constant across the two slower speed conditions. Only for the fastest movements did the gains evolve slightly different values. Also, the gains were negative only because the experimental setup, somewhat counterintuitively, was such that positive torques accelerate the joint in the direction of negative angles. Negative feedback

gains therefore imply that torque feedback is in fact positive.

In summary, the proposed extension of equilibrium-point based models for multijoint movements constitutes a simple mechanism that could explain the compensation of interaction torques, the observed synergy between elbow and shoulder joints, as well as the speed-insensitive movement strategy employed by human subjects. The fact that these features emerge simultaneously from a simple non-linear feedback controller with interjoint torque feedback suggests that the latter two might in fact be secondary outcomes of a mechanism that deals primarily with intersegmental dynamics.

6.3 Feedforward compensation

The mechanism proposed in the previous section for compensation of interaction torques relies on a feedback signal between joints that carries information about net joint torques. A possible source for this type of feedback are the proprioceptive afferents carrying signals about the tension in individual muscles (appropriately combined). A different approach could make use of information about the intended movement to "predict" instead the upcoming torques. As can be seen in the previous sections, the waveform of net joint torque has to have a sinusoidal shape with an accelerating and a decelerating pulse. The magnitude and timing of these pulses in turn is correlated with the desired movement amplitude and speed. If these details are known, an approximate time course of joint torques could therefore be "predicted". In this section we test the idea that a *somehow preprocessed* version of the virtual EP trajectory for one joint can be used to modulate the input trajectory of another joint such as to cancel out the interaction torques resulting from the motion of the two. We emphasise here the fact that we do not know a priori what exactly this preprocessing needs to achieve. An actual, precise prediction of upcoming torques might not be required, for example. As the previous section has demonstrated, all that is needed is a signal that amplifies or suppresses joint torques depending on the direction and magnitude of joint motion. The only difference is that we want to create this signal here in a feedforward manner, from information about the intended movement, rather than from proprioceptive feedback.

6.3.1 Methods

The proposed feedforward compensation mechanism works as follows. First, a linear shift in desired position is generated that moves from the initial to the desired position at a constant rate (identical to previous experiments). This constitutes the central motor command. Two such input ramps are in fact produced, one for the elbow and one for the shoulder joint. Now, for each joint we create a preprocessor. This subsystem receives both the input trajectory for the same joint as well as that for the other joint as input. Its function is to somehow modulate the original input trajectory based on information from the other joint's trajectory so that upcoming interaction torques are compensated for. Since we do not want to constrain the functionality of the preprocessing stage in any particular way, we evolve dynamic neural networks for this purpose. The type of neural network used is described in the next section.

Dynamical neural networks

Continuous-time recurrent neural networks (CTRNNs) (Beer, 1995b) are used in the following experiments as abstract models of spinal reflex circuits. The state of each node in such a network is described by

$$\tau_i \dot{y}_i = -y_i + \sum_{\forall j} w_{ji} \phi_j (y_j + \vartheta_j) + g I_i(t)$$

where y_i is the cell potential of that node, τ_i its time constant, w_{ji} the weights of incoming synapses, ϕ the sigmoidal function $\phi(x) = 1/(1+e^{-x})$ calculating the firing rate, ϑ the threshold of the node and gI gain-scaled input respectively.

Even though the above equation can be interpreted as a model of biological (non-spiking) neurons and networks, dynamical systems of this type are used here only as proxies for hypothesised functionality of yet unknown spinal circuits. In other words, these networks should be regarded proof-of-concept dynamical systems that demonstrate whether or not certain central motor commands can produce a desired movement when combined correctly. As such, they can be used to make predictions, for example, about the significance of certain types of control signals, but not about detailed connectivity in biological reflex circuits. CTRNNs were chosen because they are arguably the simplest non-linear continuous-time neural model and were shown to be universal approximators (Funahashi and Nakamura, 1993; Nakamura and Nakagawa, 2009). Also, because their dynamics are guaranteed to always converge, independent of the parameters chosen, they are well suited to evolutionary algorithms (e.g. Beer, 1996).

Used in conjunction with a genetic algorithm, the parameters of each neuron are obtained through scaling of elements in the genotype (distributed over the range [0,1]). Typically in this chapter, weights, biases and input gains are scaled to the interval $[-12, 12]$, and time constants are constrained to be at least twice the integration step size and to cover at most the length of the fitness evaluation. The Euler method with a time step of 0.005 s was used for integrating the differential equation (equal to the granularity of the physical simulation).

Experimental setup

The topology of the neural networks evolved to generate modified EP trajectories is illustrated in figure 6.6. Each network consists of four neurons and two input nodes (filled grey circles). The latter do not exhibit neural dynamics, but function as simple placeholders relaying the centrally specified monotonic shifts in desired EP. Each network receives the EP trajectory for the joint it controls as its first input, and the desired EP of the other joint as its second input. Also, the output of one of its neurons (black filled circle) constitutes the new desired EP trajectory and is used as input to the muscle-reflex system instead of the original EP ramp. The neuron's output was scaled from the range [0, 1] to the range [-1, 1]. Since the muscle-reflex system works in units of radians, the networks were therefore able to specify desired angles between -180° and +180°. Notice that there is no feedback to the networks from the muscle-reflex controller or limb dynamics. The desired EP trajectories have to be generated in a purely feedforward manner from information about the intended movement (such as the rate of change and duration of the input ramp).

The evolution of these networks was carried out incrementally. In the first stage, only one network was evolved to produce single-joint movements at the elbow. Fitness was determined as previously

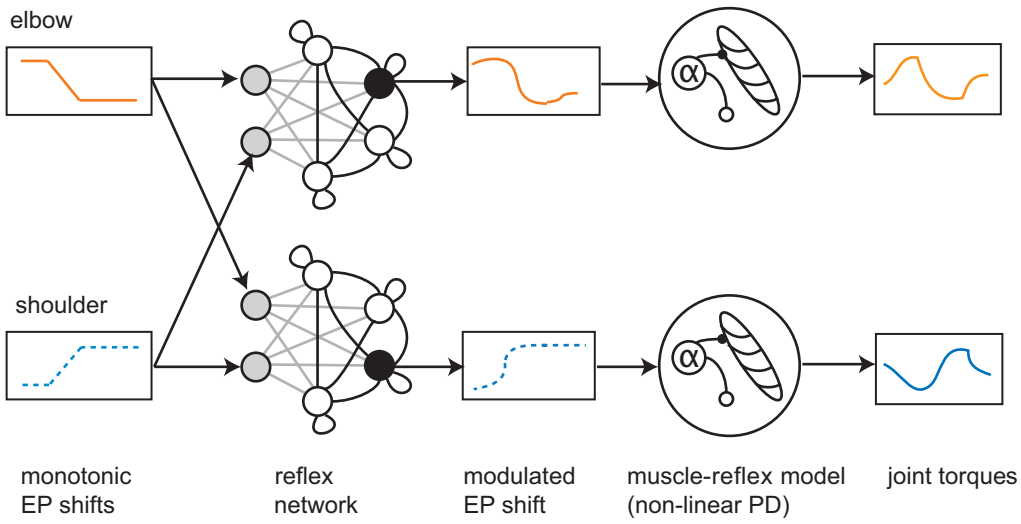

Figure 6.6: Elbow (top) and shoulder (bottom) control schemes responsible for compensation of interaction torques. From left to right: each joint is controlled by a neural network that receives as inputs both its own desired position, as well as that of the other joint. The desired positions are centrally controlled and shift monotonically from start to endpoint. Each network outputs a new EP trajectory through a dedicated neuron (black node), which is used to drive the corresponding joint's muscle-reflex model in place of the original input ramp. In other words, each network uses information about the intended movement of the other joint to transform its simple monotonic input ramp with the aim to preempt the resulting interaction torques. No feedback is present from the periphery to the network controllers.

from the difference between actual and desired minimum jerk trajectories. Three amplitudes of 22.5°, 45° and 67.5° were tested for each network instance, with desired durations of 0.15, 0.3 and 0.45 s. The time span of the monotonic EP shift was also optimised. As in previous experiments, it was constrained to be at most as long as the desired movement, but not shorter than 25% of its duration. As at this stage only single-joint movements were evolved, the network received only one input, namely its own desired EP shift. For each network evaluation, the order of trials was randomised and the desired movement randomly offset by up to 12° (so movements were not always centred around 0°). Also, at the beginning of a trial each neural state was reset to random values from an interval surrounding its bias. This was to avoid networks which perform correctly only when starting from specific initial conditions.

After the genetic algorithm had converged (no further improvement in fitness), the experiment transitioned to the second stage. Now movements at both elbow and shoulder joints were evolved. To this end, the best evolved single-joint network was extended in two ways. Firstly, the second input neuron was added with initial parameters chosen so that by default it had no influence on the network dynamics (gain and outgoing weights were set to zero). Secondly, the extended network was duplicated exactly for a setup as presented in figure 6.6. A genome encoding the extended and duplicated network was then used to seed a new population from which the GA started evolving multijoint movements. Parameters for the two subnetworks could from then on evolve independently. All in all, each genome encoded for 77 values (34 per neural network, three feedback gains per muscle-reflex controller, and three EP shift durations).

6.3.2 Results

Figure 6.7 presents the kinematics, feedback components, and torque output of the best evolved system during a 45° excursion lasting 0.3 s. Clearly, a successful strategy evolved that produces smooth multijoint movements with natural bell-shaped velocity profiles. Compare these trajectories to those generated by the uncompensated system in figure 6.2. As was the case with feedback compensation, the resulting system exploits interaction torques when these are supporting the intended movement. The forces applied at the joints in this case are smaller than in the case of opposing interaction torques (compare the first two columns to the last two). In fact, the same pattern of breaking rather than accelerating torques can be observed in the elbow. Also, the shoulder creates larger overall torques than the elbow. This is not surprising either, since the shoulder joint has to support and move a larger load than the elbow.

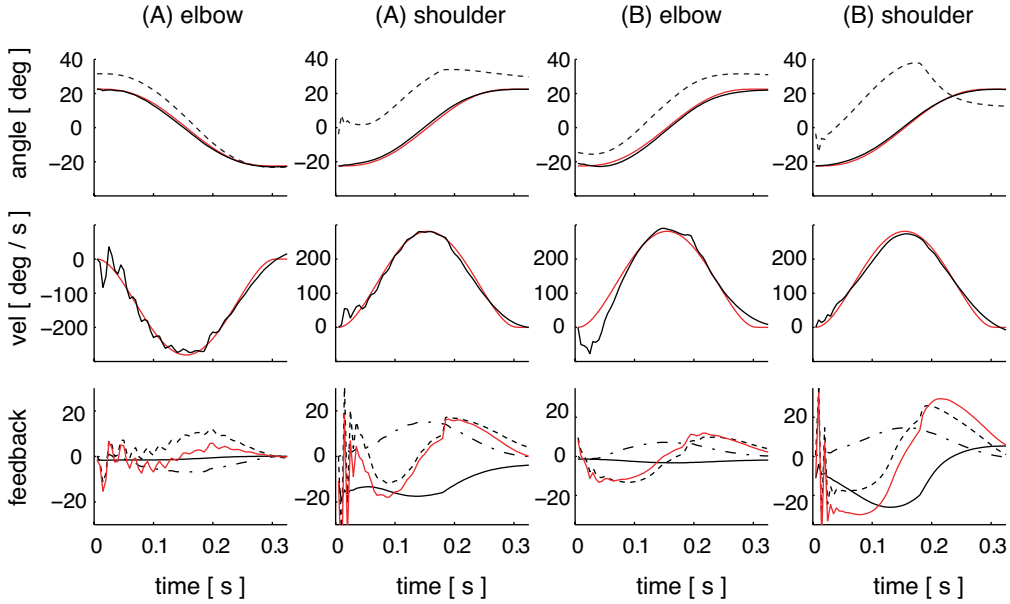

Figure 6.7: Multijoint kinematics of CTRNN model for a medium amplitude movement. Shown are angular position (top) and velocity (middle) as well as feedback response (bottom). Red lines indicate the minimum jerk trajectory in the first two rows, and the dashed line plots the virtual EP trajectory generated by the neural network. In the last row, solid black lines correspond to the positional error term, dashed to velocity error, and dash-dotted to the damping term. The red line plots final torque output.

However, several features distinguish the evolved system from the torque feedback model. Firstly, the neural network initially exhibits relatively large, and later small amplitude oscillations in its output neuron (and therefore torque output), especially at low overall output levels (leftmost column). This is certainly not desired, but does not seem to significantly affect the spatial trajectory. It would be reasonable to assume that continued optimisation, careful tuning of the fitness function and network parameter ranges, or the addition of more neurons, could produce a smoother approximation of the dynamics observed. But since we are not concerned with absolute accuracy in matching experimental data, this was not pursued here.

Secondly, the kinematics show no discernible discontinuity at peak velocity. Whereas in the torque feedback model this discontinuity spread from the ramp-shaped input signal of one joint to the

torque output of the other, this discontinuity is absorbed here by the neural network dynamics. Even though the existence of this discontinuity in the previous model merely hints at its simplifications (e.g. no low-pass filter on activation dynamics, which is a standard feature in Hill-type muscle models), the absence of it in the neural network model indicates that intuitions about a desirable and simple central command signal might be misleading. Although a ramp-shaped shift from initial to target position might seem simple to a human designer, the resulting discontinuity, especially in higher derivatives, can amplify to undesirable effect. The smooth, continuous output of a neural network, in contrast, though seemingly more complex, is possibly more appropriate for many tasks. In fact, there is no reason to assume that the nervous system more easily produces a linear, monotonic shift in a controlled variable than, say, a non-linear relaxation.

Most importantly, however, the neural network uses a mechanism for the generation of accelerating and decelerating torque pulses that is very different from the one identified in the feedback model. Firstly, observe that in many cases the desired EP trajectory (dashed in top row) does not approach the target position (red), yet the actual trajectory does (black). This is only possible, of course, if the difference between desired and actual position is not the determining factor for torque production. It can only be explained if velocity error is the main contributor instead. Indeed, the desired EP trajectory seems to be mostly offset on the angle axis, but its rate of change is rather similar to that of the minimum jerk trajectory. This is even more evident in the plots of reflex components. Here, it can easily be seen in the similarity of the two traces that net torque is mostly caused by velocity error. The whole picture is a little more complex, though. While elbow feedback gains are such that positional error is indeed negligible, in the shoulder significant forces are produced in proportion to positional error. Here, the neural network has offset the virtual EP from the target position by a larger amount. Also, analogous to the torque feedback model, in the case of opposing interaction torques the virtual trajectory initially accelerates faster, but then reverses direction before the joint relaxes towards the target (top row, right column). These changes to the virtual EP lead to a complex interaction of the three reflex components that is ultimately responsible for the correct compensation of intersegmental dynamics.

Finally, figure 6.8 presents the trajectories produced by the best evolved network for all six trials. These consist of three different amplitudes and two different directions. While the shoulder always moves in the direction of positive angles, the elbow moves either in the same or the opposite direction. Trajectories are shown only for the time period that the network was evaluated on in a given trial[3]. As can be seen in the figure, the performance described above extends both to smaller as well as larger amplitudes. Plots of angle over time are generally smooth, although elbow velocity profiles exhibit the already mentioned oscillations caused by neural output. Because the desired duration of each movement was determined from a constant average velocity, peak velocities are approximately equal. In other words, because the desired speed was fixed, one can not observe the speed-insensitive strategy that was demonstrated by the torque feedback model.

To conclude, the non-linear reflex controller when driven by a neural network is best not understood as a damped spring model, but as a complex dynamical system that balances various force components for the task at hand. The added layer of neural "computation" between central motor commands and reflex dynamics allows higher levels to interact with the motor apparatus without

[3]Fitness evaluations of smaller amplitude movements were shorter for reasons of computational efficiency.

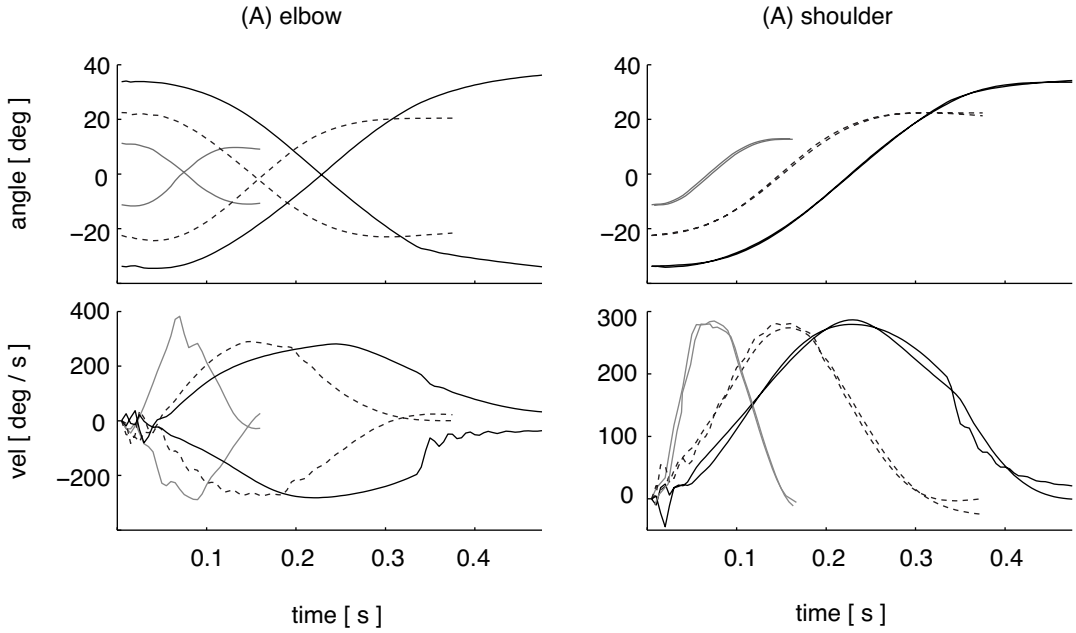

Figure 6.8: Multijoint kinematics of ANN model during movements of three different amplitudes.

regard for intersegmental dynamics.

6.4 Discussion

Two mechanisms have been proposed in this chapter for the compensation of interaction torques during multijoint movements. The first is based on interjoint feedback of net joint torques. Since intersegmental dynamics are systematically related to actively applied joint torques, information about the latter can be used to counteract the former. But how can *torques* function as corrective feedback in a motor control framework based on *positional* control? One option would involve an internal inverse dynamics model that maps required counter-torques onto positional offsets. Such a mapping can only be correct if it takes into account the geometry and dynamics of force generation of the neuromusculoskeletal system. The model developed here suggests instead that the central motor command which specifies the desired position of one joint can simply be offset in proportion to the torque created at another. In other words, the "inverse dynamics calculations" are replaced with a basic linear scaling function. The model further predicts that the virtual EP of the distal joint (elbow) is modulated by torque feedback only when joints move in opposite directions. When they move in the same direction, in contrast, only the proximal joint (shoulder) is affected. In both cases torque feedback is positive.

Translated into animal anatomy and neurophysiology the hypothesised mechanism makes the following predictions. Firstly, it assumes that active muscle forces can be sensed reliably, and transformed into either muscle torques first or joint torques directly. Such transformations could arguably be based on a combination of sensed muscle force with other proprioceptive signals according to the geometry of the articulated system (torque at the joint is equal to force times moment arm). It further predicts that spinal interneurons exist which receive afferents carrying information

about forces and which project onto α-motorneurons such as to modulate the threshold λ of the stretch reflex (offset the desired muscle length, see chapter 3). Furthermore, either the activity of these interneurons, or their synapses onto α-motorneurons need to be selectively gated depending on the relative direction of motion of the joints. Lastly, net joint torques need not be represented explicitly if information about active muscle force or torque is appropriately relayed across other joints in the chain. The required distribution of afferents could be the result of the co-development of the skeleton, the muscles and the spinal circuits innervating them.

The question then arises as to how realistic the assumptions and predictions of the torque feedback model are. Force feedback has been used previously as an integral part of other motor control models. Feldman, for example, hypothesised that it helps linearising the effect of cocontraction so that stiffness and position can be controlled independently, even when antagonist muscles are arranged asymmetrically (Feldman, 1993). It was also used to model the myotactic reflex which protects a muscle when loads exceed a safe threshold (Contreras-Vidal et al., 1997). Indeed, this was traditionally thought to be the only role of the Ib afferents from force sensing Golgi tendon organs (references in Cleland and Rymer, 1990). Several findings challenge this idea. Firstly, it is now clear that Ib afferents are in fact very sensitive to even small force levels (Jami, 1992). Secondly, the ensemble activity of Golgi tendon organs accurately encodes force information in the whole muscle (Mileusnic and Loeb, 2009). And thirdly, Ib afferent activity results in widespread inhibition as well as excitation of motoneurons innervating muscles acting at the same joint as well as distant ones (Jankowska et al., 1981; Nichols, 1989; Jankowska, 2001). It is also known that Ib inhibitory interneurons receive input from Ia afferents that carry muscle length and velocity feedback from muscle spindles. One theory suggests that Ia input confers dynamic sensitivity to Ib interneurons, which would allow for precise force regulation throughout a wide range of movements (McCrea, 1992). In conjunction, these findings suggest that force-dependent feedback could play a role in coordinating the simultaneous motion of several joints. Interestingly, McCrea (1992) points out that a hypothesis has yet to emerge that explains the widespread distribution of Ib excitation throughout the limb. The torque feedback model presented in this chapter suggests that Ib excitation could be the mechanism by which the spinal cord compensates for interaction torques during multijoint movements.

Further evidence for the use of positive force feedback in the control of movement comes from studies of invertebrates and cats. It is known, for example, that certain reflexes activating ankle extensors in the cat switch from being inhibitory during static posture (Harrison et al., 1983) to excitatory during the stance phase of walking (Pearson and Collins, 1993; Pratt, 1995). Excitatory influences were shown to originate in Golgi tendon organs (Conway et al., 1987; Donelan and Pearson, 2004) and the contribution of this positive force feedback was shown to range from 20% to as much as 50% of total muscle force (Donelan and Pearson, 2004). Regarding its role, Prochazka et al. (1997) demonstrate in computational models that such positive force feedback can, somewhat paradoxically, provide stable load compensation when functioning in concert with inherent muscle viscoelasticity, negative displacement feedback and delays in the afferent pathway. Positive feedback was also demonstrated as a means for decentralised limb coordination in the stick insect (Cruse et al., 1995), in the control of leg movements of the locust (Burrows and Pflueger, 1988), and claw movements in the crayfish (Lindsey and Gerstein, 1977). Experimental

evidence also exists for load receptor contribution to the control of body equilibrium during stance in humans (Dietz, 1998).

Last but not least, the feedback model presented in this chapter exhibits the experimentally observed linear synergy between elbow and shoulder torques, and follows the speed insensitive strategy identified in human subjects. Neither of these features were explicitly built into the system. This suggests that they could be epiphenomena of a mechanism that is primarily concerned with intersegmental dynamics. They constitute another example of features that need not be centrally planned, but could emerge from the dynamics of the underlying neuromechanical system.

Further work should address the generality of the proposed compensation mechanism. It would be interesting to know whether torque feedback gains need to be adjusted in a complex manner for a wider range of different movement amplitudes and speeds, for example. Another question is whether compensation could also be achieved with acceleration feedback instead of torque, as implicated for example in the control of balance (Welch and Ting, 2009). As acceleration is related to torque via inertia, feedback about the former, possibly in conjunction with postural feedback or information about limb characteristics, could potentially achieve the same effect. Also, it would be important to show that the proposed feedback mechanism works equally on the level of individual muscles, and not just for a joint-level model as considered in this chapter.

The feedforward model proposed for producing smooth multijoint movements is less able to make concrete predictions. First of all, since it operates solely on the level of central motor commands, it could be implemented either in the brain or in spinal reflex circuits. Further work would be needed to evolve a neural network that can control multijoint movements under a wider range of conditions. This could be analysed for specific correlations between neural activity and force production, which could then be compared to those found in the brain or the spinal cord. One prediction of the model, however, is its strong reliance on velocity error feedback. Several researchers (e.g. Bullock and Grossberg, 1992; Feldman, 1986) have noted the importance of the muscle spindle's high gain response to stretch velocity (Edin and Vallbo, 1990) for the creation of triphasic muscle bursts in models of the stretch reflex. It is not clear, however, whether an equally strong signal of velocity *error* is also present in neural activity of the spine. Though there is no theoretical argument against it, experimental observation would need to confirm the existence of such a signal.

In summary, two testable hypotheses have been proposed that can explain the compensation for interaction torques during multijoint movements. It remains to be seen whether the models generalise to the explicit control of individual muscles, and whether future neurophysiological research will confirm or reject their assumptions.

Chapter 7

Conclusion

The aim of this thesis was to examine the relationship between the material properties and dynamics of muscles and reflexes on the one hand, and the type of control signals required for coordinated movement on the other. Specifically, the framework of the equilibrium-point hypothesis was used to test whether simple monotonic shifts in desired position are sufficient to produce single- and multijoint movements of varying amplitude and speed that replicate biomechanical invariants observed in human subjects. As described in chapter 2, the EP hypothesis suggests that this can be achieved without the need for internal models by exploiting the intrinsic dynamics of muscles and neural circuits in the spine. Others have argued that motor control based on the viscoelastic properties of these subsystems is insufficient to account for fast movements and that it predicts complex control signals. Much of the criticism regarding this theory, however, is based on misconceptions about or oversimplification of the mammalian motor apparatus. It was therefore necessary to study the implications of various non-linear components of the muscle model used, so that any simplifications could be justified as not being relevant in the context of the experiments carried out (see chapter 3). Given the chosen level of biological plausibility, the following chapters set out to test the model's ability to deal with feedback delays, to produce triphasic burst patterns, to simultaneously control movement distance and duration, and to coordinate the motion of multiple joints. Also, a lumped muscle-reflex model, which combines the two components into a single equation of force production at the joint, was considered as an approximation of the detailed dynamical representation. Based on this simpler model, two mechanisms were proposed which aim to explain the compensation for interaction torques that arise in one body segment as the result of motion in another.

7.1 Summary of contributions

Properties of stable equilibria in joint space created by antagonistic muscles

The finding that non-linear material properties in skeletal muscles lead to the emergence of a stable equilibrium when one muscle acts against another is not new and forms the basis of most EP models of motor control. Chapter 3, however, illustrates in some detail how joint stability depends on

assumptions about muscle paths and moment arms, the inclusion of series elasticity (tendon) and the modelling of chemical dynamics (Ca^{2+}). It also shows that a setup consisting of two monoarticular muscles can qualitatively, and in some respects quantitatively, approximate the steady-state and transient behaviour of a system that in addition features biarticular muscles. By showing that at the chosen level of complexity the muscle simulation allows for stable control of joint position, stiffness and velocity, it justifies its use in the following chapters. Regarding the bigger picture, the chapter argues that stable joint equilibria implement synergies at the lowest level of motor control. They reduce the number of degrees of freedom that need to be controlled (from several muscle forces to a single joint position), yet allow for flexibility via tuning of response characteristics (stiffness and damping).

Material properties of muscles allow for flexible motor control and might facilitate motor learning

The second part of chapter 3 explores the implications of material properties for open-loop muscle control using pulse-step motor commands. Using a genetic algorithm to evolve control strategies, it is found that the antagonistic setup allows for more flexibility in reaching the same position than would be possible with a proportional derivative controller. An example is the use of a passive, i.e. unpowered, swing to move from an initial position to a target. Also, muscle damping characteristics are shown to smoothen the fitness landscape of pulse-step controllers. If nervous systems use such forms of control, then this property could facilitate the learning of appropriate motor commands.

Muscle-reflex dynamics driven by simple control signals reproduce biomechanical invariants

Chapter 4 introduces the λ-model, an instantiation of the EP hypothesis, and variations thereof that add velocity error as well as static coactivation components. It demonstrates that the former is crucial for high velocity movements without oscillations, and the latter for dealing with feedback delays. It is shown that this reflex model can reproduce natural kinematics of human subjects at realistic stiffness levels, even when driving a musculoskeletal system that does not feature tendon, calcium dynamics or biarticular muscles. The chapter also shows how a simple monotonic shift in desired position interacts with the reflex model to produce experimentally observed triphasic burst patterns, and allows for control of movement distance and velocity. For the latter to be feasible, however, the range of static musculoskeletal properties represented in the controller needs to be extended. The results confirm that any EP-based motor control scheme requires functions that relate the desired target not only to appropriate muscle lengths, but also to feedback gains determining the system's viscoelasticity.

A lumped model approximation of neuromuscular dynamics

For some purposes it might not be necessary or desired to simulate in detail the dynamics of several muscles and their reflex control. In chapter 5 an alternative model is developed which approximates such dynamics with a single equation of force production that exhibits equilibrium dynamics at the joint level. It is shown that elastic and viscous forces need to be non-linear functions of joint position and velocity in order to reproduce human kinematic data during single-joint

movements. Crucially, this model demonstrates how assumptions about muscle and reflex dynamics affect predictions about the kind of control signals needed for smooth targeted movements. While the detailed muscle-reflex simulation produced the smoothest movements with a shift in desired position as long as the desired movement, the lumped model predicts a shift of only half the duration.

Compensation for intersegmental dynamics during multijoint movements

The detailed muscle model, driven in feedforward or feedback mode, as well as the lumped muscle-reflex model, both failed to account for the intersegmental dynamics that occur by necessity during multijoint movements. Chapters 3–5 demonstrate that it is not sufficient to drive each joint in isolation when force production is limited to realistic levels. Two mechanisms were therefore proposed in chapter 6, which couple the control of individual joints so that interaction torques are compensated for correctly. One is based on the distribution of force feedback across the joints in a limb, and the other on feedforward adjustments of control signals in relation to the desired movement duration and amplitude. While both show potential in reproducing human performance, the former is simpler and makes more explicit and testable predictions. It also suggests that experimentally observed elbow-shoulder synergies as well as the so-called speed-insensitive movement strategy, might be epiphenomena of a system that is primarily responsible for the compensation of intersegmental dynamics. Both models are the first to indicate that the nervous system might not need an internal representation of limb dynamics to achieve this.

7.2 Future work

The work started in this thesis opens many avenues to be explored. One direction to follow concerns the chosen level of realism and model complexity. Although a relatively complete muscle model was studied in chapter 3, several simplifications were made in consecutive experiments. For example, the series elastic element was omitted based on the fact that the short tendons found in the human arm should have a negligible effect on its dynamics. Also, calcium dynamics and biarticular muscles were not included, while muscle paths were assumed to vary linearly with joint angle and moments arms to be constant. The complete model was pruned this way because it allowed for an easier relationship to be established between a given target position and the required muscle lengths. Arguably, the conclusions in this thesis are general enough not to depend on such details. A logical next step would be to show that this is in fact true.

Another simplification was the omission of the effect of gravity. This is a common technique in biomechanical studies, and usually implemented by executing movements in the horizontal plane only. It is justified if one is primarily concerned with the dynamic forces involved in a given movement, but not with the static forces required for counteracting the effect of gravity on a limb. Though this was the case here, it would be interesting to examine how control signals need to be adapted to account for external loads (the fact that EP models can account for internal loads has been shown in this thesis).

The range of movements studied could also be extended. Here, we only considered movements involving two hinge joints, each revolving towards a target angle. Human arm movements, of

course, involve more joints, many more muscles, and spatial trajectories in three dimensions. The models studied in this thesis could be incrementally extended to account for more complex bodily configurations as well as task requirements. Others have already shown, for example, that asymmetry in muscle attachment could be compensated for in the spine so that higher levels only "see" symmetrical structures. Eventually, it would be desirable to show that an EP model extended with the mechanisms proposed in this thesis can produce natural multijoint movements when controlling an anatomically correct arm model in three dimensions and under the effect of gravity.

Another route for further investigation concerns the neurophysiological evidence for the mechanisms proposed in this thesis. Though it was shown that velocity error feedback is crucial for fast movements, and that force feedback can be used to cancel interaction torques, it is still unclear whether the required circuitry actually exists in the spinal cord. We know of interneurons that encode the velocity of muscle contraction and tension, but their patterns of connectivity with other inter- and motorneurons has not yet been fully established. Also, a technique is required for separating reflex and centrally specified components of shifts in motorneuron thresholds (the λ command). At different points in this thesis, reflex models predicted monotonic motor commands of either the same duration as the intended movement or of half its duration. If the actual motor command could be identified, this could help to disambiguate between the different model assumptions.

Muscle-reflex models were evolved in this thesis based on a fitness function that minimises jerk in joint angle trajectories. As reviewed in chapter 2, many other optimality criteria have been proposed that account for the invariants observed in human movements. One advantage of the evolutionary approach is that the fitness criterion can easily be changed. It would be interesting to test whether different optimality assumptions lead to different types of reflex models or evolved motor commands. For example, neural network controllers could be modified to include signal-dependent noise, and evolved to minimise endpoint variance at the arm. According to the minimum variance theory, resulting trajectories should be smooth as a consequence, since abrupt changes in motor commands would lead to more variability (error) in the final position. The optimality measure could have significant effects on predicted reflex gains and motor commands. In this thesis, controllers were evolved to reduce overshoot and oscillations at all cost (as a result of minimising jerk). But in human subjects these features can in fact be observed, especially during fast movements. Another question is, therefore, whether the same results are obtained if such constraints are relaxed.

This thesis has demonstrated that reflex gains need to be adjusted to match the viscoelasticity of the system to the speed and amplitude requirements of the desired movement. Further work would be needed to determine whether this adjustment can take place on lower levels of the motor hierarchy, for example through simple heuristics implemented in spinal circuits, or whether a precise internal model is required for relating reflex gains to the intended motion. Another problem is how either of these would be acquired. Models exist for learning forward and inverse internal models of the body. But an open question is whether spinal circuits co-develop with the body in such a way as to reflect the dynamical interactions of its segments. An appropriate organisation of feedback in the spinal cord can in theory compensate for interaction torques, gravity, or the asymmetry of muscle

attachment (see e.g. Feldman, 1993; Bullock and Grossberg, 1991). All this could be tested with a more detailed neural model of spinal reflexes.

The thesis has also demonstrated that the dynamical systems approach is a valid methodology for studying questions of motor control. As shown throughout the previous chapters, in the EP-hypothesis *control* of motor behaviours is best understood as the appropriate selection of parameters of a coupled neuro-musculoskeletal system, while the *execution* of a motor behaviour is simply the relaxation of its dynamics towards a stable equilibrium. While the selection of control parameters (such as reflex gains) is relatively simple – it does not require an internal model of bodily dynamics – it necessitates kinematic representations of body geometry. The difference between force-control and EP-control (as implemented here), is thus not whether or not internal models are used, but rather concerns the nature of the models. The force-control hypothesis requires detailed computational processes that calculate the inverse transformation from desired movement to individual motor neuron firing rates, in other words, detailed and accurate predictive simulations of the body and the external world. The EP hypothesis, in contrast, suggests that the body (specifically the neuro-musculoskeletal periphery) is "its own best model" (Brooks, 1991), and responds to centrally triggered shifts in parameters with the autonomous execution of movements. Furthermore, as argued above, the kind of kinematic representations required by the EP-hypothesis could in theory be embodied in distributed peripheral networks co-developing with the body. Arguably, referring to such an organisation of feedback structures as "internal models" would stretch the meaning of the word.

It is also worth pointing out that kinematic maps were required in this thesis because the experiments, somewhat artificially, defined a movement task as moving from one specific set of angles to another. Natural movement tasks are usually driven by other goals, and are often defined in visual space, as when reaching for an object in the environment. In such situations, the EP hypothesis proposes a hierarchical control scheme (Feldman, 2010). As described in section 4.1.3, for multiple muscles it is suggested that shifts in individual threshold lengths are controlled by a signal comprising two components: a reciprocal part R, the referent configuration, which shifts the thresholds of antagonistic muscles in the same direction in joint space to control equilibrium position; and a co-contraction part C that shifts the thresholds in opposite directions in order to modulate the stiffness of the joint. The referent configuration R, by specifying a basis set of muscle lengths beyond which muscles become activated, essentially establishes the origin of a frame of reference for muscle activations. For the control of movement at the joint level, the central nervous system does not need to concern itself with activating individual muscles, but only with shifting the referent configuration R. In the hierarchical scheme, it is further suggested that the referent joint configuration does not need to be specified explicitly. Firstly, because ontogenetically formed neural structures are thought to distribute shifts in threshold lengths such that asymmetries in muscle configurations are automatically accounted for. In other words, R can be shifted linearly from one joint angle to another, while the underlying neural structures shift muscle thresholds in relation to the geometry of the musculoskeletal system. Secondly, the joint referent R itself is controlled within a higher-level frame of reference. For example, when reaching for an object, the central nervous system establishes as a task goal a shift of the hand referent position in visual space. Lower level referents, such as the joint referent, are in turn defined with respect to the

frame of reference of the hand. In other words, to reach for a particular point in space, a shift in referent hand position results in a shift of referent joint angles such that the hand moves in the direction of the target. On this level too, the relationship between the different frames of reference (how joint referents move in response to shifts in the hand referent) is implemented by ontogenetically formed neural structures. Now, in this thesis the lower level of the hierarchy was studied in isolation. Experiments evaluated only whether artificially established referent configurations in joint space (i.e. poses) could be achieved smoothly by different types of controllers. Arbitrary poses were selected as "tasks" and the referent configuration R determined using a look-up table of muscle lengths and joint angles. Neither were the neural structures considered that shift muscle threshold lengths in response to a shift in joint referent, nor the higher-level frames of reference responsible for establishing task-specific shifts in the joint referent in the first place. One of the most valuable extensions of the work presented here could therefore investigate if the requirement for internal kinematic maps can be relaxed in a framework that is based on tasks defined in external space, and which includes the (neural) implementation of hierarchical frames of reference.

7.3 Conclusion

To conclude, this thesis has demonstrated that the intrinsic material properties of muscles and the dynamics of low-level reflexes simplify the "computational" problems involved in the control of limb movements. It has confirmed that equilibrium-point models can account for single- and multijoint movements of various speeds and amplitudes and thereby refuted claims to the contrary. Furthermore, it has shown that this can be achieved with simple control signals, and without requiring inverse dynamics calculations. The thesis also demonstrated that the approach of co-evolving bodily parameters and neural control structures using biomechanically inspired optimality criteria is a promising avenue that should be further explored. It remains to be seen whether neurophysiological research will verify or falsify the predictions made in this thesis concerning the types of feedback control employed in human multijoint arm movements.

Bibliography

Abraham, R. and Shaw, C. D. (1992). *Dynamics: The Geometry of Behavior*. Addison Wesley Publishing Company, 2 edition.

Agmon-Snir, H. and Segev, I. (1993). Signal delay and input synchronization in passive dendritic structures. *Journal of Neurophysiology*, 70(5):2066–2085.

Akazawa, K. and Okuno, R. (2006). Estimating Torque-Angle relations of human elbow joint in isovelocity flexion movements. *IEICE - Trans. Inf. Syst.*, E89-D(11):2802–2810.

Ali, M. S., Hou, Z. K., and Noori, M. N. (1998). Stability and performance of feedback control systems with time delays. *Computers & Structures*, 66(2-3):241–248.

Allen, C. and Stevens, C. F. (1994). An evaluation of causes for unreliability of synaptic transmission. *Proceedings of the National Academy of Sciences of the United States of America*, 91(22):10380–10383.

Atkeson, C. and Hollerbach, J. (1985). Kinematic features of unrestrained vertical arm movements. *J. Neurosci.*, 5(9):2318–2330.

Balasubramaniam, R. and Feldman, A. G. (2004). Guiding movements without redundancy problems. In Jirsa, V. K. and Kelso, J. A. S., editors, *Coordination Dynamics*. Springer, New York.

Balnave, C. D. and Allen, D. G. (1996). The effect of muscle length on intracellular calcium and force in single fibres from mouse skeletal muscle. *The Journal of Physiology*, 492(Pt 3):705–713.

Barto, A. G. (1999). Learning to reach via corrective movements. *IEE Seminar Digests*, 1999(49):6.

Barto, A. G., Fagg, A. H., Sitkoff, N., and Houk, J. C. (1999). A cerebellar model of timing and prediction in the control of reaching. *Neural Computation*, 11(3):565–94.

Bastian, A. J., Martin, T. A., Keating, J. G., and Thach, W. T. (1996). Cerebellar ataxia: abnormal control of interaction torques across multiple joints. *Journal of Neurophysiology*, 76(1):492–509.

Beamish, D., Bhatti, S., Wu, J., and Jing, Z. (2008). Performance limitations from delay in human and mechanical motor control. *Biological Cybernetics*, 99(1):43–61.

Beer, R. (1996). Towards the evolution of dynamical neural networks for minimally cognitive behavior. In Maes, P., Mataric, M., Meyer, J., Pollack, J., and Wilson, S., editors, *From animals to animats 4: Proceedings of the Fourth International Conference on Simulation of Adaptive Behavior*, pages 421–429, Cape Cod, Massachusetts. MIT Press.

Beer, R. (2009). Dynamical systems and embedded cognition. In Frankish, K. and Ramsey, E., editors, *The Cambridge Handbook of Artificial Intelligence*. Cambridge University Press, Cambridge, UK.

Beer, R. D. (1995a). A dynamical systems perspective on agent-environment interaction. *Artif. Intell.*, 72(1-2):173–215.

Beer, R. D. (1995b). On the dynamics of small continuous-time recurrent neural networks. *Adapt. Behav.*, 3(4):469–509.

Belenkii, V. E., Gurfinkel, V. S., and Pal'tsev, E. I. (1967). Control elements of voluntary movements. *Biofizika*, 12(1):135–141.

Bellman, R. (1961). *Adaptive Control Processes: A Guided Tour*. Princeton University Press.

Bellomo, A. and Inbar, G. (1997). Examination of the equilibrium point hypothesis when applied to single degree of freedom movements performed with different inertial loads. *Biological Cybernetics*, 76(1):63–72.

Bennett, D. J., Hollerbach, J. M., Xu, Y., and Hunter, I. W. (1992). Time-varying stiffness of human elbow joint during cyclic voluntary movement. *Experimental Brain Research. Experimentelle Hirnforschung. Expérimentation Cérébrale*, 88(2):433–442.

Bennett, K. M. and Lemon, R. N. (1996). Corticomotoneuronal contribution to the fractionation of muscle activity during precision grip in the monkey. *Journal of Neurophysiology*, 75(5):1826–1842.

Bizzi, E., Accornero, N., Chapple, W., and Hogan, N. (1984). Posture control and trajectory formation during arm movement. *J. Neurosci.*, 4(11):2738–2744.

Blakemore, S. J., Wolpert, D. M., and Frith, C. D. (1998). Central cancellation of self-produced tickle sensation. *Nat Neurosci*, 1(7):635–640.

Brooks, R. A. (1990). Elephants don't play chess. *Robotics and Autonomous Systems*, 6(1-2):3–15.

Brooks, R. A. (1991). Intelligence without reason. *IJCAI'91 Proceedings of the 12th international joint conference on Artificial intelligence*, 1:569—595.

Brown, I. and Loeb, G. (2000). A reductionist approach to creating and using neuromusculoskeletal models. In Winters, J. and Crago, P., editors, *Biomechanics and Neuro-Control of Posture and Movement*, pages 148–163. Springer-Verlag, New York.

Brown, I. E., Cheng, E. J., and Loeb, G. E. (1999). Measured and modeled properties of mammalian skeletal muscle. II. the effects of stimulus frequency on force-length and force-velocity relationships. *Journal of Muscle Research and Cell Motility*, 20(7):627–643.

Bryson, A. E. and Ho, Y. (1975). *Applied optimal control*. Taylor & Francis.

Bullock, D. and Grossberg, S. (1988). Neural dynamics of planned arm movements: emergent invariants and speed-accuracy properties during trajectory formation. *Psychol Rev*, 95(1):49–90.

Bullock, D. and Grossberg, S. (1991). Adaptive neural networks for control of movement trajectories invariant under speed and force rescaling. *Human Movement Science*, 10:3–53.

Bullock, D. and Grossberg, S. (1992). Emergence of tri-phasic muscle activation from the nonlinear interactions of central and spinal neural network circuits. *Human Movement Science*, 11(1-2):157–167.

Burke, D., Gracies, J. M., Mazevet, D., Meunier, S., and Pierrot-Deseilligny, E. (1994). Nonmonosynaptic transmission of the cortical command for voluntary movement in man. *The Journal of Physiology*, 480 (Pt 1):191–202.

Burrows, M. and Pflueger, H. J. (1988). Positive feedback loops from proprioceptors involved in leg movements of the locust. *Journal of Comparative Physiology A*, 163(4):425–440.

Carr, C. E. and Konishi, M. (1988). Axonal delay lines for time measurement in the owl's brainstem. *Proceedings of the National Academy of Sciences of the United States of America*, 85(21):8311–8315.

Cleland, C. L. and Rymer, W. Z. (1990). Neural mechanisms underlying the clasp-knife reflex in the cat. i. characteristics of the reflex. *J Neurophysiol*, 64(4):1303–1318.

Contreras-Vidal, J. L., Grossberg, S., and Bullock, D. (1997). A neural model of cerebellar learning for arm movement control: cortico-spino-cerebellar dynamics. *Learn Mem*, 3(6):475–502.

Conway, B. A., Hultborn, H., and Kiehn, O. (1987). Proprioceptive input resets central locomotor rhythm in the spinal cat. *Experimental Brain Research. Experimentelle Hirnforschung. Expérimentation Cérébrale*, 68(3):643–656.

Corcos, D. M., Gottlieb, G. L., and Agarwal, G. C. (1989). Organizing principles for single-joint movements. II. a speed-sensitive strategy. *J Neurophysiol*, 62(2):358–368.

Cruse, H., Bartling, C., and Kindermann, T. (1995). High-Pass filtered positive feedback. decentralized control of cooperation. In *Proceedings of the Third European Conference on Advances in Artificial Life*, pages 668–678. Springer-Verlag.

de Lussanet, M. H. E., Smeets, J. B. J., and Brenner, E. (2002). Relative damping improves linear mass-spring models of goal-directed movements. *Human Movement Science*, 21(1):85–100.

Debicki, D. B. and Gribble, P. L. (2004). Inter-Joint coupling strategy during adaptation to novel viscous loads in human arm movement. *J Neurophysiol*, 92(2):754–765.

Debicki, D. B. and Gribble, P. L. (2005). Persistence of inter-joint coupling during single-joint elbow flexions after shoulder fixation. *Exp Brain Res*, 163(2):252–257.

Dennett, D. and Pylyshyn, Z. (1987). Cognitive wheels: The frame problem of AI. In *The Robot's Dilemma: The Frame Problem in Artificial Intelligence*, pages 64, 41. Ablex Publishing Co.

Dietz, V. (1998). Evidence for a load receptor contribution to the control of posture and locomotion. *Neuroscience and Biobehavioral Reviews*, 22(4):495–499.

Donelan, J. M. and Pearson, K. G. (2004). Contribution of force feedback to ankle extensor activity in decerebrate walking cats. *J Neurophysiol*, 92(4):2093–2104.

Dudek, D. M. and Full, R. J. (2006). Passive mechanical properties of legs from running insects. *J Exp Biol*, 209(8):1502–1515.

Edin, B. B. and Vallbo, A. B. (1990). Dynamic response of human muscle spindle afferents to stretch. *Journal of Neurophysiology*, 63(6):1297–1306.

Feldman, A. and Latash, M. (2005). Testing hypotheses and the advancement of science: recent attempts to falsify the equilibrium point hypothesis. *Exp Brain Res*, 161:91–103.

Feldman, A. G. (1966). Functional tuning of the nervous system with control of movement or maintenance of a steady posture. *Biophysics*, 11:565–578.

Feldman, A. G. (1979). Central and reflex mechanisms in the control of movement. *Moscow: Nauka*.

Feldman, A. G. (1986). Once more on the equilibrium-point hypothesis (lambda model) for motor control. *Journal of Motor Behavior*, 18(1):17–54.

Feldman, A. G. (1993). The coactivation command for antagonist muscles involving ib interneurons in mammalian motor control systems: an electrophysiologically testable model. *Neurosci Lett*, 155(2):167–170.

Feldman, A. G. (2010). Space and time in the context of equilibrium-point theory. *Wiley Interdisciplinary Reviews: Cognitive Science*, pages n/a–n/a.

Feldman, A. G., Adamovich, S. V., Ostry, D. J., and Flanagan, J. R. (1990). The origin of electromyograms - explanations based on the equilibrium point hypothesis. In Winters, J. and Woo, S., editors, *Multiple Muscle Systems: Biomechanics and Movement Organization*, pages 195–213. Springer Verlag, New York.

Feldman, A. G. and Latash, M. L. (1982). Afferent and efferent components of joint position sense; interpretation of kinaesthetic illusion. *Biological Cybernetics*, 42(3):205–214.

Feldman, A. G. and Levin, M. F. (1995). Positional frames of reference in motor control: Origin and use. *Behavioral and Brain Sciences*, 18(4):723–806.

Feldman, A. G., Ostry, D. J., and Levin, M. F. (1995). Velocity-dependent coriolis force perturbations: An explanation of the positional errors and adaptation. *Neuroscience Abstracts*, 21:681.

Feldman, A. G., Ostry, D. J., Levin, M. F., Gribble, P. L., and Mitnitski, A. B. (1998). Recent tests of the equilibrium-point hypothesis (lambda model). *Motor Control*, 2(3):189–205.

Fitts, P. M. (1954). The information capacity of the human motor system in controlling the amplitude of movement. *Journal of Experimental Psychology*, 47(6):381–391.

Flash, T. and Gurevich, I. (1997). Models of motor adaptation and impedance control in human arm movements. In Morasso, P. and Sanguineti, V., editors, *Self-organization, Computational Maps and Motor Control*, pages 423–481. Elsevier, Amsterdam.

Flash, T. and Hogan, N. (1985). The coordination of arm movements: an experimentally confirmed mathematical model. *J Neurosci*, 5(7):1688–1703.

Flash, T. and Sejnowski, T. J. (2001). Computational approaches to motor control. *Current Opinion in Neurobiology*, 11(6):655–662.

Floreano, D. and Mondada, F. (1994). Automatic creation of an autonomous agent: genetic evolution of a neural-network driven robot. In *Proceedings of the third international conference on Simulation of adaptive behavior : from animals to animats 3: from animals to animats 3*, pages 421–430, Brighton, United Kingdom. MIT Press.

Franklin, T. C. and Granata, K. P. (2007). Role of reflex gain and reflex delay in spinal stability–a dynamic simulation. *Journal of Biomechanics*, 40(8):1762–7.

Fu, Q. G., Flament, D., Coltz, J. D., and Ebner, T. J. (1995). Temporal encoding of movement kinematics in the discharge of primate primary motor and premotor neurons. *Journal of Neurophysiology*, 73(2):836–854.

Funahashi, K. and Nakamura, Y. (1993). Approximation of dynamical systems by continuous time recurrent neural networks. *Neural Networks*, 6(6):801–806.

Garner, B. A. and Pandy, M. G. (2001). Musculoskeletal model of the upper limb based on the visible human male dataset. *Computer Methods in Biomechanics and Biomedical Engineering*, 4(2):93–126.

Garner, B. A. and Pandy, M. G. (2003). Estimation of musculotendon properties in the human upper limb. *Annals of Biomedical Engineering*, 31(2):207–220.

Gelder, T. V. (1997). The dynamical hypothesis in cognitive science. *Behavioral and Brain Sciences*, 21:615—665.

Georgopoulos, A. P., Ashe, J., Smyrnis, N., and Taira, M. (1992). The motor cortex and the coding of force. *Science (New York, N.Y.)*, 256(5064):1692–1695.

Georgopoulos, A. P., Kalaska, J. F., Caminiti, R., and Massey, J. T. (1982). On the relations between the direction of two-dimensional arm movements and cell discharge in primate motor cortex. *The Journal of Neuroscience: The Official Journal of the Society for Neuroscience*, 2(11):1527–1537.

Giesl, P. and Wagner, H. (2007). Lyapunov function and the basin of attraction for a single-joint muscle-skeletal model. *Journal of Mathematical Biology*, 54(4):453–464.

Gomi, H. and Kawato (1996). Equilibrium-point control hypothesis examined by measured arm stiffness during multijoint movement. *Science*, 272(5258):117–120.

Gomi, H. and Kawato, M. (1997). Human arm stiffness and equilibrium-point trajectory during multi-joint movement. *Biological Cybernetics*, 76(3):163–171.

Gomi, H. and Osu, R. (1996). Human arm stiffness and viscosity in interaction with environments on a horizontal plane. *Nippon Telegraph and Telephone Corporation*.

Gomi, H. and Osu, R. (1998). Task-Dependent viscoelasticity of human multijoint arm and its spatial characteristics for interaction with environments. *J. Neurosci.*, 18(21):8965–8978.

Gomi, H., Shidara, M., Takemura, A., Inoue, Y., Kawano, K., and Kawato, M. (1998). Temporal firing patterns of purkinje cells in the cerebellar ventral paraflocculus during ocular following responses in monkeys i. simple spikes. *Journal of Neurophysiology*, 80(2):818–831.

Gottlieb, G. L. (1998). Muscle activation patterns during two types of voluntary single-joint movement. *J Neurophysiol*, 80(4):1860–1867.

Gottlieb, G. L., Corcos, D. M., Agarwal, G. C., and Latash, M. L. (1990). Organizing principles for single joint movements. III. speed-insensitive strategy as a default. *Journal of Neurophysiology*, 63(3):625–636.

Gottlieb, G. L., Song, Q., Hong, D. A., and Corcos, D. M. (1996). Coordinating two degrees of freedom during human arm movement: load and speed invariance of relative joint torques. *J Neurophysiol*, 76(5):3196–3206.

Graziano, M. (2006). The organization of behavioral repertoire in motor cortex. *Annual Review of Neuroscience*, 29(1):105–134.

Gribble, P. L., Mullin, L. I., Cothros, N., and Mattar, A. (2003). Role of cocontraction in arm movement accuracy. *J Neurophysiol*, 89(5):2396–2405.

Gribble, P. L. and Ostry, D. J. (1996). Origins of the power law relation between movement velocity and curvature: modeling the effects of muscle mechanics and limb dynamics. *Journal of Neurophysiology*, 76(5):2853–2860.

Gribble, P. L. and Ostry, D. J. (1999). Compensation for interaction torques during single- and multijoint limb movement. *J Neurophysiol*, 82(5):2310–2326.

Gribble, P. L. and Ostry, D. J. (2000). Compensation for loads during arm movements using equilibrium-point control. *Exp Brain Res*, 135(4):474–482.

Gribble, P. L., Ostry, D. J., Sanguineti, V., and Laboissiere, R. (1998). Are complex control signals required for human arm movement? *J Neurophysiol*, 79(3):1409–1424.

Gribble, P. L. and Scott, S. H. (2002). Method for assessing directional characteristics of non-uniformly sampled neural activity. *Journal of Neuroscience Methods*, 113(2):187–197.

Guenther, M. and Ruder, H. (2003). Synthesis of two-dimensional human walking: a test of the lambda-model. *Biological Cybernetics*, 89(2):89–106.

Haken, H., Kelso, J. A. S., and Bunz, H. (1985). A theoretical model of phase transitions in human hand movements. *Biological Cybernetics*, 51(5):347–356.

Harnad, S. (1990). The symbol grounding problem. *Phys. D*, 42(1-3):335–346.

Harris, C. M. and Wolpert, D. M. (1998). Signal-dependent noise determines motor planning. *Nature*, 394(6695):780–784.

Harrison, P. J., Jankowska, E., and Johannisson, T. (1983). Shared reflex pathways of group i afferents of different cat hind-limb muscles. *The Journal of Physiology*, 338:113–128.

Harvey, I., Husbands, P., and Cliff, D. (1994). Seeing the light: artificial evolution, real vision. In *Proceedings of the third international conference on Simulation of adaptive behavior : from animals to animats 3: from animals to animats 3*, pages 392–401, Brighton, United Kingdom. MIT Press.

Hatze, H. (1981). *Myocybernetic control models of skeletal muscle : characteristics and applications*. University of South Africa, Pretoria.

Hidler, J. and Rymer, W. (2001). Effects of motoneuron properties on reflex stability in spastic subjects: a simulation study. In *Engineering in Medicine and Biology Society, 2001. Proceedings of the 23rd Annual International Conference of the IEEE*, volume 2, pages 1178–1181 vol.2.

Hill, A. V. (1938). The heat of shortening and the dynamic constants of muscle. *Proceedings of the Royal Society of London. Series B, Biological Sciences (1934-1990)*, 126(843):136–195.

Hogan, N. (1984). An organizing principle for a class of voluntary movements. *J. Neurosci.*, 4(11):2745–2754.

Holdefer, R. N. and Miller, L. E. (2002). Primary motor cortical neurons encode functional muscle synergies. *Experimental Brain Research. Experimentelle Hirnforschung. Expérimentation Cérébrale*, 146(2):233–243.

Holst, E. and Mittelstaedt, H. (1950). Das reafferenzprinzip. *Naturwissenschaften*, 37(20):464–476.

Hooper, S. L., Guschlbauer, C., Blumel, M., Rosenbaum, P., Gruhn, M., Akay, T., and Buschges, A. (2009). Neural control of unloaded leg posture and of leg swing in stick insect, cockroach, and mouse differs from that in larger animals. *J. Neurosci.*, 29(13):4109–4119.

Iida, F. (2005). Cheap design approach to adaptive behavior: Walking and sensing through body dynamics. In *International Symposium on Adaptive Motion of Animals and Machines*.

Jami, L. (1992). Golgi tendon organs in mammalian skeletal muscle: functional properties and central actions. *Physiological Reviews*, 72(3):623–666.

Jankowska, E. (2001). Spinal interneuronal systems: identification, multifunctional character and reconfigurations in mammals. *The Journal of Physiology*, 533(1):31–40.

Jankowska, E., Johannisson, T., and Lipski, J. (1981). Common interneurones in reflex pathways from group 1a and 1b afferents of ankle extensors in the cat. *The Journal of Physiology*, 310:381–402.

Jeannerod, M. (1997). *The cognitive neuroscience of action*. Blackwell.

Jones, K. E., Hamilton, A. F., and Wolpert, D. M. (2002). Sources of signal-dependent noise during isometric force production. *Journal of Neurophysiology*, 88(3):1533–1544.

Jones, L. A. (1989). Matching forces: constant errors and differential thresholds. *Perception*, 18(5):681–687.

Jordan, M. I. (1993). Computational aspects of motor control and motor learning. In Heuer, H. and Keele, S., editors, *Handbook of Perception and Action: Motor Skills*. Academic Press, New York.

Kalman, R. (1960). A new approach to linear filtering and prediction problems. *Transactions of the ASME – Journal of Basic Engineering*, 82:45, 35.

Karniel, A. (2002). Three creatures named 'forward model'. *Neural Netw*, 15(3):305–307.

Karniel, A. and Inbar, G. F. (1999). The use of a nonlinear muscle model in explaining the relationship between duration, amplitude, and peak velocity of human rapid movements. *J Mot Behav*, 31(3):203–206.

Kawato, M. (1999). Internal models for motor control and trajectory planning. *Curr Opin Neurobiol*, 9(6):718–727.

Kawato, M., Furukawa, K., and Suzuki, R. (1987). A hierarchical neural-network model for control and learning of voluntary movement. *Biological Cybernetics*, 57(3):169–185.

Kelso, J. A. (1984). Phase transitions and critical behavior in human bimanual coordination. *Am J Physiol Regul Integr Comp Physiol*, 246(6):R1000–1004.

Kelso, J. A. S. and Tuller, B. (1984). A dynamical basis for action systems. In Gazzaniga, M., editor, *Handbook of Cognitive Neuroscience*. Plenum, New York.

Kistemaker, D., Soest, A. V., and Bobbert, M. (2007a). A model of open-loop control of equilibrium position and stiffness of the human elbow joint. *Biological Cybernetics*, 96(3):341–350.

Kistemaker, D. A., Soest, A. K. J. V., and Bobbert, M. F. (2007b). Equilibrium point control cannot be refuted by experimental reconstruction of equilibrium point trajectories. *J Neurophysiol*, 98(3):1075–1082.

Kistemaker, D. A., Soest, A. V., and Bobbert, M. F. (2006). Is equilibrium point control feasible for fast Goal-Directed Single-Joint movements? *J Neurophysiol*, 95(5):2898–2912.

Konhilas, J. P., Irving, T. C., and de Tombe, P. P. (2002). Length-dependent activation in three striated muscle types of the rat. *The Journal of Physiology*, 544(Pt 1):225–236.

Lackner, J. R. and Dizio, P. (1994). Rapid adaptation to coriolis force perturbations of arm trajectory. *Journal of Neurophysiology*, 72(1):299–313.

Lacquaniti, F., Licata, F., and Soechting, J. F. (1982). The mechanical behavior of the human forearm in response to transient perturbations. *Biological Cybernetics*, 44(1):35–46.

Lacquaniti, F., Terzuolo, C., and Viviani, P. (1983). The law relating the kinematic and figural aspects of drawing movements. *Acta Psychologica*, 54(1-3):115–130.

Lan, N., Li, Y., Sun, Y., and Yang, F. S. (2005). Reflex regulation of antagonist muscles for control of joint equilibrium position. *Neural Systems and Rehabilitation Engineering, IEEE Transactions on [see also IEEE Trans. on Rehabilitation Engineering]*, 13(1):60–71.

Latash, M. (1993). *Control of human movement*. Human Kinetics Publishers, Champaign IL.

Latash, M. L. and Gottlieb, G. L. (1991). Reconstruction of shifting elbow joint compliant characteristics during fast and slow movements. *Neuroscience*, 43(2-3):697–712.

Lemay, M. A. and Crago, P. E. (1996). A dynamic model for simulating movements of the elbow, forearm, an wrist. *Journal of Biomechanics*, 29(10):1319–30.

Lindsey, B. G. and Gerstein, G. L. (1977). Reflex control of a crayfish claw motor neuron during imposed dactylopodite movements. *Brain Research*, 130(2):348–353.

Loeb, G. E., Brown, I. E., and Cheng, E. J. (1999). A hierarchical foundation for models of sensorimotor control. *Exp Brain Res*, 126:1–18.

Macefield, G. and Gandevia, S. C. (1992). Peripheral and central delays in the cortical projections from human truncal muscles. rapid central transmission of proprioceptive input from the hand but not the trunk. *Brain: A Journal of Neurology*, 115 Pt 1:123–135.

Martin, V. (2005). *A dynamical systems account of the uncontrolled manifold and motor equivalence in human pointing movements : a theoretical study*. Doctoral thesis, Ruhr-Universitaet Bochum.

Matthews, P. B. (1959). The dependence of tension upon extension in the stretch reflex of the soleus muscle of the decerebrate cat. *The Journal of Physiology*, 147(3):521–546.

Matthews, P. B. C. (1970). The origin and functional significance of the stretch reflex. In Andersen, P. and Jansen, J. K. S., editors, *Excitatory Synaptic Mechanisms*, pages 301–315. Universitetsforlaget, Oslo.

McCrea, D. A. (1992). Can sense be made of spinal interneuron circuits? *Behavioral and Brain Sciences*, 15:633–643.

McGeer, T. (1990). Passive dynamic walking. *The International Journal of Robotics Research*, 9(2):62–82.

McIntyre, J. and Bizzi, E. (1993). Servo hypotheses for the biological control of movement. *Journal of Motor Behavior*, 25(3):193–202.

Mehta, B. and Schaal, S. (2002). Forward models in visuomotor control. *J Neurophysiol*, 88(2):942–953.

Merton, P. A. (1953). Speculations on the Servo-Control of movement. In Wolstenholme, G. E. W., editor, *Ciba Foundation Symposium - The Spinal Cord*, Novartis Foundation Symposia. John Wiley & Sons, Ltd., Chichester, UK.

Meyer, D. E., Abrams, R. A., Kornblum, S., Wright, C. E., and Smith, J. E. (1988). Optimality in human motor performance: ideal control of rapid aimed movements. *Psychological Review*, 95(3):340–370.

Meyer, D. E., Keith-Smith, J. E., Kornblum, S., Abrams, R. A., and Wright, C. E. (1990). Speed-accuracy tradeoffs in aimed movements: Toward a theory of rapid voluntary action. In *Attention and performance 13: Motor representation and control.*, pages 173–226. Hillsdale, NJ, England: Lawrence Erlbaum Associates, Inc.

Miall, R. C., Weir, D. J., Wolpert, D. M., and Stein, J. F. (1993). Is the cerebellum a smith predictor? *Journal of Motor Behavior*, 25(3):203–216.

Micheau, P., Kron, A., and Bourassa, P. (2003). Evaluation of the lambda model for human postural control during ankle strategy. *Biological Cybernetics*, 89(3):227–236.

Mileusnic, M. P. and Loeb, G. E. (2009). Force estimation from ensembles of golgi tendon organs. *Journal of Neural Engineering*, 6(3):036001.

Morasso, P. (1981). Spatial control of arm movements. *Experimental Brain Research*, 42(2):223–227.

Mussa-Ivaldi, F. A. (1988). Do neurons in the motor cortex encode movement direction? an alternative hypothesis. *Neuroscience Letters*, 91(1):106–111.

Nakamura, Y. and Nakagawa, M. (2009). Approximation capability of continuous time recurrent neural networks for non-autonomous dynamical systems. In *Artificial Neural Networks – ICANN 2009*, volume 5769 of *Lecture Notes in Computer Science*, pages 593–602. Springer, Berlin / Heidelberg.

Nakano, E., Imamizu, H., Osu, R., Uno, Y., Gomi, H., Yoshioka, T., and Kawato, M. (1999). Quantitative examinations of internal representations for arm trajectory planning: minimum commanded torque change model. *J Neurophysiol*, 81(5):2140–2155.

Newell, A. and Simon, H. A. (1976). Computer science as empirical inquiry: symbols and search. *Commun. ACM*, 19(3):113–126.

Nichols, T. R. (1989). The organization of heterogenic reflexes among muscles crossing the ankle joint in the decerebrate cat. *The Journal of Physiology*, 410:463–477.

Nichols, T. R. and Houk, J. C. (1976). Improvement in linearity and regulation of stiffness that results from actions of stretch reflex. *J Neurophysiol*, 39(1):119–142.

Nolfi, S. and Floreano, D. (2000). *Evolutionary robotics : the biology, intelligence, and technology of self-organizing machines*. MIT Press, Cambridge Mass.

Ostry, D. J. and Feldman, A. G. (2003). A critical evaluation of the force control hypothesis in motor control. *Exp Brain Res*, 153(3):275–288.

Pandy, M. G., Zajac, F. E., Sim, E., and Levine, W. S. (1990). An optimal control model for maximum-height human jumping. *Journal of Biomechanics*, 23(12):1185–1198.

Pearson, K. G. and Collins, D. F. (1993). Reversal of the influence of group ib afferents from plantaris on activity in medial gastrocnemius muscle during locomotor activity. *Journal of Neurophysiology*, 70(3):1009–1017.

Pfeifer, R. (2007). *How the body shapes the way we think : a new view of intelligence*. MIT Press, Cambridge Mass.

Pfeifer, R. and Iida, F. (2005). Morphological computation: Connecting body, brain and environment. *Japanese Scientific Monthly*, 58(2):48–54.

Pigeon, P., Yahia, L., and Feldman, A. G. (1996). Moment arms and lengths of human upper limb muscles as functions of joint angles. *Journal of Biomechanics*, 29(10):1365–70.

Pilon, J. and Feldman, A. (2006). Threshold control of motor actions prevents destabilizing effects of proprioceptive delays. *Experimental Brain Research*, 174(2):229–239.

Pilon, J., Serres, S. D., and Feldman, A. (2007). Threshold position control of arm movement with anticipatory increase in grip force. *Experimental Brain Research*, 181(1):49–67.

Polit, A. and Bizzi, E. (1979). Characteristics of motor programs underlying arm movements in monkeys. *J Neurophysiol*, 42(1):183–194.

Popescu, F., Hidler, J. M., and Rymer, W. Z. (2003). Elbow impedance during goal-directed movements. *Experimental Brain Research*, 152(1):17–28.

Pratt, C. A. (1995). Evidence of positive force feedback among hindlimb extensors in the intact standing cat. *J Neurophysiol*, 73(6):2578–2583.

Prochazka, A., Gillard, D., and Bennett, D. J. (1997). Implications of positive feedback in the control of movement. *J Neurophysiol*, 77(6):3237–3251.

Read, H. L. and Siegel, R. M. (1996). The origins of aperiodicities in sensory neuron entrainment. *Neuroscience*, 75(1):301–314.

Revonsuo, A. and Newman, J. (1999). Binding and consciousness. *Consciousness and Cognition*, 8(2):123–127.

Roszek, B., Baan, G. C., and Huijing, P. A. (1994). Decreasing stimulation frequency-dependent length-force characteristics of rat muscle. *Journal of Applied Physiology (Bethesda, Md.: 1985)*, 77(5):2115–2124.

Sabatini, B. L. and Regehr, W. G. (1996). Timing of neurotransmission at fast synapses in the mammalian brain. *Nature*, 384(6605):170–172.

Schmidt, R. A., Zelaznik, H., Hawkins, B., Frank, J. S., and Quinn, J. T. (1979). Motor-output variability: a theory for the accuracy of rapid motor acts. *Psychological Review*, 47(5):415–451.

Scholz, J. P. and Schöner, G. (1999). The uncontrolled manifold concept: identifying control variables for a functional task. *Experimental Brain Research*, 126(3):289–306.

Scholz, J. P., Schöner, G., and Latash, M. L. (2000). Identifying the control structure of multijoint coordination during pistol shooting. *Experimental Brain Research*, 135(3):382–404.

Schwartz, A. B. (1993). Motor cortical activity during drawing movements: population representation during sinusoid tracing. *Journal of Neurophysiology*, 70(1):28–36.

Scott, S. H., Sergio, L. E., and Kalaska, J. F. (1997). Reaching movements with similar hand paths but different arm orientations. II. activity of individual cells in dorsal premotor cortex and parietal area 5. *Journal of Neurophysiology*, 78(5):2413–2426.

Shadlen, M. N. and Newsome, W. T. (1994). Noise, neural codes and cortical organization. *Current Opinion in Neurobiology*, 4(4):569–579.

Shadlen, M. N. and Newsome, W. T. (1998). The variable discharge of cortical neurons: implications for connectivity, computation, and information coding. *The Journal of Neuroscience: The Official Journal of the Society for Neuroscience*, 18(10):3870–3896.

Shadmehr, R. and Mussa-Ivaldi, F. (1994). Adaptive representation of dynamics during learning of a motor task. *J. Neurosci.*, 14(5):3208–3224.

Shidara, M., Kawano, K., Gomi, H., and Kawato, M. (1993). Inverse-dynamics model eye movement control by purkinje cells in the cerebellum. *Nature*, 365(6441):50–52.

Slocum, A. C., Downey, D. C., and Beer, R. D. (2000). Further experiments in the evolution of minimally cognitive behavior: From perceiving affordances to selective attention. In Meyer, J., Berthoz, A., Floreano, D., Roitblat, H., and Wilson, S., editors, *From Animals to Animats 6: Proceedings of the Sixth International Conference on Simulation of Adaptive Behavior*, pages 430–439. MIT Press.

Smith, L. and Thelen, E. (1993). *A dynamic systems approach to development : applications*. MIT Press, Cambridge Mass.

Soechting, J. and Lacquaniti, F. (1981). Invariant characteristics of a pointing movement in man. *J. Neurosci.*, 1(7):710–720.

St-Onge, N., Adamovich, S. V., and Feldman, A. G. (1997). Control processes underlying elbow flexion movements may be independent of kinematic and electromyographic patterns: experimental study and modelling. *Neuroscience*, 79(1):295–316.

St-Onge, N. and Feldman, A. G. (2004). Referent configuration of the body: a global factor in the control of multiple skeletal muscles. *Experimental Brain Research. Experimentelle Hirnforschung. Expérimentation Cérébrale*, 155(3):291–300.

Sternad, D. and Schaal, S. (1999). Segmentation of endpoint trajectories does not imply segmented control. *Experimental Brain Research*, 124(1):118–136.

Strogatz, S. (1994). *Nonlinear Dynamics And Chaos: With Applications To Physics, Biology, Chemistry, And Engineering (Studies in nonlinearity)*. Perseus Books Group.

Suzuki, M., Shiller, D. M., Gribble, P. L., and Ostry, D. J. (2001). Relationship between cocontraction, movement kinematics and phasic muscle activity in single-joint arm movement. *Exp Brain Res*, 140(2):171–181.

Thelen, E., Schöner, G., Scheier, C., and Smith, L. B. (2001). The dynamics of embodiment: a field theory of infant perseverative reaching. *The Behavioral and Brain Sciences*, 24(1):1–34; discussion 34–86.

Todorov, E. (2000). Direct cortical control of muscle activation in voluntary arm movements: a model. *Nat Neurosci*, 3(4):391–398.

Todorov, E. and Jordan, M. I. (2002). Optimal feedback control as a theory of motor coordination. *Nat Neurosci*, 5(11):1226–1235.

Turvey, M. T. (1990). Coordination. *Am Psychol*, 45(8):938–953.

Uno, Y., Kawato, M., and Suzuki, R. (1989). Formation and control of optimal trajectory in human multijoint arm movement. minimum torque-change model. *Biological Cybernetics*, 61(2):89–101.

Vallbo, A. B. (1970). Discharge patterns in human muscle spindle afferents during isometric voluntary contractions. *Acta Physiologica Scandinavica*, 80(4):552–566.

Vallbo, Å. B. (1971). Muscle spindle response at the onset of isometric voluntary contractions in man. time difference between fusimotor and skeletomotor effects. *The Journal of Physiology*, 218(2):405–431.

van Beers, R. J., Baraduc, P., and Wolpert, D. M. (2002). Role of uncertainty in sensorimotor control. *Philos Trans R Soc Lond B Biol Sci*, 357(1424):1137–1145.

van Soest, A. J. and Bobbert, M. F. (1993). The contribution of muscle properties in the control of explosive movements. *Biological Cybernetics*, 69(3):195–204.

van Vreeswijk, C. and Sompolinsky, H. (1996). Chaos in neuronal networks with balanced excitatory and inhibitory activity. *Science*, 274(5293):1724–1726.

Wachholder, K. and Altenburger, H. (1926). Beitraege zur physiologie der willkuerlichen bewegung. *Pfluegers Archiv European Journal of Physiology*, 214(1):642–661.

Wagner, H. and Blickhan, R. (1999). Stabilizing function of skeletal muscles: an analytical investigation. *J Theor Biol*, 199(2):163–179.

Webb, B. (2004). Neural mechanisms for prediction: do insects have forward models? *Trends Neurosci*, 27(5):278–282.

Welch, T. D. J. and Ting, L. H. (2009). A feedback model explains the differential scaling of human postural responses to perturbation acceleration and velocity. *J Neurophysiol*, 101(6):3294–3309.

Winters, J. M. and Stark, L. (1985). Analysis of fundamental human movement patterns through the use of in-depth antagonistic muscle models. *IEEE Trans Biomed Eng*, 32(10):826–839.

Wolpert, D., Ghahramani, Z., and Jordan, M. (1995). An internal model for sensorimotor integration. *Science*, 269(5232):1880–1882.

Wolpert, D. M., Doya, K., and Kawato, M. (2003). A unifying computational framework for motor control and social interaction. *Philos Trans R Soc Lond B Biol Sci*, 358(1431):593–602.

Wolpert, D. M. and Ghahramani, Z. (2000). Computational principles of movement neuroscience. *Nature Neuroscience*, 3:1212–1217.

Won, J. and Hogan, N. (1995). Stability properties of human reaching movements. *Experimental Brain Research*, 107(1):125–136.

Wu, C. H., Houk, J. C., Young, K. Y., and Miller, L. E. (1990). Nonlinear damping of limb motion. In Winters, J. and Woo, S., editors, *Multiple muscle systems: Biomechanics and movement organization*, pages 214–235. Springer, New York.

Zahalak, G. I. (1981). A distribution moment approximation for kinetic theories of muscular contraction. *Math. Biosci.*, 55:89–114.

Zajac, F. E. (1989). Muscle and tendon: properties, models, scaling, and application to biomechanics and motor control. *Crit Rev Biomed Eng*, 17(4):359–411.

Zajac, F. E., Neptune, R. R., and Kautz, S. A. (2002). Biomechanics and muscle coordination of human walking. part i: introduction to concepts, power transfer, dynamics and simulations. *Gait & Posture*, 16(3):215–232.

Zakotnik, J., Matheson, T., and Dürr, V. (2006). Co-contraction and passive forces facilitate load compensation of aimed limb movements. *The Journal of Neuroscience: The Official Journal of the Society for Neuroscience*, 26(19):4995–5007.